NOTE TO USERS

Université d'Ottawa · University of Ottawa

Université d'Ottawa · University of Ottawa

FACULTÉ DES ÉTUDES SUPÉRIEURES ET POSTDOCTORALES

FACULTY OF GRADUATE AND POSTDOCTORAL STUDIES

PAP, Ilona

AUTEUR DE LA THÈSE - AUTHOR OF THESIS

M.A.Sc. (Chemical Engineering)

GRADE - DEGREE

Department of Chemical Engineering

FACULTÉ, ÉCOLE, DÉPARTEMENT - FACULTY, SCHOOL, DEPARTMENT

TITRE DE LA THÈSE - TITLE OF THE THESIS

Productivity Enhancement in Optical Semiconductor Manufacturing: Early Warning of Failures in Bhet Laser Fabrication

Jules Thibault / David McLean

DIRECTEUR DE LA THÈSE - THESIS SUPERVISOR

EXAMINATEURS DE LA THÈSE - THESIS EXAMINERS

G. Neale

A. Maccki

J.-M. De Koninck, Ph.D.

LE DOYEN DE LA FACULTÉ DES ÉTUDES SUPÉRIEURES ET POSTDOCTORALES

SIGNATURE

DEAN OF THE FACULTY OF GRADUATE AND POSTDOCTORAL STUDIES

Productivity Enhancement in Optical Semiconductor Manufacturing: Early Warning of Failures in BHet Laser Fabrication

by

Ilona Pap

A thesis submitted to the Faculty of Graduate and Postdoctoral Studies in partial fulfillment of the requirement for the degree of

Master of Applied Science

in the

Department of Chemical Engineering

UNIVERSITY OF OTTAWA

Your file Votre référence
ISBN: 0-494-01571-3
Our file Notre référence
ISBN: 0-494-01571-3

ABSTRACT

There are unique challenges in the fabrication and testing of optical semiconductor devices because, unlike typical silicon semiconductor devices, which can be tested cost-effectively on the wafer, many optical devices can only be 'fully' tested once the individual die is bonded to a heat sink. As a result, both the manufacturing process and test strategy need to be capable of predicting yields and product quality attributes based on limited sampling from a batch of the product. The large number of product quality and process variables that are measured for each device when it is manufactured makes it almost impractical to manually analyze them for valuable decision-making information. There is a need for understanding the complex, interactive effects of process variables on the product quality variables as well as automated analysis and discovery tools for extracting useful knowledge from the raw data. Such knowledge could have a significant impact on productivity and quality improvement. The objective of the present study is to identify useful correlations amongst the numerous process variables and to develop simple empirical models to predict important process quality indicators.

Quality is assessed using statistical data analysis, focusing on the primary functions of major failures. Validation of the data set also demonstrated that linear models were accurate in predicting new data points for some of the output variables, whereas the variation of some output variables could not be explained using the available industrial data bank. Some models were powerful in making predictions and to provide a clearer insight in determining the key factors in manufacturing of BHet. BHet is a directly modulated laser operating at 2.5 Gb/s and reaches up to 360 km. Application of this research for failure prediction at an early stage of the manufacturing line could result in a dramatic reduction in the number of defective wafers that are completely processed and thereby lowering the overall manufacturing cost.

RÉSUMÉ

Il y a de nombreux défis dans la fabrication et la vérification des produits à base de semi-conducteurs optiques parce que, contrairement aux produits utilisant des semi-conducteurs de silicium typiques, qui peuvent être vérifiés économiquement sur la gaufrette, beaucoup de produits optiques peuvent seulement être 'entièrement' vérifiés une fois la puce est placée sur un dissipateur thermique. Par conséquent, le procédé industriel et la stratégie de vérification doivent être capables de prédire le rendement et la qualité du produit basé sur un échantillonnage restreint à partir d'un lot de production. Le grand nombre de variables décrivant la qualité du produit et des variables de procédé qui sont mesurées pour chaque produit au cours de la fabrication rend presque impossible la procédure d'évaluation des données sans utiliser des outils automatiques d'analyse. Il est nécessaire de comprendre les effets complexes et interactifs des variables de procédé sur les variables de qualité du produit. Pour ce faire, des outils d'analyse performants sont nécessaires pour extraire la connaissance utile contenue dans les données brutes. De telles connaissances pourraient avoir un impact significatif sur l'amélioration de la productivité et de la qualité du produit fini. L'objectif de cette étude est d'identifier des corrélations utiles parmi les nombreuses variables de procédé et développer des modèles empiriques simples pour prédire certains indicateurs importants de la qualité du produit.

La qualité est évaluée en utilisant l'analyse statistique des données, avec une emphase sur les variables qui sont une cause majeure d'échec. La validation des données a démontré qu'un modèle linéaire était suffisamment précis pour obtenir de bonnes prédictions pour plusieurs variables mais pas pour toutes les variables de la banque de données. La modélisation est assez performante pour permettre de faire de bonnes prédictions et a permis de mettre en évidence les principaux facteurs impliqués des produits BHet. La prédiction d'échecs, tôt dans la fabrication du produit, permettrait une réduction significative du nombre de gaufrettes qui auraient à être fabriqués complètement et, par conséquent, une réduction du coût de fabrication.

ACKNOWLEDGEMENTS

Many people have contributed to my thesis. First and foremost, I would like to thank my supervisors, **Dr. Jules Thibault** and **Dr. David McLean,** for all the long and interesting conversation we had from which I have always greatly benefited, and for motivating me to higher achievements and for providing me continual guidance throughout this work. I am very appreciative for the numerous editorial comments and corrections done to my written work. There were many times I needed someone to talk to and they were always there to listen and to point me in the right direction.

I thank **John Reilly** for his love, vulnerability, wisdom, and strength that have inspired me to be the best I could be. I am grateful to him for sharing what we have learned together. Thank you John, for your encouragement and positive spirit, which continue to help me through my difficult times.

I would like to thank Ben, Nassem, Roopa, David Moore, Treena and Bruce for their encouragement and help throughout the many difficulties encountered during this research work. I really enjoyed working with them in this exciting area of research. I wish them all the best in the years to come.

Finally, I would like to express my grateful thanks to my family, my husband **Denes Pap,** and to my two lovely sons (evils at times), **David** and **Robert**, for their comprehension and sacrifices, and for not spending as much time with them as I used to. Without their love, support, understanding and patience this work would not have been possible.

Signature: _____ Date: _____

TABLE OF CONTENTS

LIST OF TABLES

LIST OF FIGURES

CHAPTER 1

INTRODUCTION

Semiconductor companies are faced with tremendous time-to-market pressure due to product cycles getting shorter and shorter with each new generation of wafer technology and selling prices declining rapidly after new products are introduced. The semiconductor manufacturing process in Nortel Networks, Carling Campus begins with bare InP (Indium Phosphide) wafers and builds the desired devices using a series of precise layering steps. Each step occurs in one of the three processing areas: growth, fabrication and testing.

Indium Phosphide (InP) is the most promising material and has an advantage over the more matured Si and Gallium-Arsenide (GaAs) technologies. When compared to GaAs, InP has higher electron velocity, higher radiation hardness and better heat-conducting property. The advantage of InP crystal material allows higher frequency operation and lower power requirements. Therefore, InP is widely used for the manufacture of microwave devices, high-frequency devices and optoelectronic integrated circuits (OEICs) which are indispensable for wireless technology and satellite communications Still, the promise of InP process technology is often overshadowed by concerns regarding high fabrication cost, low yield and unproven reliability of devices.

Unlike typical silicon semiconductor devices, which can be tested cost-effectively on the wafer, many InP devices can only be 'fully' tested once the individual die is bonded to a heat sink. As a result, both the manufacturing process and test strategy need to be capable of predicting yields and product quality attributes based on limited sampling from a batch of products. The large number of process variables that are measured for each device when it is manufactured, makes it almost impractical to manually analyze them for valuable decision making information. There is a need for understanding the complex, interactive effects of process variables on the product quality

variables, as well as automated analysis and discovery tools for extracting useful knowledge from the raw data.

Fabrication of BHet (Buried Heterostructure laser) directly modulated laser is a very complex process with a large number of processing steps. The process described in this thesis, pertains specifically to the one used at Nortel Networks, Carling Campus.

Most process variables associated with the BHet manufacturing process are recorded in computer databanks using a lot number. A lot number is an identification number used to track the lot throughout the manufacturing process. One of the problems associated with using this wealth of process information is the difficulty to trace the history of the lot due to the use of multiple data bases. To ensure that the processing steps are carried out correctly and in the right order, a computer control system is used to control the process flow of batches through the manufacturing process. The manufacturing process can be divided into four main areas: Metal Organic Chemical Vapor Deposition (MOCVD), Laser Gratings, Wafer Fabrication and Wafer Testing. All four areas use different database control systems for data storage, and the method of collection and units have evolved over time, making data mining more difficult.

The construction and validation of a coherent and complete database, covering the entire processing sequence, represented the major effort of this work. More than one year was required to understand and gather all the information that is now contained the data bank used in this thesis.

After gathering all data and organizing it into more friendly and readable form, a series of statistical tests were performed to extract useful information and determine interrelationships between all process variables. This information was instrumental to develop predictive models.

Initially, it is desired to use these models to predict, at any step in the process, the probability of occurrence of failures of the final product. Knowing as early as possible that a manufactured device has a high probability of failure would be very helpful to process engineers who may decide to terminate the fabrication of this device or to take remedial action, if possible, to correct the detected fault. In either case, significant saving could be achieved.

The specific objectives of the thesis are:

1. Build an industrial data bank and carry out exploratory data analyses in order to validate the data bank, to calculate useful statistics of all variables and to determine interrelationship amongst all process variables.
2. Determine relationships between product performance and intermediate product characteristics.
3. Develop predictive models relating output variables and fail codes to intermediate product characteristics, and forecasting potential problems.

This thesis mainly consists of four chapters: **Chapter 2** gives the reader a broad understanding of general IC manufacturing processes, which is followed by a detailed description of BHet laser manufacturing process. **Chapter 3** describes in detail how the final data bank was obtained. **Chapter 4** discusses some exploratory data analysis techniques that were used to correlate input and output variables. **Chapter 5** presents some predictive models that were developed as pre-emptive failure diagnostic, and presents a methodology to efficiently use these models. This thesis ends with conclusions and recommendations.

CHAPTER 2

BRIEF DESCRIPTION OF THE IC MANUFACTURING AND BHET PROCESS

2.0 INTRODUCTION

The intent of this chapter is to provide a general description of an Integrated Circuit (IC) manufacturing process and, in particular, to describe the main steps required in Nortel's manufacturing of BHet laser, which is the process that will be studied in this thesis. It is important to observe that 95% of the products manufactured at Nortel and Paignton plants are destined for the telecommunication industry. The demand for information transfer is increasing exponentially. The maximum data transfer rate and the distance an electrical signal can travel through cables before needing amplification is limited. On the other hand, optical fiber communication systems, using lasers as the transmission mode, allow higher data transfer rates and longer distances before the signal needs to be regenerated.

2.1 General processing Steps Involved in Wafer[1] Fabrication

The manufacture of any integrated circuit[2], including BHet laser, contains the same fundamental transformation steps. Typically, wafer fabrication involves a series of photolithography steps, chemical vapour deposition (CVD), diffusion, etching, and metallization steps. These steps are combined in a predetermined order (work flow) to produce the desired final product. These will be described in the following sections.

2.1.1 Chemical Vapour Deposition (CVD)

CVD is used extensively in the semiconductor industry and has played an important role by allowing the deposit of very thin films on the surface of a wafer (Medou, 1997). During chemical vapour deposition, the constituents of a vapour phase, often diluted with an inert carrier gas, react at a hot surface to deposit a solid film. In CVD, the diffusive-convective transport to the substrate involves intermolecular collisions. In the reaction chamber, the reactants are adsorbed on the heated substrate surface and the atoms undergo migrations and film-forming reactions. Gaseous by-products are desorbed and removed from the reaction chamber. The reaction forming a solid material does not always occur on or close to the heated substrate (heterogeneous reaction) but can also occur in the gas substrate (homogeneous reaction).

The thermal energy is the sole driving force in high temperature CVD reactors; for lower temperature deposition an additional energy is needed. Radio Frequency (RF), using electromagnetic radiation can be used to enhance the deposition process. This process is known as plasma enhanced CVD (PECVD). Plasma Enhanced Chemical Vapor Deposition (PECVD) is a technique in which one or more gaseous reactors are used to form a solid insulating or conducting layer on the surface of a wafer enhanced by the use of a vapor containing electrically charged particles or plasma, at lower

[1] Indium phosphide can be supplied as ingots or ingot sections or as-cut, etched or polished wafers. All indium phoshide wafers are individually laser scribed with ingot and slice identity to ensure perfect traceability. Wafers can be supplied with either the major or minor flat prepared to an orientation tolerance of ± 0.02° to aid cleavage in laser manufacturing operations.

[2] Another name for a chip, an integrated circuit (IC) is a small electronic device made out of a semiconductor material. The first integrated circuit was developed in the 1950s.

temperatures. PECVD reactors have the capability of also using the plasma for etching and cleaning the wafer prior to the deposition step. This in situ cleaning prepares the deposition surface, eliminating the problem of added contamination picked up during the loading step. PECVD uses lower substrate temperatures, is fast, and provides good film adhesion and good coverage. The main disadvantages of using PECVD are the use of chemicals (e.g., hydrogen) and this technique is prone to particulate contamination.

2.1.2 Photolithography

The most widely used form of lithography[3] is photolithography[4]. In the IC industry, pattern transfer from masks onto thin films is accomplished exclusively via photolithography. Accurate alignment and exposure of a series of successive patterns lead to complex multilayered ICs.

Photolithography is one of the most critical operations in semiconductor processing. It is the process that sets the surface dimensions on the various parts of the devices and circuits. The goal is first to create in and on the wafer surface a pattern whose dimensions are as close to the design requirements as possible. The second goal is the correct placement (alignment) of the circuit pattern on the wafer. The entire circuit pattern must be correctly placed on the wafer surface and the individual parts of the circuit must be in the correct position relative to each other. The effects of misaligned

---

[3] Lithography was invented by Aloysius Senefelder (1771 – 1834), in Bavaria. The word comes from the Greek; lythos – stone, grapho – to write. The concept of lithography is based on the mutual incompatibility of oil and water; the capacity of limestone to absorb and retain water and the disposition of oily substances to adhere to limestone. The highly polished nature of the surface is receptive to the oil that is spread over it. Senefelder discovered that by chemically treating the surface of limestone, and drawing onto it with a grease crayon, only the areas touched by the grease crayon would take the printing ink. Therefore, by drawing onto the treated stone in this way, inking it, covering it with a damp paper and running it through a printing press, the image is transferred exactly onto the paper.

[4] Photolithography is a process used in semiconductor device fabrication to transfer a pattern to the surface of a wafer or substrate. The transfer of this pattern will allow for the definition of features to be etched in an underlying film

mask layers can cause the entire circuit to fail. Transferring the image from the reticle or mask onto a wafer surface layer is a ten-step procedure.

The basic photolithography process involves application of photoresist to the wafer, masking, exposing the resist with the desired pattern, and developing the resist, which chemically removes the unwanted portions. This leaves the wafer surface exposed only in areas where surface treatment at the next step is required. Bake steps partially evaporate photoresist solvents by heating. Upon completion of the above stages, the wafers travel back into the diffusion or another slightly different cycle of deposition, or metallization. They then return to photolithography for the next mask step, and so on until all steps of the process are completed.

Control of the dimensions and alignment are difficult tasks because each of the individual process steps is sensitive to errors. Because of the number of steps in each patterning operation and the number of mask layers, the masking process is the chief source of wafer defects. Figure 2.1 shows a wafer which is coated with a photoresist and exposed to ultraviolet light causing the exposed portion of the wafer to undergo a chemical reaction.

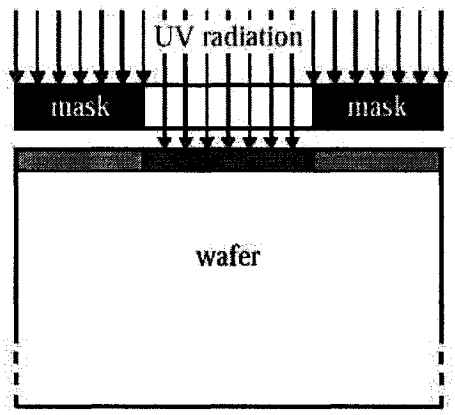

Figure 2.1 Basic patterning process

2.1.3 Etching

Etching is the process of removing the top layers(s) from the wafer surface through the openings in the resist pattern. When a mask is used to protect specific areas of the substrate surface, the goal of etching is to precisely remove the exposed material.

The mask material may be a photoresist or some other material, such as nitride, that is unaffected by the etching chemicals. Etching can be conducted using either wet chemicals or dry gas processes.

Wet etching is a blanket name that covers the removal of material by immersing the wafer in a liquid bath of the chemical etchant. Wet etchants fall into two broad categories; isotropic etchants and anisotropic etchants. Wet etching in general relies on oxidation-reduction reactions. Wet etchants are selected for their ability to uniformly remove the top wafer layer without attacking the underlying material. It is desired to have as good selectivity as possible. Wet etching is still largely used in several applications because it is relatively simple to implement and a complete batch is able to contain up to 20 substrates, which can be treated in one operation. That constitutes a considerable saving of time. On the other hand, it is necessary for chemical processing to rinse abundantly and dry the substrates. The rinsing is also done in vats. During the rinsing with deionized water, the resistivity of water is controlled in order to determine the quantity of contaminant ions still desorbed by substrates. The problems associated with wet etching are incomplete etch, over etching, undercutting, selectivity, and anisotropic or isotropic etching of the sidewalls.

Dry etching is a generic term that refers to the etching techniques in which gases are the primary etch medium, and the wafers are etched without wet chemicals or rinsing. The wafers enter and exit the system in a dry state. After a typical etch in a carbon containing RIE, the top 30 Å is heavily damaged, with an extensive concentration of Si-C bonds. RIE processes done in a hydrogen-containing ambient also have Si- H defects that can be observed as deep as 300 Å. Hydrogen may penetrate several microns into the surface where it can deactivate dopants in the substrate. .Major advantages of the dry etching are low temperature dependence, the etch rate change is relatively constant, reduced chemicals consumption with associated lower cost and environmental impact. Also one of the advantages is a cleaner process, less susceptible to problems. It leads to more precise pattern transfers and is easier to operate.

2.1.4 *Diffusion*

When dopants[5] atoms need to be introduced into an InP wafer, dopants are allowed to selectively diffuse through the windows etched in an oxide masking layer. This step allows dopants to enter those areas of the semiconductor wafer surface that are not masked with SiO_2 or Si_3N_4, incorporating important electrical characteristics. Dopants are divided in two categories related to their charge: negative (N) and positive (P). N dopants include phosphorus, antimony and arsenic while P dopants include boron, gallium and aluminium. Diffusion is accomplished in a high temperature furnace, typically in the range of 900°C to 1200°C. The dopants are driven into the wafer by the heat from the furnace. The depth (and width) of the diffusion is controlled by the time the wafer remains in the furnace, and by the temperature of the furnace.

The goal of a diffusion process is the creation of a specific number (concentration) of dopants atoms at the wafer surface, and of N-P or P-N junction[6] at specific distance below the wafer surface.

2.1.5 *Metallization*

When the internal circuit within the wafer has been fabricated, it is necessary to make the appropriate interconnections between the various devices as well to link the devices to the outside world to send and receive information.

The wafer fabrication process is mainly comprised of three major steps. In the first step, the active and passive components are incorporated when the successive layers of the wafer are progressively added. The last step comprises a series of intermediate steps where the completed chip surface is covered with a protective or passivation layer. The step in between consists of a series of processes where one or more layers of a conducting metal are deposited on the wafer surface and a patterning process that leaves the circuit components electrically connected. These latter processes are called metallization.

---

[5] A substance, such as boron, added in small amounts to a pure semiconductor material to alter its conductive properties for use in transistors and diodes

[6] The interface at which the conductivity type of a material changes from P type to N type or vice versa.

There are three techniques that are commonly used to create electrical contacts: thin-film vacuum evaporation, sputtering and electroplating.

Vacuum Evaporation consists of placing a small charge of the metal to be deposited in a crucible and to heat this metal to generate vapour. Some of the vapour will accumulate as a thin film on the surface of the wafer. This operation occurs under very high vacuum.

Sputtering which has largely replaced vacuum evaporation in wafer fabrication consists of applying a high voltage across two parallel plates, in a vacuum chamber separated by 10 cm or less. One plate, called the target, is judiciously chosen to emit a high-energy ion flux that will migrate to the other plate on which the wafers are located. It is therefore possible to deposit thin films of various metals.

Electroplating consists of submerging the wafer into an electrolytic solution and using it as a cathode to deposit a thin film of a given metal.

2.2 Detailed Description of the Processing Steps Involved in the Fabrication of BHet Laser

Most semiconductor optoelectronic devices, other than silicon, InP photodetectors, and InP lasers, are made from Heterostructure. A Heterostructure is one that is made using more than one material. These materials are important because: the use of different materials allows to control the location of the electrons and holes in the devices, this being very critical for the functioning of the device; the different refractive indices of the different materials allow to make waveguides and mirror structures; the structures can be made to control the operating wavelength; and in advanced optoelectronic devices, the different materials allow to quantum-confine the electrons and holes in very thin layers, enabling quantum-mechanically engineered devices.

The following sequence presents the detailed fabrication steps of BH directly modulated laser. The purpose of each general process step is given, along with a short explanation. Finally, the inspection procedures required to determine acceptable completion of the step are described. Any wafer that does not meet the inspection criteria is noted and further processing of the wafer is stopped.

2.2.1 *Main Processing Steps Involved in the Fabrication of BHet Laser*

Laser is an acronym for **L**ight **A**mplification by **S**timulated **E**mission of **R**adiation. The first semiconductor laser was invented and demonstrated in 1962 (Kapon, 1999). The semiconductor laser is essentially a dielectric optical waveguide terminated by facets, or mirrors, to form a resonant cavity. As opposed to a **L**ight **E**mitted **D**evice (LED), whose output results from spontaneous emission, the output of a laser results from stimulated emission and is coherent.

When a wafer has completed the MOCVD (Metal Organic Chemical Vapour Deposition) growth process, some important variables need to be measured and must fall within some predetermined ranges for the wafer to be accepted and allowed to proceed further. Some of these variables are the: QWQB[7], Average PL[8] Wavelength, InP Peak doping levels, etc.

To successfully grow one crystalline material onto another, lattice constants need to be very closely matched, otherwise the epitaxial layer has a very large number of crystalline defects, which tends to significantly degrade device performance and can result in a catastrophic failure.

In the step of growing blocking layer, the doping level is a very important characteristic. Hydrides of group VI or IV elements (e.g., H_2S or SiH_4) are used for N-type doping. Metal organic compounds of group II elements (e.g., diethyl zinc) or group IV (carbon) from trimethyl gallium are used for P-type doping. Usually the elements of group III starts in the form of metal-organic compounds and elements of the group V are initially in the form of hydrides (e.g., triethyl gallium ($Ga(C_2H_5)_3$)).

The next step, one of the critical steps in manufacturing of BHet laser, is the Gain-Coupled Grating Fabrication or known in its short form as Grating. In this step, the active region is etched to form a grating with the characteristics of reflecting light of a specific wavelength back in the laser cavity with the objective of increasing the intensity of light.

---

[7] Quantum Well Quantum Barrier
[8] Photoluminescence

An important characteristic of the gratings is the depth. If the grating is too deep, due to excessive etching, the gain of the laser is affected. The grating period is also important because it ultimately determines the wavelength of the light, which is created inside the laser. The grating acts like a wavelength filter because it only reflects a very specific wavelength of light.

In a homojunction laser the active region is defined by the diffusion length of the minority carriers, whereas in a heterojunction laser the active region is defined by the heterojunction boundaries. The heterojunction also helps in confining the optical mode and forming a dielectric waveguide.

The grating overgrowth consists of InP only, a single point Photoluminescence spectroscopy (PL) measurement of the wavelength is taken, to monitor any effects the overgrowth had on the first growth wavelength. A PL intensity map is also required to monitor the spatial uniformity of the resulting intensity.

The last step in the growth steps is a final blanket overgrowth of BH laser (Figure 2.3) In this step, a special procedure must be observed during growth to ensure the incorporation of a sufficiently high concentration of Zn in the InGaAs contact layer. Growth layer is Zn-doped InP layer. When this layer is completed, the InGaAs contact layer is then grown. A single point X-ray technique is required to verify lattice matching of the InGaAs. A single point Photoluminescence spectroscopy (PL) measurement of wavelength is required to monitor any effects the overgrowth had on the first growth wavelength.

Upon acceptance at the end of the MOCVD process the wafer goes to a chemical plasma vapour deposition (PECVD) step where silicon dioxide or silicon nitride is deposited. The purpose of this step is to prepare the surface of the wafer which will be used as the etch mask for defining the ridge. Dielectric is a material that conducts no current when it has a voltage across it. At the completion of this step, the wafer should be free of haze and visible streaks, and differences in thickness of dielectric are recorded. The thickness uniformity of the SiO_2 must be better than 6% ((max-min) / (2 *average)). If the deposited SiO_2 fails to meet the acceptance criteria, it must be stripped in B-HF (Buffer Hydrofluoric acid) and this step must be repeated.

When dielectric is deposited and the thickness measurement meets the specifications, the wafer is sent to the ridge lithography. Ridge lithography defines the laser ridge. The ridge must be aligned perpendicular to the major flat of the wafer. The critical dimension measurement (CD) of the ridge is useful information in assessing the width of the patterned photo resist ridges. If the ridges are poorly defined or cannot be adjusted to meet the ridge width criteria across the wafer, rework has to be done.

Once the ridge mask pattern is transferred into the oxide, the rest of the oxide has to be removed in a dry etch process (Figure 2.2). The dry etch process, called Reactive Ion Etching[9] (RIE), uses a mixture of CF_4/H_2. This step includes the initial O_2 descum[10] if desired, to achieve the required ridge width. This step can be separated from the CF_4/H_2 etch to allow for careful adjustment of the ridge width before etching the SiO_2. SiO_2 should be completely removed in unmasked areas. If some SiO_2 remains, RIE must be repeated until the SiO_2 is completely removed in unmasked areas. With the CF_4/H_2 in RIE, 20 % over etch is allowed. When SiO_2 is completely removed from unmasked areas, the next step is to remove the remaining photoresist which covers masked areas to protect it from etch process and repeated Critical Dimension (CD) measurement is required. Critical dimensions describe the widths of the lines and spaces of critical circuit patterns as well as the area of contacts. After recording a width of the ridge, one more etch remains, but this time the ridge is etched into epitaxial InGaAs and InP grown semiconductor layers. The InGaAs capping layer and InP buffer layer are etched to a certain depth. When the ridge etch is completed, using a wet etch chemistry, which selectively removes the remaining InP and stops at the etch stop layer, the etch depth has to be measured using a Dektak (ridge high measurement instrument) and the depth has to be recorded. The etch depth should be ± 0.2 μm. Etch depths of 0.7–1.6 μm are acceptable but values outside this limit indicate a potential problem with the etch process and should be examined carefully.

When the wafer has completed the etch process and meets all requirements for continuing the process, the wafer goes back for a Silicon Dioxide and Nitride Deposition. Silicon dioxide and nitride are deposited over the ridge structure to provide electrical isolation of P-contact and to provide optical confinement for the ridge wave-guide. At the

[9] Etching process that combines plasma and ion beam for removal of the surface layer.
[10] Removing a scum and residue after

completion of this step, the wafer should be free of haze and visible streaks. The thickness uniformity of the SiO_2 and silicon Nitride must be better than 6%. If the deposit silicon dioxide or nitride fails to meet the acceptance criteria, the procedure must be repeated.

After the deposition of a silicon dioxide and nitride layer, the wafer is ready for the next lithography step, called ridge via[11] lithography. This process step defines the via pattern that will be used to open the contact to the top of the ridge. The PMGI[12] coating should look uniform and no photoresist should remain on top of the ridge. If more than 15% of the wafer does not meet these criteria rework is required.

The wafer is now ready for a last etch step in the fabrication of BHet laser, called Ridge Via Etch. This process step removes both the silicon nitride and the silicon dioxide from the top of the ridge before P-metal deposition. Inspections of ridge areas are required to determine if the silicon nitride and silicon dioxide have been completely removed. At this step it is very important to record the position of any areas on the wafer where dielectric remains on the top of the ridge.

Finally the wafer arrives for last lithography step, called Bilayer[13] (PMMG and PMGI) Lithography: P-contact. This process step provides the pattern for the P-contact metallization. After P-contact lithography, the wafer goes for a P-metal deposition on top of the bilayer lithography and it is then patterned by dissolving the photoresist/PMMA, and lifting off a portion of the metal. The deposited P-metal (usually is a TiPtAu) should look uniform and smooth. Metal coverage of the ridge sidewalls is important for acceptable device performance. This deposition process must be monitored periodically to ensure that sidewalls coverage is > 1200 Å (> 40% of top metal thickness). The excess metal is then lifted off and the contact is annealed[14].The patterned P-contact metal is used in order to reduce the capacitance of the device.

---

[11] device contact, via means opening

[12] Polymethylglutarimide (PMGI) is a positive resist with very unique material and performance properties

[13] Polymethyl methacrylate PMMA positive resists, designed to provide high contrast, high resolution in lithographic processes. PMMA is often used as a protective layer in III-V device wafer thinning applications.

[14] A high temperature processing step

After the P-metal deposition, the wafer is ready for lap[15] and polish. Wafer is thinned to promote uniform cleaving with smooth facets. Wafer is lapped to a thickness ±20 μm and polished to a final thickness of ±15 μm. The final thickness of the wafer has to be recorded.

The very last step in the fabrication of BH laser is the deposition of N-metal on the back of the wafer. The thickness of the N-metal is measured using Dektak instrument. The wafer is ready for scribing[16] and cleaving into individual bars.

The minimum quantity of bars required from each quarter for Wafer Verification is 3. After the bars are cut into individual chips, some chips usually chosen at random are used for further testing, including some chips that will be submitted to "life-test". In a life test, conditions to which the chips will be exposed are selected in order to accelerate the failure mechanisms. These latter tests usually use elevated temperature, humidity, voltage, pressure, vibration, and a combination of these conditions. Figure 2.4 presents an overall overview of Fabrication, Testing and Packaging of the Si device.

In this thesis the specific focus will be only on the test data from the Wafer Verification testing (Appendix F).

Table 2.-1 provides a summary of the main process steps with their associated measurements taken during the manufacturing process.

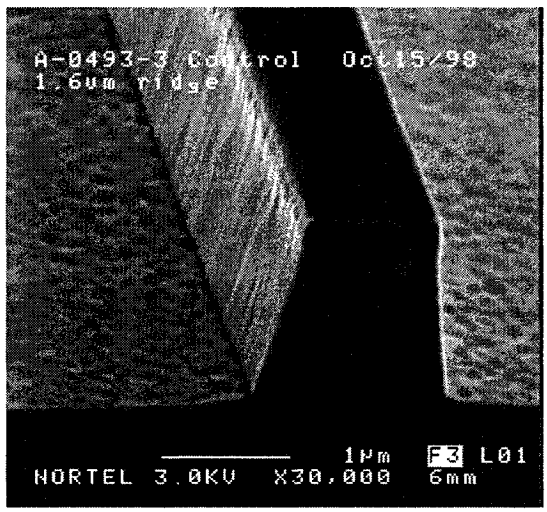

Figure 2.2 SEM images which represents the process step the Ridge definition

[15] Thinning wafer

[16] Means lines are used to separate die on the wafer. The wafer will be cleaved along the scribe lines into chips.

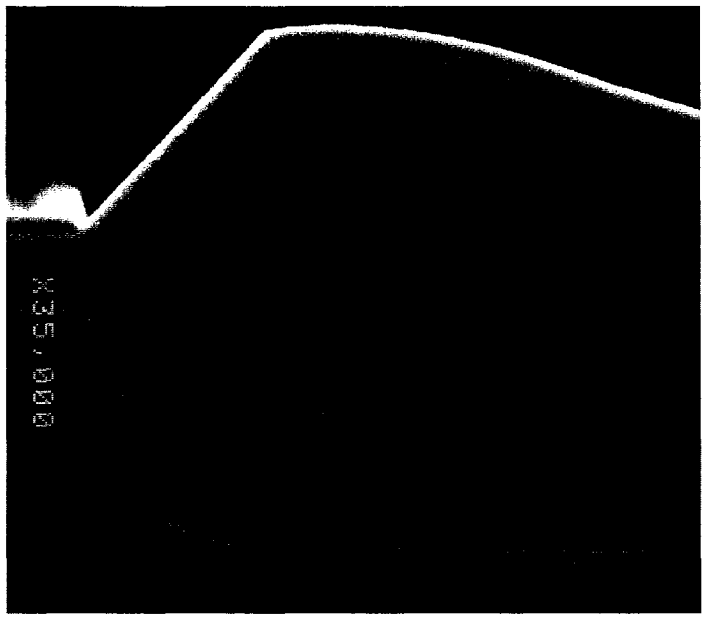

Figure 2.3 Overgrowth of Blocking layer

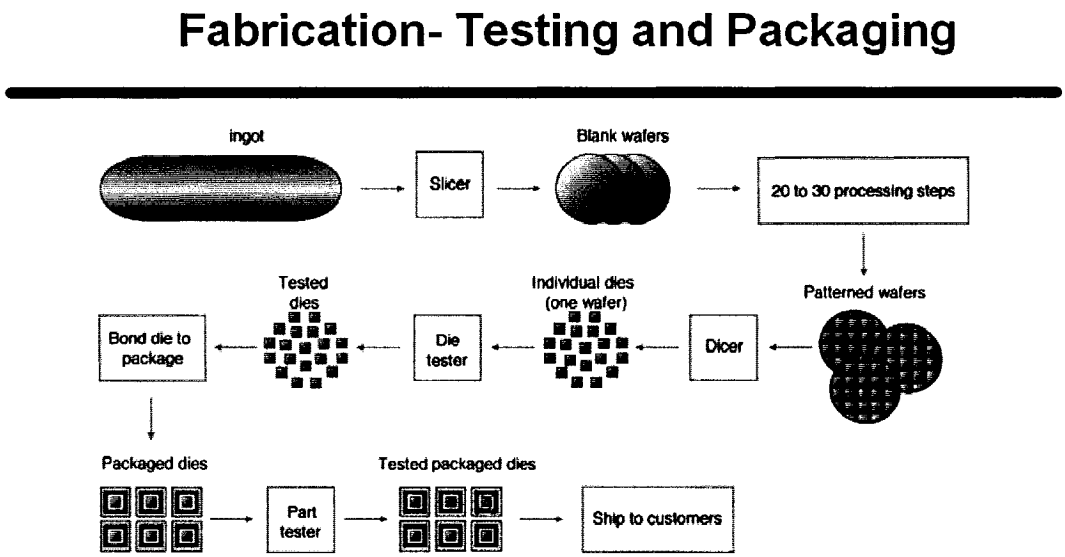

Figure Source: D. Patterson and J. Hennessey, *Computer Organization and Design*, Morgan Kafumann, 1996

Figure 2.4 General overview of Fabrication, Testing and Packaging of Si Device

Table 2-1 Summary of the main process steps and their measurements

Process Step	Description	Collected Data
Wafer First Growth MOCVD	**Grow active laser layers onto wafer substrate**	**Lasing Wavelength**
Grating Lithography	**Create Grating resist pattern**	**Grating pitch**
Grating Semiconductor Etch	**Transfer Grating pattern into top grown layers of wafer**	**Grating depth**
MOCVD Over Growth	**Overgrow Grating with InP layers**	**Intensity and pick Wavelength**
Ridge Dielectric Deposition	Ridge dielectric etch mask	Thickness, Uniformity
Ridge Lithography	Create resist ridge pattern on top of mask	Resist Ridge Width, Uniformity
Ridge Dielectric Mask Etch	Using resist pattern, etch dielectric to create hard mask	Dielectric Ridge Width, Uniformity
Ridge Semiconductor Etch	Using hard mask pattern, etch InP material to create ridge	Ridge Height, Uniformity
Ridge Selective Area lithography	Create resist ridge pattern on top of ridge Only	Visual Inspection
Ridge Dielectric Mask Etch	Using resist pattern, etch dielectric to leave hard mask	Visual Inspection
Selective PnP MOCVD Overgrowth	**Selectively grow PNP blocking layer**	**Inspection**
Final InP MOCVD Overgrowth	**Grow Final InP/InGaAs contact layer**	**Inspection**

Process Step	Description	Collected Data
Wide Ridge Dielectric Deposition	Device Ridge dielectric etch mask	Thickness, Uniformity
Wide Ridge Lithography	Create resist ridge pattern on top of mask	Visual Inspection
Wide Ridge Dielectric Mask Etch	Using resist pattern, etch dielectric to create hard mask	Visual Inspection
Wide Ridge Semiconductor Etch	Using hard mask pattern, etch InP material to create Device ridge	Ridge Height, Uniformity
Ridge Clad Dielectric Deposition	Ridge contact insulation layer	Thickness, Uniformity
P-Contact Via Lithography	Create resist pattern on top of dielectric	Visual Inspection
P-Contact Via Dielectric Mask Etch	Using resist pattern, etch dielectric to create contact Via hole	Visual Inspection
P-Metal Lithography	Create resist pattern on top of dielectric	Resist Thickness, Uniformity
P-Metal Deposition	Deposit device P-Metal contact	Thickness, Contact Resistance
EP-Metal Lithography	Create Electro-Plate resist pattern	Visual Inspection
EP-Metal Deposition	Deposit Thick Electro-plated Metal on top of P-Metal	Visual Inspection
Lap & Polish	Reduce wafer thickness to enable bar cleave at Facet Coat	Thickness, Uniformity
N-Metal Deposition	Deposit device Back side N-Metal contact	Thickness
Bar Cleave	Cleave wafer into bars for Facet Coat	Visual Inspection
Ar & Hr Facet Coating	Coat the front and back of bars	AR & HR Reflectance

CHAPTER 3

BUILDING THE DATA BASE

3.0 INRODUCTION

In order to meet the objectives of this thesis, reliable historical data had to be extracted from the process records. This chapter describes the database systems used at Nortel and the approach developed to assemble the data required for this work. Although it was initially thought that this would be a simple task, almost nine months were spent creating the final database.

Recall that the four main processing areas involved in manufacturing this device were:

- GROWTH: In this area, high quality epitaxial active layers are put down on the wafer.(Table 2-1 in blue colour)
- GRATING: In this area, the grating responsible for locking the laser to a specific wavelength is created through a series of microlithographic procedures.(Table 2-1 in orange colour)
- WAFER FAB: In this area, the remaining processing steps are performed to make the final device structure. (Table 2-1 in black colour)
- WAFER VERIFICATION (WaVe): In this area, the wafer is broken into individual devices, which are mounted and performance tested (known as TEST).

Unfortunately, each of the four processing areas used different database systems for control and data storage, each on a different server. In addition, the method of collection had evolved over the time span of interest, leaving data scattered over different databases. Moreover, different wafer identifiers were used in each area with no link between them. Very often missing information had to be filled in manually, which was a very time consuming task.

3.1 Product Identification

The fabrication of wafers for the BH laser device is a very complex process. To ensure that the correct processing steps are carried out in the right order using the correct operating conditions (recipe), a computerized system is used to control the process flow and recipe selection, as well as data collection for all wafers. This system is called "**PROMIS**", the **PR**oduction **O**peration **M**anagement **I**nformation **S**ystem. The current identification procedure for any product, including the BHet, will now be described.

3.1.1 The current identification procedure for BHet

There is a unique number that is physically laser-scribed onto the back of each wafer by the wafer substrate manufacturer (e.g., 123467.007). The form of this number varies from company to company, but always identifies the boule number and the wafer number in that boule. (InP wafers are grown as a sausage shaped crystal (boule) that is sliced into wafers, much like salami.) This number is known as the COMPID; COMPID stands for Component Identification.

A PROMIS LOTID (e.g., 3G19846.1) is assigned to a wafer as it leaves the pre-manufacturing stock room. Along with the LOTID, each lot is assigned a PARTID, which identifies the process flow (the sequence of process steps and recipes to be followed). A label with the LOTID, PARTID and COMPID is placed on the outside of the box containing the wafers (up to eight) making up the lot (or batch). The same information is contained in a bar code on the label to facilitate tracking. This label is used to identify and track the lot throughout the process. The LOTID is used by all four process areas. This is where the Holy Grail of wafer identification is found; in reality, it has been evolving during the last three years, with different numbers used in the four different process areas.

The processing of each lot is controlled by tracking it into and out of each piece of equipment in the process. PROMIS does not allow a lot to be tracked into the wrong piece of equipment, nor does it allow the process flow to continue when data are missing

or the entered data constitute an out-of-control signal in the database. PROMIS stores all processing information: the time when a lot was tracked in, which operator tracked it in, into which piece of equipment the lot was tracked, the actual operating conditions and product specifications related to the current stage of processing.

Sometimes, a mistake occurs while a batch is being processed. When this happens, the operator has to reprocess the batch in what is called a rework loop. PROMIS captures all of the processing steps that were carried out on each batch for a particular processing level. This processing sequence can be used to screen out batches that have been reworked. This does not significantly affect the size of the database because the number of reworked batches is low in the InP manufacturing process.

At any point in the process, an entire lot may be completely scrapped and sent for waste treatment. This happens whenever all the wafers within a lot do not meet requirements and cannot be recovered through rework. These lots are referred to as scrap lots. However, it is sometimes possible to recover a lot or, at least, some of the wafers within it that could meet standards through rework. In such cases, the lot is split into two or more lots: a parent lot and one or more split lots. Usually, these split lots do not emerge from the entire process at the same time. The delay between the emergence of the parent lot and the emergence of the split lots can be several weeks. This happens whenever the split is stocked for further design or new tests. Consequently, the data for split lots are spread over "islands of data" in PROMIS. Moreover, a link between parent and split lots does not exist. This problem with split lots was a source of frustration in extracting the data required for this work. The same problem commonly has arisen when customer complaints are filed on a single chip that was sold, for example, three months ago. It was then very difficult to diagnose the source of the problem. Information about when processing occurred, which recipe, process, and equipment were used could not be extracted. The procedure for extracting the required data will now be described.

3.2 Data Extraction and Sorting

The purpose of this section is to provide an overview of the database system and the difficulties encountered in extracting the data required for this study. Finding a common

link between databases, identifying and removing rogue entries and creating a usable data structure took the author over one year of effort.

The biggest problem in the extraction of the data was matching the results from **D**ata **C**ollection **O**perational **P**rocedures **(DCOPs)** at each step in the process with the correct WAFERID. This was due to a number of factors:

- different databases
- different tracking numbers (WAFERID)
- different data entry protocols.

The data used for this project, covered BHet production for the period January, 2000 to January, 2001. During this time, the methods used and the types of data collected evolved. At the start of the period, data for the original wafers were stored in FilemakerPro databases in all four processing areas. Then, Wafer Fab changed from the FilemakerPro database to a PROMIS database. Shortly after, Growth and Grating also moved to a PROMIS database, but used a different PROMIS tracking number. The evolution of the data collection systems can be classified into four distinct structures and is summarized in Table 3.1.

Table 3-1 Evolution of the Data Collection System

Evolution of the data collection system										
Structure	**Growth**				**Grating**		**Wafer Fab**		**Test**	
	Serial Number	**Wafer Number**	**First Growth Nunber**	**Database**	**Tracking Number**	**Database**	**Tracking Number**	**Database**	**First Growth Number**	**Database**
1	G068090	62986.03	A-3206-4	**FILEMAKER PRO**	A-3206-4	**FILEMAKER PRO**	A-3206-4	**FILEMAKER PRO**	A-3206-4	**FILEMAKER PRO**
2	G068090	62986.03	A-3206-4	**FILEMAKER PRO**	A-3206-4	**FILEMAKER PRO**	80140016.1	**PROMIS**	A-3206-4	**FILEMAKER PRO**
3	PROMIS 3G19846.1	62986.03	A-3206-4	**FILEMAKER PRO**	PROMIS "3G"	**FILEMAKER PRO**	80140016.1	**PROMIS**	A-3206-4	**FILEMAKER PRO**
4	PROMIS 3G19846.1	62986.03	A-3206-4	**PROMIS**	PROMIS "3G"	**PROMIS**	PROMIS "3G"	**PROMIS**	A-3206-4	**FILEMAKER PRO**

Structure 1

The first row of Table 3.1 shows the original wafer identification system based on the FilemakerPro database. A FilemakerPro auto-generated serial number (e.g., "**G068090**") was assigned in Growth and is entered in the first column, labelled 'Serial Number'. The COMPID is provided in the second column. When the processing steps in Growth were completed, the first growth number (e.g., A-3206-4, indicating the fourth wafer of run 3206 in reactor A) was added. This number is of particular value since wafers from the same growth run have very similar device performance and wafers from the same growth run are used as health checks for the other process areas. This number was then used to track wafers through Grating, Wafer Fab and WaVe (Test).

Structure 2

In the second structure, Wafer Fab implemented a new tracking number (e.g., 80140016.1, representing the first wafer of batch 80140016) and switched to using the PROMIS database. Growth, Grating and Test continued to use FilemakerPro and the First Growth Number for tracking.

Structure 3

In the third structure, Growth changed from a FilemakerPro serial number (e.g., **G068090**) to a PROMIS number (e.g., **3G19846.**1) to be used along with the first growth number. Grating also switched to using the PROMIS number. Both Growth and Grating, along with WaVe, continued to use FilemakerPro as their database. Wafer Fab continued using the tracking number (e.g., 80140016.1) and the PROMIS database.

Structure 4

The fourth and final structure saw use of the PROMIS tracking number (e.g., **3G19846.1**) in Growth, Grating and Wafer Fab, with all three areas using the PROMIS database. On the other hand, the Test area still used FilemakerPro as their database system and the first growth number as their tracking number.

As mentioned in Chapter 2, after processing in Wafer Fab, the wafer is sent to WaVe. Unlike typical silicon semiconductor devices, which can be tested cost-effectively on the wafer, many InP devices can only be 'fully' tested once the individual die or chip is bonded to a heat sink. A minimum of three bars was taken from each quarter for testing. The bars were cut into chips and a minimum of 60 chips were randomly selected

for further testing. Altogether 100-200 chips were tested and the test results had to be linked to the original wafer. Difficulties in finding this link will be later described.

To compile a single overall database for analysis, data had to be extracted from all the individual databases and matched by a single identifying wafer number. The number used in WaVe, called "WAFERID", is the first growth number (e.g., A-3206-4). Data were extracted in seven steps. These steps are described in the following sections.

3.2.1 Step One

Extraction of the data started at WaVe by using the SQL language to look for the performance measurements associated with specific first growth numbers (e.g., A-3206-4).

Table 3.2 shows an example of the output table from the SQL script that was developed to extract test data. The first column is the WAFERID, which consisted of the first growth number. Some test data for each WAFERID are listed in the subsequent columns.

3.2.2 Step Two

The next step was the extraction of data from the Wafer Fab PROMIS database. PROMIS is a very extraction-unfriendly propriety database; in fact, Nortel had already done work to copy the data from PROMIS to an industry-standard Oracle database. Business Objects software was used to extract data from this Oracle database. Firstly, all DCOP data were extracted by DCOP and PROMIS LOTID (e.g., 80140016.1). This was done by selecting the BHet PARTID and then extracting all pertinent DCOPs and LOTIDs. The main mass of data was extracted by this method. In case of some split lots individual DCOP blocks of data were extracted using the extraction tools built into PROMIS. These tools allow data to be extracted one DCOP at a time. This was very useful when there was missing data from the database or when some DCOP changed over the period of interest.

Figure 3.1 is an example of output as seen on the monitor during the PROMIS extraction followed with detailed explanation below.

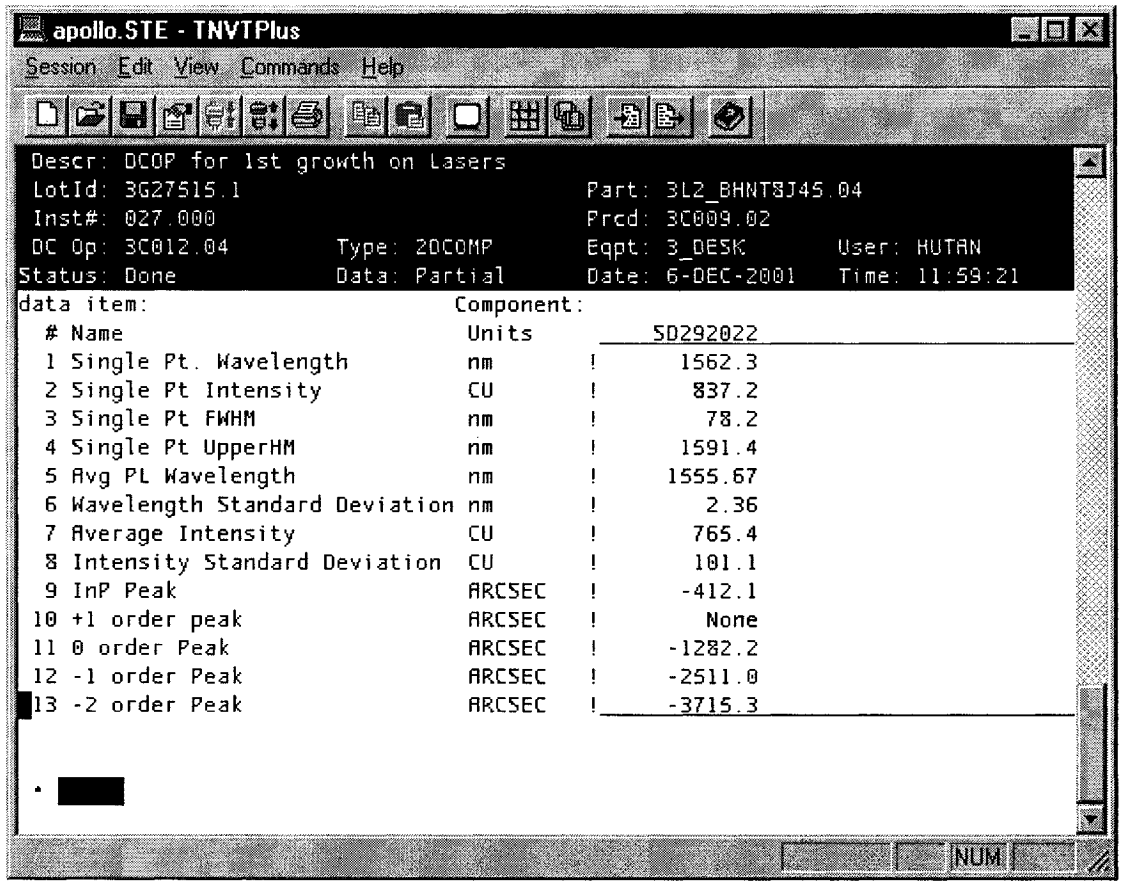

Figure 3.1 PROMIS data extraction output seen on the monitor during extraction

Descr: DCOP	Description (name) of the DCOP
LotId 3G20231.1	Contains lot identification used to track the lot throughout the manufacturing process
Part: 3L2_BHNT8J45.04	Refers to product type which means L-band BHet laser
Inst#: 001.000	The instruction Number in the Recipe.
Prcd: 3C014.04	The Procedure Number
DC Op: 3C016.01	The identification number of the DCOP.
Type: 2DCOMP	The type of DCOP
Eqpt: 3A_RCTOR	Equipment used during this collection.
User: HUTAN	Name of the operator who processed and finished this step
Status: Done	Shows that this processing step is finished and it is ready for the next step
Date: 5-NOV-2001	Date and time when data were entered
Time: 14:36:46	

Table 3-2 Typical Segment of the EXCEL Output File Following SQL Data Extraction

1	2	3	4	5	10	12	13	14
WAFERID	**ITH2L**	**REAR POWER**	**I_5MW**	**EFF_M2**	**VF_10MW**	**PKWL_ITHX**	**SMSR_5MW**	**SBAND_5MW**
A-2931-2	9.934	2.905	33.646	0.222	0.952	1581.55469	34.556	2.928
A-3255-8	8.642	2.342	29.508	0.256	0.929	1537.88231	40.290	3.060
A-3311-2	7.773	2.210	30.034	0.246	0.941	1541.51206	46.208	77.948
A-3327-5	9.429	2.122	33.149	0.229	0.926	1530.41837	45.245	3.260
A-3346-2	8.428	2.320	29.944	0.252	0.918	1547.70949	42.783	3.498
A-3346-4	9.538	2.069	29.975	0.259	0.938	1548.89796	42.338	3.055
A-3346-5	8.865	2.733	31.986	0.246	0.950	1541.491	46.685	3.516
A-3346-6	9.394	2.185	30.677	0.253	0.905	1546.29064	44.869	3.319
A-3347-4	9.157	2.297	29.902	0.253	0.899	1548.39277	38.184	3.070
A-3350-4	11.829	2.284	30.163	0.288	0.923	1549.84868	35.684	2.098
A-3352-2	8.066	2.102	29.148	0.248	0.960	1541.384	42.753	3.144
A-3353-2	8.691	2.951	29.428	0.264	0.921	1532.13784	43.308	3.131
A-3353-3	7.553	2.214	28.192	0.259	0.916	1533.58541	46.930	3.839
A-3355-6	8.109	2.373	31.112	0.234	0.970	1530.47075	50.665	4.281
A-3356-4	9.679	2.216	31.119	0.250	0.935	1532.7047	44.524	3.243
A-3357-4	7.836	2.112	29.195	0.249	0.925	1525.79935	41.879	2.942
A-3357-8	7.086	1.878	27.670	0.260	0.900	1532.46112	45.673	3.626

3.2.3 Step Three

The next step in collecting the information for this project was to extract data from the two Growth databases. This started with the input data from the original FilemakerPro database, and then the remaining data were extracted from the PROMIS Growth database by LOTID and COMPID, using the Business Objects software from that copied Oracle database.

3.2.4 Step Four

After step three, the Grating data were extracted from FilemakerPro and PROMIS databases by using COMPID and LOTID.

3.2.5 Step Five

All extracted data from the Growth, Fab and Grating databases were first stored as text files. These text files from each area were then read into separate EXCEL files. The Test data were extracted directly into the first EXCEL sheet.

3.2.6 Step Six

Data from the three EXCEL files (Growth, Grating, Fab) were merged into one large file and then merged with the test data file, to create a single data table for data analysis. The biggest problem was finding a link in the wafer data between each EXCEL file, with no connecting field. The only physical number was the COMPID, but, unfortunately, it was not used in the Grating and Test areas, it was available in Growth and Fab but not tracked into PROMIS or FilemakerPro.

A solution was reached, whereby the COMPID was extracted from Oracle database and added to all four EXCEL tables. The EXCEL VLOOKUP feature allows data in one table to be compared with data in a second table and the matching data to be added to the first table. For example, LOTID is matched and COMPID was added to Tables 1 and 2. The first step was to add a blank COMPID column to the Fab and Growth table and then the COMPID and LOTID were extracted from the Fab and Growth databases into a separate file. Matching the LOTID in the new file to the LOTID in the Fab and Growth tables, the COMPID was added to the Fab and Growth table using the VLOOKUP feature. Now the Growth table contained the LOTID, COMPID, and first growth number. The COMPID was added to the Test data table by matching the first growth number from the Growth table. As a final step, the COMPID was added to the Grating table by matching with the LOTID from the Fab data table. Now four separate tables were created, all with COMPID. Then a master EXCEL table was created and all data from each table were added to the master table, one data field at a time by using EXCEL VLOOKUP.

When the final table was created, it became apparent that there were many missing values Individual wafers had to be manually searched for the missing data from all databases. These wafers were ones that had been split from the main process batch or for which collection flow changed during process life cycle. Table 3.3 shows a sample of

the EXCEL sheet that was developed to merge the Growth, Grating, Fab, and Test data. The first column contains the LOTID from Wafer Fab, followed in the second column with COMPID. The third column contains the WAFERID, which refers to the first Growth number, other columns contain output measurements from the Test and some input measurements from Growth and Fab.

3.2.7 Step Seven

Another difficulty was data-inconsistency arising from changes in the units of test values and different DCOPs between databases and over time. The same set of data, extracted from multiple database systems using different data formats, appeared to be data for a different variable. After compiling the data for analysis, this resulted in gaps along with multiple names for the same data. Dealing with this was a most time-consuming part of the data gathering process!

The use of different units for the same variable was not identified until exploratory data analysis was undertaken. In such cases, the magnitudes of the variables fell into different categories depending upon the units reported. This clustering showed up clearly as potentially abnormal behaviour in several plots (e.g., scatter plots, histograms). Once identified, resident engineers confirmed that this was due to a difference in the DCOP. Moreover, data for every variable were then examined for this type of problem.

The occurrence of apparently incomplete data sets, resulting from changes in DCOPs (with different names) over time or split lots or equipment changes, was indicated by gaps in the data sets associated with the common DCOPs. Data identified by one DCOP resulted in a gap in the same data set for the other DCOP. This required a manual search for the DCOP containing the missing data. Once found, the VLOOKUP feature was used to combine the results.

Table 3-3 PROMIS Data Extraction Output

LOTID (wafer from Fab)	COMPID	WAFERID	ITH2L	EFF_M2	REAR POWER	3C012.04, DCOP for 1st growth on Lasers,Avg PL Wavelength	3C012.04, DCOP for 1st growth on Lasers, InP Peak	pitch calculation	8GBH3 Enter Lasing WaveLength	8GBH1.01, Enter GRATING PERIOD (nm):	8GBH1.01, Enter EXPOSURE TIME (sec):	8GBH3., Enter GRATING DEPTH for BH from SRS mapper.	8MM13.04, Enter thickness measure. for each wafer (1000A SiO2)	8M008.03, and 8M197.01 Enter data for ridge litho CDs, measur.	8M007.03, Enter the ridge heights for each wafer	8M263.01, Enter EP-Metal thickness for all wafers. (13000A)
3G19846.1	S8384059	A-2931-2	9.934	0.222	2.905	1002.9	1540.40	238.0	1517	237.96	187	655.7	1004.61	2.04	2.99	11395.83
3G20627.1	SA571018	A-3255-8	8.642	0.256	2.342	1031.2	1556.97	0.0	1556.97	241.64	372	683.5	991.59	2.06	2.89	10608.58
3G15650.1	SA087091	A-3311-2	7.773	0.246	2.210	806.1	1563.59	0.0	1563.59	242.32	453	702.7	2059.86	2.06	2.84	10640.89
3G11596.1	63651.022	A-3327-5	9.429	0.229	2.122	958.3	1602.61	248.1	1579.52	248.13	187	0	970.4	1.69	2.76	10534.41
3G14728.1	SA008005	A-3346-2	8.428	0.252	2.320	1070.6	1566.63	243.2	1548.51	243.22	573	625	988.5	2.07	3.01	10240
3G14729.1	SA008003	A-3346-4	9.538	0.259	2.069	1058.2	1567.86	243.2	1548.51	243.4	577	635.74	980.9	2.08	2.65	11394.67
3G14730.1	SA008002	A-3346-5	8.865	0.246	2.733	1059.2	1563.73	242.2	1542.14	242.21	578	719	903.5	2.06	3.03	11594.29
3G14731.1	S9746011	A-3346-6	9.394	0.253	2.185	1174.0	1564.78	243.0	1546.92	242.99	557	60.5	1025.7	2.06	2.76	13790.5
3G14717.1	SA086049	A-3347-4	9.157	0.253	2.297	1005.4	1566.68	243.2	1548.51	243.4	577	638.6	1025.7	2.06	2.76	13790.5
3G14736.1	S9746017	A-3350-4	11.829	0.288	2.284	1162.6	1574.08	243.9	1552.52	243.88	468	594.3	990.64	2.04	3.12	10096.8
3G14764.1	S6665013	A-3352-2	8.066	0.248	2.102	1120.1	1563.70	242.2	1542.14	242.21	578	722	903.5	2.06	3.03	11471.58
3G17038.1	SA175008	A-3353-2	8.691	0.264	2.951	1177.6	1552.55	0.0	1552.55	240.62	453	707.5	965.17	1.97	2.68	10902
3G17049.1	SA175027	A-3353-3	7.553	0.259	2.214	1134.4	1553.67	0.0	1553.67	240.8	453	714.2	991.59	2.06	2.89	10608.58
3G17051.1	S9746003	A-3355-6	8.109	0.234	2.373	1207.2	1554.04	0.0	1554.04	240.8	453	727.6	993.82	1.92	2.91	11322.61
3G15654.1	SA316029	A-3356-4	9.679	0.250	2.216	1288.1	1554.30	0.0	1554.3	240.92	453	722.6	993.82	1.92	2.91	11322.61
3G11595.1	SA748012	A-3357-4	7.836	0.249	2.112	1222.9	1546.29	239.7	1527.99	239.69	153	0.82	984.56	2.04	3.08	11570.87
3G17040.1	SA086013	A-3357-8	7.086	0.260	1.878	1263.2	1551.95	0.0	1551.95	240.62	453	731.2	974.33	2.01	3.52	13074
3G14775.1	SA316017	A-3365-1	7.657	0.248	2.604	927.5	1560.58	241.6	1538.19	241.65	575	688	1027.9	2.07	3.45	10916.47
3G14784.1	SA740017	A-3366-5	8.709	0.232	2.253	1057.7	1559.17	241.5	1537.4	241.51	573	614	1025.7	2.06	2.76	13790.5
3G14785.1	SA748015	A-3366-6	6.722	0.236	2.173	862.0	1561.01	241.6	1538.19	241.65	575	722	1027.9	2.07	3.45	10916.47
3G14796.1	SA739084	A-3370-1	8.632	0.247	2.178	1094.4	1563.79	242.2	1542.14	242.21	578	728	903.5	2.06	3.03	11594.29
3G14835.1	SA567009	A-3373-8	9.394	0.235	2.393	1012.4	1590.06	246.4	1568.77	246.43	481	723.4	2059.86	2.06	2.84	10640.89
3G14818.1	SA743022	A-3376-7	9.960	0.250	2.929	1199.1	1566.78	243.2	1548.51	243.4	573	619	1028.19	2.07	3.06	12470
3G11632.1	63659.063	A-3425-4	12.676	0.214	2.106	568.6	1598.89	247.7	1577.03	247.75	188	657.7	970.4	1.69	2.76	10534.41
3G11600.1	64224.026	A-3426-4	11.574	0.243	2.300	639.0	1602.31	248.1	1579.52	248.13	187	671.7	0	0	2.9	10484
3G11702.1	64220.015	A-3427-2	13.743	0.233	1.988	641.1	1609.65	249.8	1590.41	249.87	187	737.6	985.43	2.05	2.74	12527
3G11703.1	64220.014	A-3427-3	10.738	0.229	2.257	628.8	1609.67	249.8	1590.41	249.87	187	739.9	0	0	3.4	12156
3G11705.1	64322.012	A-3427-5	10.712	0.234	2.345	638.2	1608.95	249.7	1589.57	249.69	187	727	970	1.7	2.71	27093.39
3G11708.1	64239.02	A-3427-8	13.330	0.244	2.883	689.1	1606.27	249.4	1587.88	249.48	185	650.7	1010.5	2.06	2.96	2823.71
3G11621.1	64322.013	A-3428-1	12.989	0.245	2.401	571.0	1618.49	251.2	1598.89	251.14	212	627.8	1040.16	2.07	2.81	5235.37
3G11612.1	64322.025	A-3429-8	11.622	0.229	3.368	580.8	1620.64	252.4	1601.46	252.36	170	0	972.93	1.8033	2.68	10706.27
3G11613.1	64239.018	A-3430-1	13.241	0.228	2.191	682.1	1622.42	252.1	1604.88	252.09	186	218.4	967.64	1.89	2.87	11160
3G11652.1	64191.014	A-3431-8	12.409	0.235	2.353	651.3	1622.41	251.8	1603.17	251.83	183	230.6	972.93	1.8	2.68	10706.27
3G11653.1	63659.005	A-3434-1	8.593	0.252	2.086	914.1	1570.57	243.6	1550.92	243.63	575	676	964.18	1.94	2.67	12196
3G11671.1	63659.069	A-3437-5	9.912	0.237	3.021	908.2	1566.54	243.1	1547.72	243.11	195	652	1010.5	2.06	2.96	2823.71

3.3 CONCLUSIONS

Several process characterization projects involving extraction of large sets of historical data had previously been attempted at Nortel, but all were severely hampered by an inability to extract reliable data in a timely fashion. The conclusions from this study listed below offer some useful insight into the nature of this problem and how it might be overcome. The results of our data extraction experience have potential industrial benefit for two aspects of process improvement: 1) improving the efficiency of future data extraction tasks and 2) improving the design of new data base systems. The specific conclusions are presented below as they would pertain to these areas.

Concerning improvement of the efficiency of data extraction tasks:

- A seven step-data extraction and sorting procedure was developed which allowed the desired data to be extracted and assembled in an easy-to-use EXCEL spreadsheet format. This procedure allowed the use of effective SQL scripts and Business Objects for the manipulation of the Oracle data bases and the VLOOKUP feature of EXCEL for assembling the final data base.

Concerning the design of a new data base system:

- Create a single, easy-to-use data base system that is accessible to a large group of people, with varying degrees of skills and needs. All of the users should be allowed access to only the data they need and have the training and tools to do so. This is paramount for optimal use of the data and for enhancing opportunities for process improvement.

CHAPTER 4

EXPLORATORY DATA ANALYSIS

4.0 INTRODUCTION

Once the available data for BHet processing from all four processes were assembled into a usable EXCEL spreadsheet, an initial exploratory analysis was performed to characterize the input and output variables in terms of their location (mean/median values), dispersion (range/standard deviation), distribution (histogram) and systematic relationships between variables (correlation). Due to the large number of input and output variables, it was necessary to attempt reducing the dimensionality of the problem to correspond to the actual information available in the historical data set. Of particular interest was the identification of major nonconformities in the BHet product, those input variables (i.e., product characteristics measured during the fabrication process) for which the data displayed highest correlation with critical product quality variables and any strong correlations between the input variables themselves and also between the output variables themselves. With this done, predictive modeling could be focused on the primary problems encountered in production using inputs providing greatest potential for early forecasting of product failure.

Standard exploratory data analysis tools (e.g., Montgomery (2001)) were used to carry out this preliminary analysis, including box plots, histograms, scatter plots, correlation matrices and Pareto diagrams.

4.1 Nature of the Data Set

The fabrication of the BHet laser device and the extraction of process and product quality data have been described in Chapters 2 and 3. Recall that the standard sampling protocol for testing the product involved taking three bars (consisting of 60 chips) from each quarter resulting in 240 being tested. In some instances this number would vary as a result of broken or defective parts of a wafer or the need for special testing requirements. The size of the resulting database was very large, consisting of 20 220 rows (chips) from 158 wafers along with 59 columns made up of 13 output (product quality) variables and 46 input (device characteristics measured at different stages of fabrication) variables. These data are available on CD from the thesis supervisors, Professors Thibault and McLean.. Since the values of the input variables for all the chips from the same wafer were identical, it was decided to average the product quality variables (outputs) over each wafer thereby reducing variability in the outputs as well as the dimensionality of our analysis. This reduced data set is found in Appendix B.

In addition, the overall pass/fail status of each chip tested along with the fail code (type of failure) for chips that failed testing was available. These data were also averaged over each wafer. The data for each chip is also included on the CD.. The averaged data are found in Appendix F.

4.2 Major Sources of Nonconformities

Reduction of nonconformities is a primary goal of process improvement. Consequently, a first step in the analysis of the process data was to determine the frequency of occurrence of each fail code over the period of study. Although a total of 33 failure codes were possible for the BHet device, in the data set provided for this study, only 17 were encountered. These are listed and briefly described in Appendix D. The results of the frequency analysis are shown in Figure 4.1. There are 19 286 chips in total (the rest of the chips were deleted form the data bank due missing values) where 10770 chips passed the test and 8518 chips failed because of different failures. Clearly, the fail

code, SMSR ...too low, occurred most frequently. (SMS -Side Mode Suppression Ratio in Decibels, which is defined as the ratio between the main device lasing wavelength and the next brightest peak). To more easily identify the relative importance of each fail code a Pareto analysis was carried out.

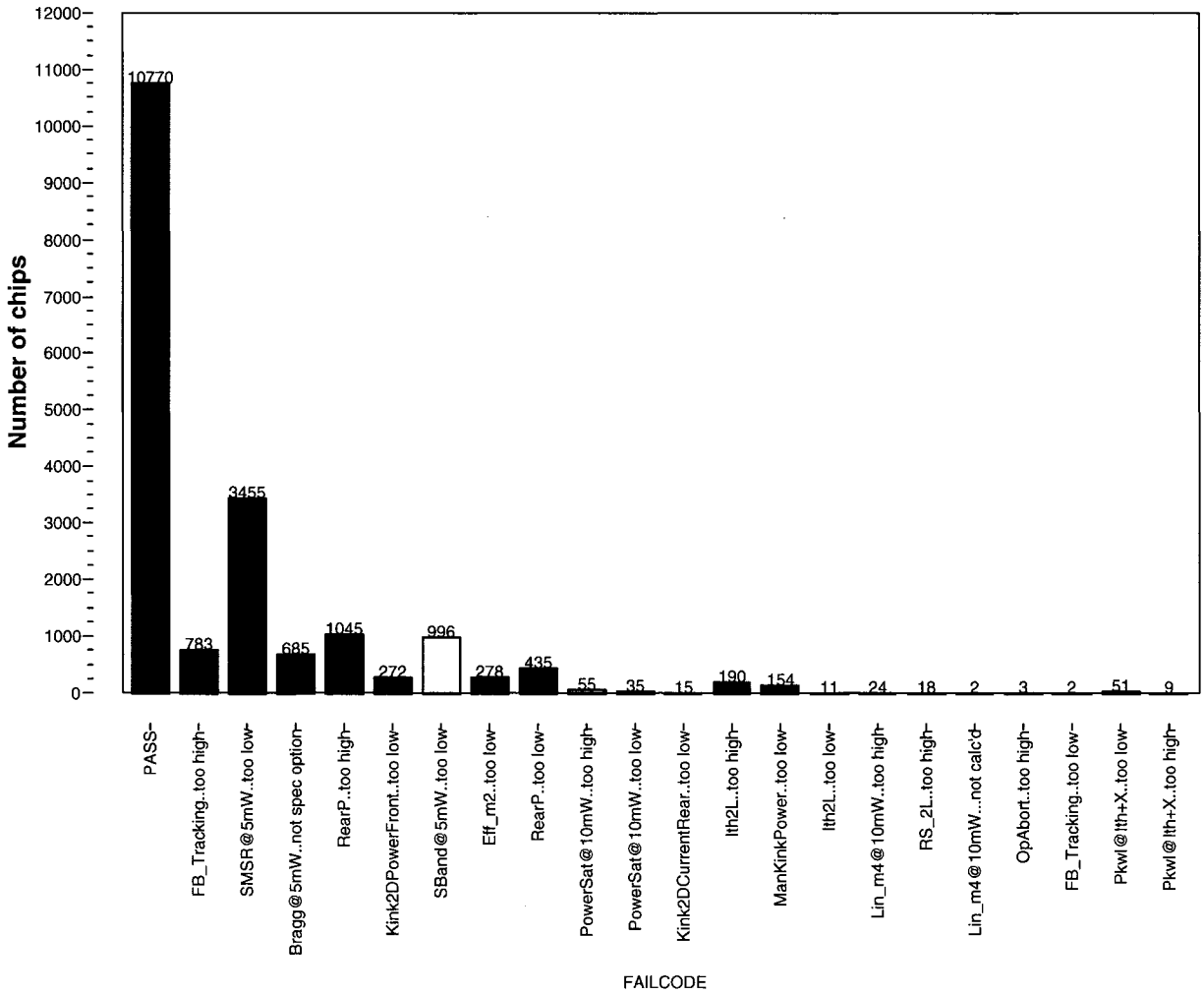

Figure 4.1 Number of occurrences of each fail code over the period under study

Using JMP statistical analysis software, the Pareto chart in Figure 4.2 was produced. Bars indicate the number of chips tested that failed as a result of the indicated fail code, while the solid line indicates the cumulative percentage of failures as fail codes are added in order of their individual contribution to failure. The sequence of bars identifies the order of importance of the fail codes.

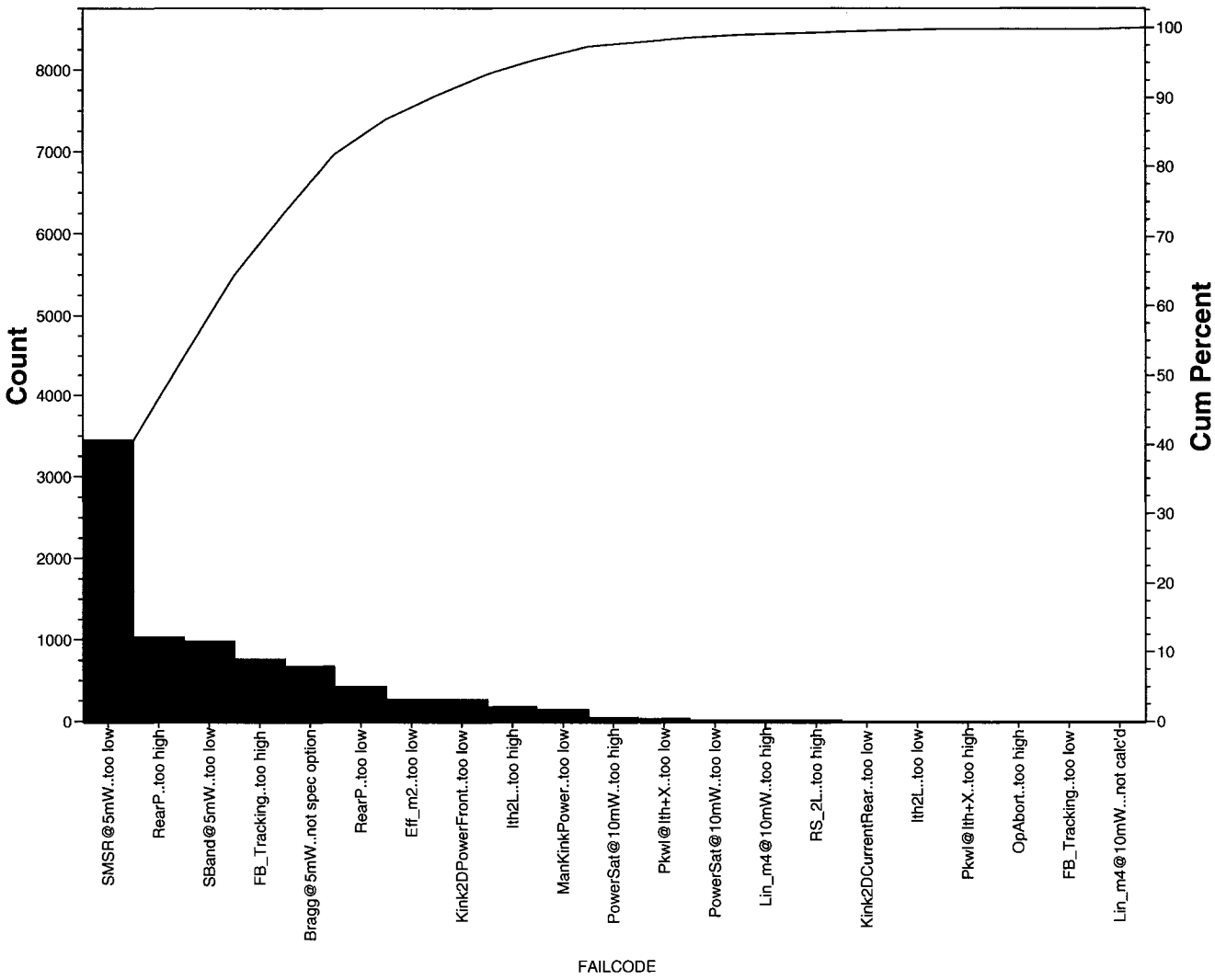

Figure 4.2 Pareto chart for BHet fail codes over the ten-month study period.

The cumulative curve shows that SMSR...too low, Rear Power...too high, SBand...too low, FB Tracking...too high, Bragg...not in spec, Rear Power...too low, and Efficiency...too low represented over 90% of the failures. SMSR...too low was clearly the most common type of nonconformity, accounting for approximately 40% of the failures.

It should be noted that the findings of this Pareto analysis are unfortunately the result of an incomplete reporting of fail codes assigned to each chip. Only a single fail

code was entered into the data base for each failed chip. As a result, other fail codes that could also have been assigned to the failed chip did not appear in the data base or the analysis. The protocol for assignment of fail codes, in such cases, was not at all clear but seemed to depend upon the order of testing and engineering judgement. The testing is done in two sequences, first where the device electrical properties is measured, and in the second sequence where the wavelength characteristics are measured. Under the assumptions that the Pareto analysis was not strongly distorted by this problem and that this production period represented typical operation, subsequent analysis was primarily focused on the seven major indicators of process performance listed in the previous paragraph.

4.3 Stability of Product Quality

To examine the stability of the process the monthly averages of five primary nonconformities were plotted for the ten-month period as shown in Figure 4.3. Trends in product quality are evident. There is some indication that changes in production took place in April and May. The fraction defectives related to Rear Power...too high and ...too low clearly decreased during April and May, while SBand...too low and FB Tracking...too high increased over the same period of time. This behaviour suggests that some compromise existed between these pairs of fail codes. Discussions with the process engineers did not reveal any physical reason for this phenomenon. In fact they were surprised to see such a pattern. Over this same period of time, the failure code, SMSR...too low, continued to increase, indicating a worsening problem over the entire ten-month period. The engineers had become aware of this problem, but had found no opportunity to investigate.

The monthly number of chips tested and the fraction defective were plotted over the study period in Figure 4.4. The black line indicates the number of tested chips per month. The monthly fraction of defectives is also shown in orange. The number of chips tested implies a ramping up of production for the first nine months, with a cutback occurring in October. This cutback corresponds to a planned shut down of the facility. The fraction defectives displayed an upwards shift in May with a partial return to lower

levels in July. The overall monthly fraction defectives range from 28% to 38%, indicating significant potential for process improvement.

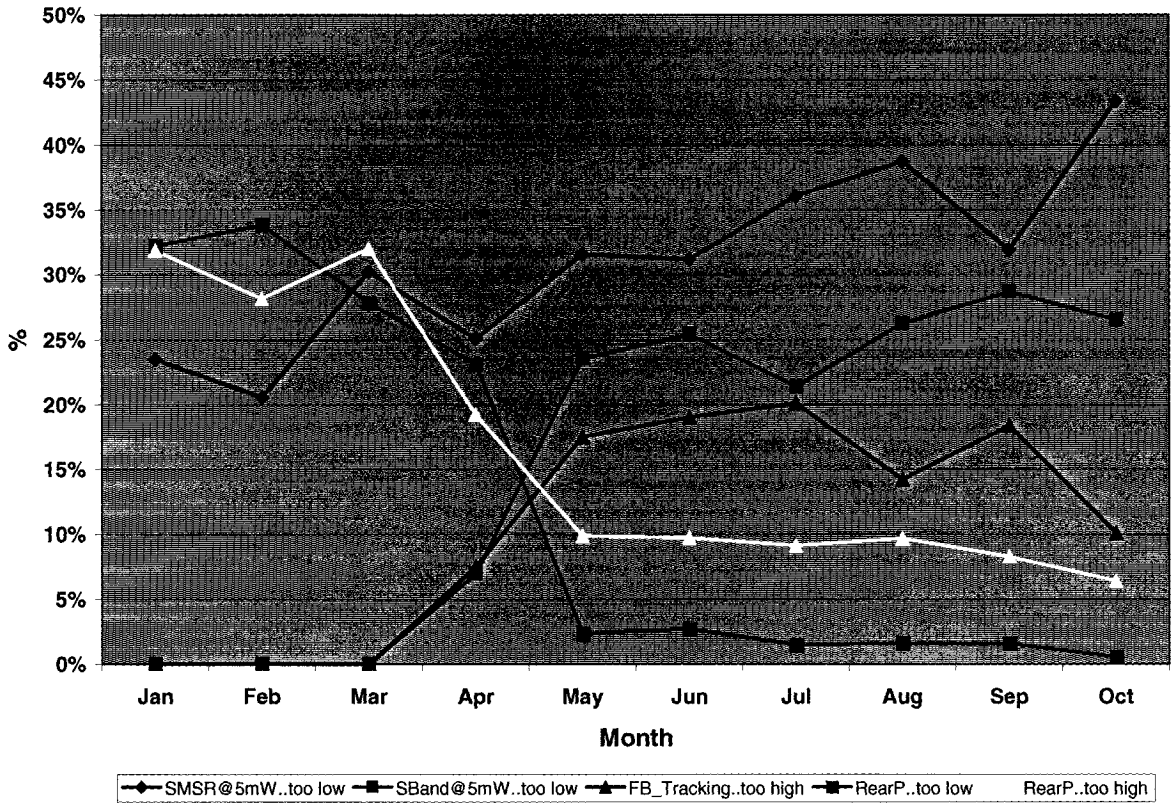

Figure 4.3 Fraction of tested chips resulting in selected fail codes over the ten-month study period

To investigate changes in occurrences of the various fail codes over the ten-month period, the percentage of the chips that passed testing along with the percentage of chips tested which failed under specific fail codes for each month were determined and displayed in Figure 4.5. In essence this figure helps to show if there is a problem with a large number of failures in a small number of wafers or a small number of wafers with a large number of failures.

In this figure, the red bars represent the number of wafers falling into a certain range of percentages of chips that passed on that wafer. For example, only one wafer had 0 to 10% of its chips pass, two wafers had 10 to 20% of its chips pass and fifty-one wafers had 50 to 60% of its chips pass. By adding the numbers of wafers in each category

a cumulative probability can be determined. For example adding the number of wafers in the three highest bins shows that 110 (51+43+16) wafers have more that 50% of their chips meeting specification. Ideally, most wafers should fall in the highest bin.

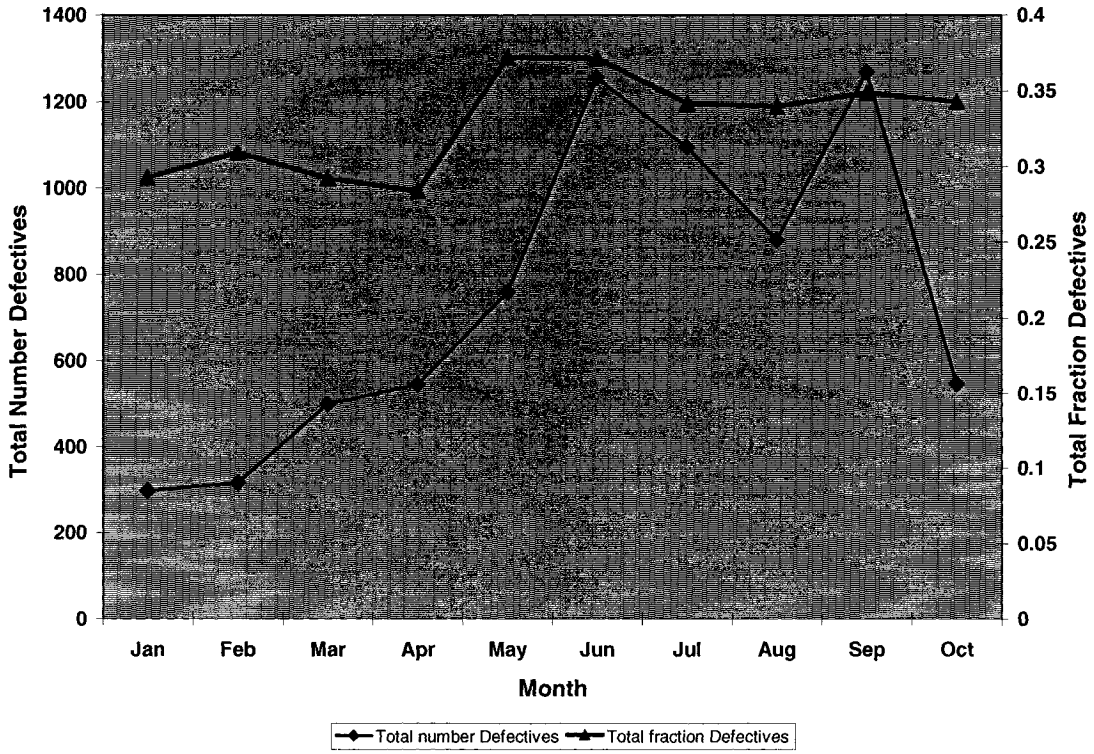

Figure 4.4 Total Number of Defectives and Fraction of Defectives over the ten-month study period

Interpretation of the bars for fail codes is somewhat different. These bars represent the number of wafers for which the specific fail code accounts for the specified range of percentages of chips that failed on that wafer. For example, the first blue bar, representing SMSR...too low, indicates that 45 wafers have 0 to 10% of their chips failing due to SMSR...too low. Ideally, most wafers should not have any fail code bars or at least have most wafers in the lowest bin. In the case of SMSR...too low, 20 (18+2) wafers have more than 30% of their chips failing as a result of this fail code. This provides further support for directing efforts towards improving the control of SMSR

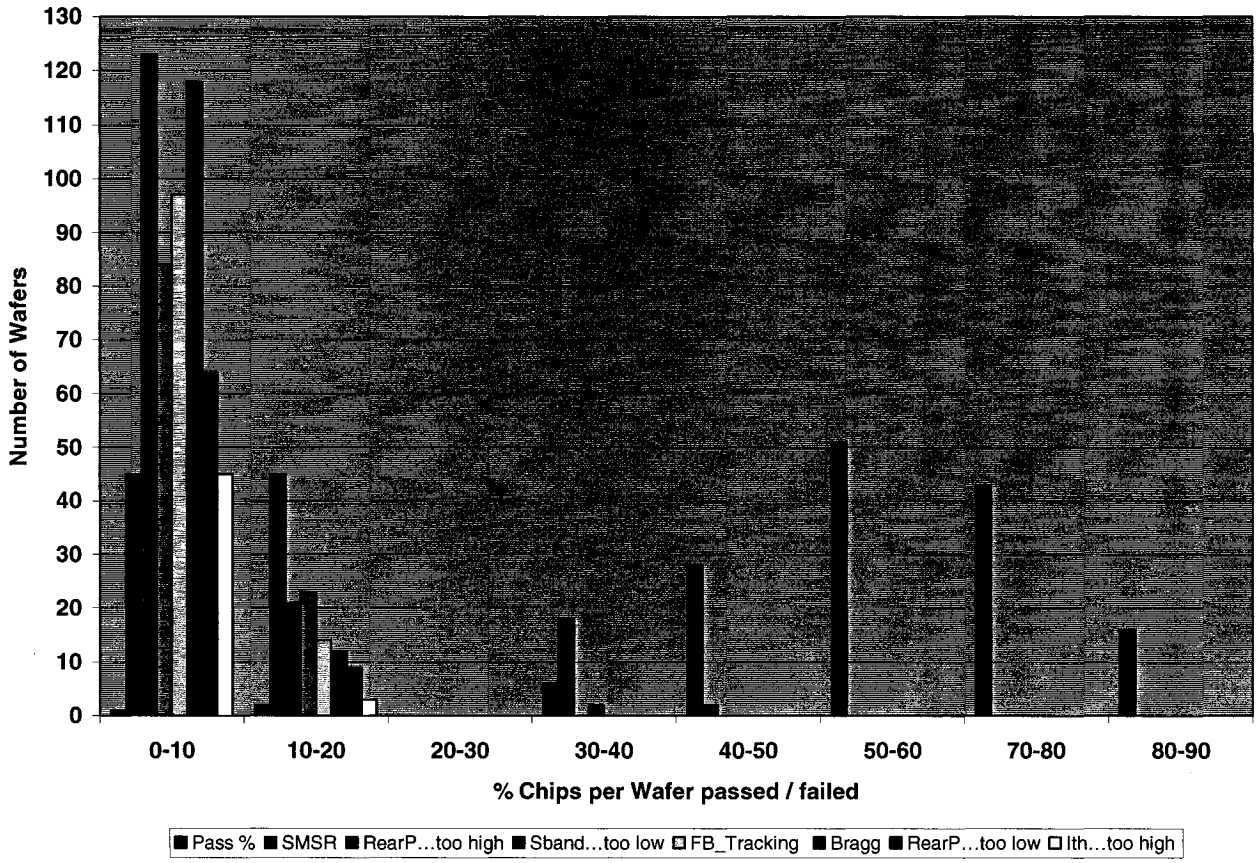

Figure 4.5 Distribution of failures/passes over wafers and chips

4.4 Variability and Correlation Analysis

Having identified the major reasons for nonconformities, it was decided to examine the potential for predicting process outputs based upon information contained in process input variables. Due to the large number of input and output variables a simple correlation analysis was used to identify potential relationships among the variables. To do this, scatter plots between all combinations of the variables were carried out along with the calculation of the corresponding correlation coefficients. The scatter plots were found to be most useful for identifying outliers in the data set. Although they did display the existence of correlation, the same information was more effectively displayed in terms of a correlation matrix. These are presented in Appendix G.(Refer to Appendices A

and B (shown in process order) plus the input/output shown in Appendix A). Due to the high dimensionality of our data set, it was not feasible to present a large number of scatter plots.

Of particular interest were high correlations between process input variables and output variables. The correlations between the input variables (variables 22 to 59) and output variables (variables 2 to 21) including measured outputs, fail code percentages and pass % were searched for high absolute values. Such values provided indications of potential input variables for predicted variables developed in Chapter 5. The search for high correlations was carried out using the software in Appendix C.

Boxplots were constructed and examined for each output variable (Figures 4.6, 4.7 and 4.8) In most cases they showed considerable variability and some potential outliers. After careful examination of these rogue points, they were discarded as long as justifiable reasons could be found. Outliers should be investigated carefully. Often they contain valuable information about the process under investigation or the data gathering and recording process. Before considering the possible elimination of these points from the data, it is recommended to understand why they appeared. Exploring why outliers exist can provide many clues to the development of better models. Outliers may indicate that an important range of the data has been ignored that is worth knowing about. The "common sense" test is often the best solution.

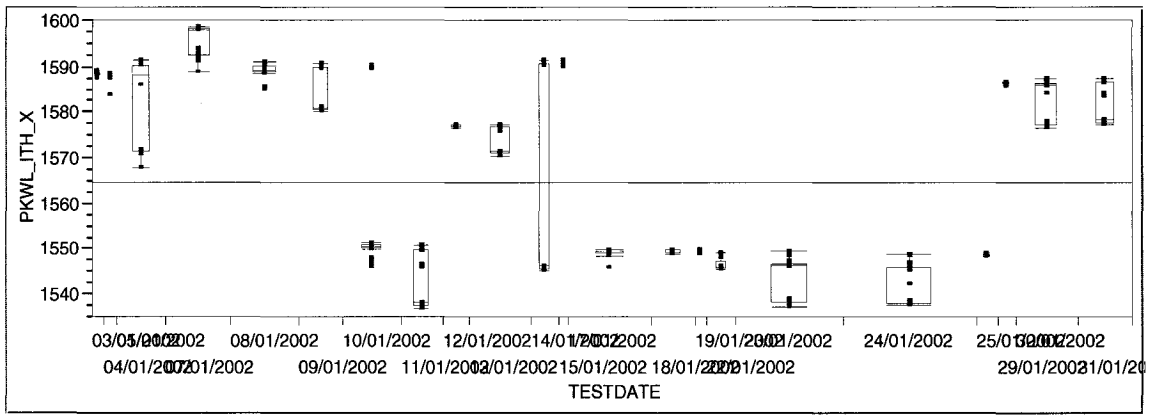

Figure 4.6 An example of PKWL_ITH_X in order by the testdata

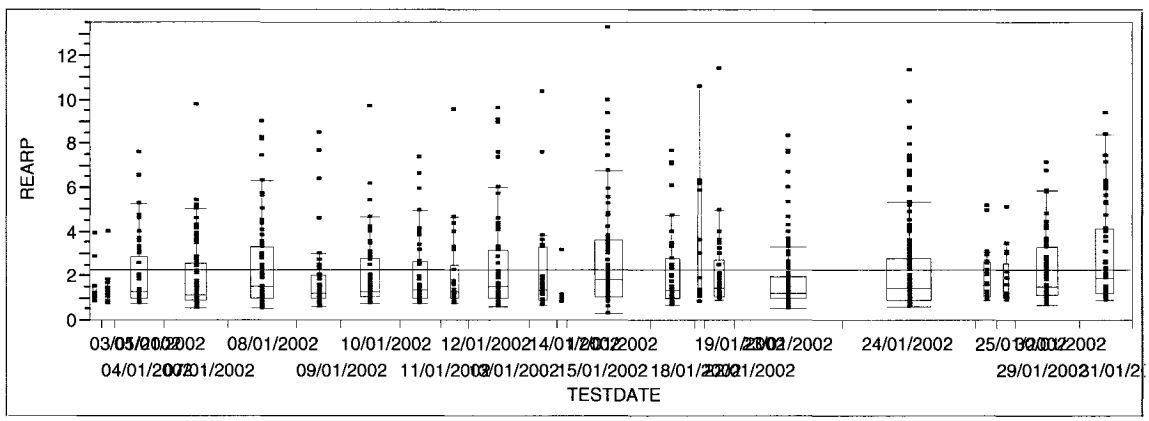

Figure 4.7 An example of RearPower in order by the testdata

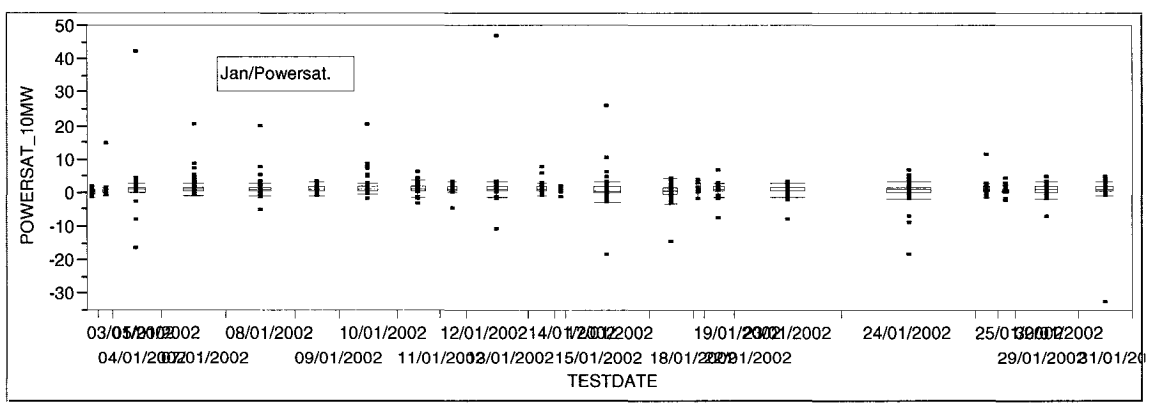

Figure 4.8 An example of PowerSaturation_10MW in order by the testdata

Table 4-1 Master Table with some outputs and their recorded values

WAFERID	FAILCODE	ITH2L	REARP	I_5MW	EFF_M2	KINKPOWERM1	VF_5MW	PKWL_ITH_X	SMSR_5MW
A-2959-7C	PASS	7.392	0.9	27.33	0.256	24.26	0.81	1587.756	46.4
A-2959-7C	SMSR@5mW..too low	8.033	1.69	25.93	0.266	25.28	0.8	1588.497	21.8
A-2959-4C	PASS	8.491	1.17	27.9	0.261	24.87	0.82	1590.443	47.1
A-3325-1A	RearP..too high	13.911	7.58	44.6	0.192	1.51	0.91	1571.008	41.8
A-2959-4C	PASS	8.234	1.21	30.24	0.232	21.94	0.83	1590.411	45
A-3325-1A	PASS	11.268	1.21	27.65	0.314	28.8	0.83	1571.822	47.9
A-3325-1A	PASS	9.99	3.3	31.6	0.253	2.38	0.85	1571.397	50.5
A-3325-1A	PASS	10.976	0.88	27.39	0.306	27.92	0.84	1571.526	48.9
A-2959-4C	PASS	8.773	2.08	31.05	0.229	21.69	0.83	1590.809	45.2
A-2959-4C	PASS	8.704	0.87	25.85	0.298	28.08	0.81	1590.554	49.1
A-2959-4C	RearP..too high	9.824	5.31	41.7	0.169	1.63	0.88	1590.502	46.6
A-2959-4C	PASS	9.412	0.89	27.85	0.275	25.61	0.81	1591.043	47.7
A-2959-4C	PASS	10.926	2.58	33.08	0.241	2.38	0.84	1591.125	44.2
A-3325-1A	PASS	11.202	4.74	35.75	0.228	2.19	0.87	1571.274	48.3
A-3325-1A	PASS	10.984	1.02	28.94	0.284	26.43	0.83	1571.938	48.8
A-3325-1A	PASS	10.921	0.96	27.58	0.305	28.2	0.84	1571.797	49.8
A-3325-1A	SMSR@5mW..too low	14.575	3.58	32.41	0.256	16.36	0.86	1571.754	27.9
A-3325-1A	SMSR@5mW..too low	16.243	4.02	39.76	0.212	17.88	0.9	1567.977	17.6
A-3325-1A	PASS	10.319	0.99	28.46	0.284	26.59	0.83	1571.913	47.7
A-2423-3C	SMSR@5mW..too low	9.616	3.91	40.86	0.156	14.3	0.91	1593.766	20.5
A-2423-3C	PASS	9.494	3.48	34.68	0.216	2.12	0.86	1597.953	49.8
A-2423-3C	PASS	7.534	1.12	30.6	0.224	21.58	0.85	1598.109	47.2
A-2423-3C	SMSR@5mW..too low	9.309	2.11	28.39	0.254	23.71	0.84	1598.287	33.6
A-2423-3C	Eff_m2..too low	9.889	2.87	44.82	0.126	11.69	0.92	1594.161	28.8
A-2423-3C	PASS	7.708	1.12	31.39	0.22	21.18	0.85	1598.055	47.1
A-2423-3C	PASS	8.425	1.03	29.38	0.243	22.6	0.84	1598.606	47.4
A-2423-3C	PASS	7.769	1.01	30.08	0.231	22.13	0.84	1598.432	46.5
A-2423-3C	Eff_m2..too low	10.149	2.63	32.08	0.143	3.48	0.86	1598.219	26.6
A-2423-3C	PASS	8.053	0.87	29.04	0.243	22.89	0.84	1598.578	46.6
A-2423-3C	PASS	8.438	1.56	30.78	0.234	22.34	0.85	1598.378	48.5
A-2423-3C	RearP..too low	8.613	0.66	27.15	0.272	25.52	0.83	1598.344	43
A-2423-3C	PASS	7.829	1.12	29.96	0.234	22.01	0.84	1598.351	46.2

4.5 CONCLUSIONS

Based on the previous analysis the following conclusions can be presented:

- There appear to be seven major fail codes that caused 90 % of the failures in the fabrication of BHet laser devices.
- There is strong evidence of poor control in the process over the ten-month period studied as noted by the overall high occurrence of nonconformities, a strong upward trend in the SMSR...too low fail code, opposing shifts in the occurrence of fail codes related to Rear Power...too low and Rear Power...too high (decreasing) compared to SBand...too low and FB_Tracking...too high (increasing) and shifts in the overall percent defective.
- Greater knowledge for process improvement could be obtained by entering all fail codes related to each chip failure into the WaVe (Test) data base. This would also help to remove the current ambiguity in interpreting fail code data.

CHAPTER 5

MODELLING

5.0 INTRODUCTION

Currently, there is no formal forecasting model in the manufacturing of BHet laser. If forecast is required, the mean value of some recent data points is calculated and it is assumed that this value will prevail in the future. This procedure has some limitations since it does not account for the correlation existing among various variables of the process nor does it consider potential significant drifts in the process. As a result, planning and production personnel would greatly benefit from having a systematic and reliable prediction tool.

Production of BHet laser is a very complex and long process where many variables are involved in the manufacturing. One of the main difficulties for this type of industry is the prediction of key output variables, and the probability of failure of a particular product.

The objective of this chapter is therefore to assess the feasibility of using simple models to predict the values of key process outputs and their probability of failure. These models, linear and non-linear, would ideally be used as early as possible in the process sequence to allow process engineers to take the appropriate control action. In InP batch process industries, a given failure may depend on a large number of input variables. The input variables that have the highest correlation coefficients with a particular output or failure should be used to develop a regression model. In this study, the complete data bank has 150 records, each record containing 59 columns or pieces of information. Among these 59 columns, 37 are values of input process variables. Three techniques were used to obtain regression models: stepwise regression analysis, generation of all linear models using a specialized computer program, and neural networks.

5.1 Linear Models

5.1.1 Stepwise Regression

Stepwise regression is a technique that can be used to sequentially build linear models by selecting a set of input variables to explain the maximum variability of a given output variable. Stepwise regression can be used in two different ways: forward stepwise regression and backward stepwise regression.

In the forward stepwise regression, the model is built progressively by adding at each step, the independent variable that will provide the most improvement to the fit of the model. This procedure is followed until adding another variable does not result in a significant improvement in the fit. In the backward stepwise regression, the initial model contains all independent variables, and the variables that have the least impact for explaining the variability of a given output variable is removed at each step. This procedure is repeated until the removal of one variable has a significant impact on the fit of the model.

Stepwise regression is a fairly efficient technique provided that the data bank is complete. Unfortunately, the industrial data bank that was gathered for this work had missing information that was scattered throughout the data bank. In stepwise regression, when a missing information or outlier appeared in one column, a whole row (data record) has to be eliminated because there was a possibility that the variable associated with this column could be used in the model. This restriction had for consequence to reduce significantly the size of the data bank and, as a result, the validity of the model.

For this reason, stepwise regression was abandoned. Instead, it was decided to write a specific computer program that would selectively eliminate a record when missing information was encountered in one the selected input variables. The listing of this computer program, written in FORTRAN, is given in Appendix C.

5.1.2 *Specialized Computer Program*

The objective of the computer program, written specifically for this thesis, is to assist process engineers to analyze the data bank to find correlation coefficients among all input and output variables and to use this information as a basis to determine the best linear models. For each output variable, for which a predictive model is sought, a number of possible input variables are retained by the program, based on correlation coefficients. The computer program then automatically generates all possible linear models with one, two, three and four input variables that minimize the sum of squares of the prediction errors and calculates the regression coefficients for each model. As an example, Table 5-1 gives a summary of the best models for the peak wavelength (PKWL) having from one to four input variables. It is important to note that the regression models are performed using data that were normalized between -1 and +1. The model parameters β_i are from the following model:

$$E(Y) = \beta_0 + \beta_1 X_1 + \beta_2 X_2 + \beta_3 X_3 + \beta_4 X_4 \qquad \textbf{(5.1)}$$

Table 5-1 also provides useful statistics to analyze the quality of each model: the standard deviation of the residuals, the average prediction error, the correlation coefficient between the real and predicted values, and the average value of the absolute value of residuals.

5.1.3 *PKWL Model*

Once the FORTRAN program was created, all models were generated using this program. In Table 5-1, the one-variable model for PKWL, using the pitch as the input variable, has a correlation coefficient of 0.959. The two-variable model was generated by adding the single point wavelength as the second input variable, and the corresponding correlation coefficient increased to 0.960, which is not a statistical significant increase. Additional input variables did not improve the prediction. Therefore, for the PKWL, a one-variable model is sufficient for an accurate prediction of its value. In the Table 5-1, the Min and Max values represent the minimum and maximum values of the actual measured test data for PKWL. For the chip to be acceptable, the PKWL value should be between 1516-1625 nm.

Table 5-1 Summary of best models for output PKWL (Column 11)

Number of inputs	Number of points	Input value	Min	Max	Parameter Values (using scaled inputs and outputs)					σ	ε	Correlation coefficient (y, ŷ)	|ε|
					β0	β1	β2	β3	β4				
1	140	32	1477.00	1617.00	0.0488	0.8808				7.99	0.0008	0.959	7.97
2	139	32 30	1477.00	1617.00	-0.0110	0.7956	0.1746			7.82	0.0059	0.960	7.80
3	139	32 29 28	1477.00	1617.00	-0.0315	0.8004	0.1388	-0.0711		7.77	0.0151	0.960	7.74
4	139	32 45 30 42	1477.00	1617.00	-0.0269	0.6663	0.1853	0.1725	-0.0392	7.76	0.0118	0.961	7.73

The most significant contribution to the PKWL is the pitch calculation (input column 32), which is generated prior to the grating manufacture.

Figure 5.1 shows the plot of the PKWL with one input variable as a function of second number. The predictive model nicely tracks the actual value of the PKWL.

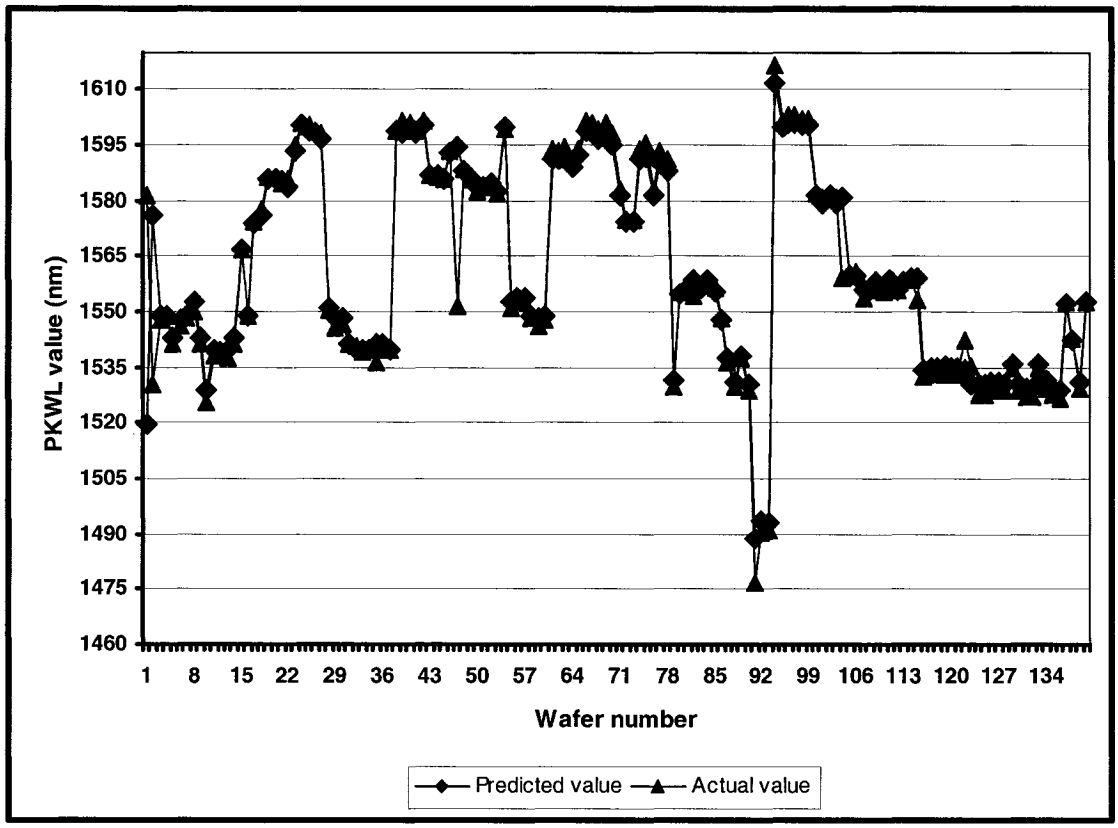

Figure 5.1 Plot of PKWL: Predicted versus Actual values for the one-variable model

To determine the model adequacy, model predictions have been examined in various ways. First, the model was used to predict if the PKWL value of a given wafer would fall within the required specifications, and therefore determine if the wafer would be acceptable. These predictions were compared with the actual outcome of the wafer. A histogram of the number of good and wrong predictions is presented in Figure 5.2. This figure shows that the model predicted the fate of the wafer with a success rate of 100%. The results of this particular output were expected given the good fit of the model.

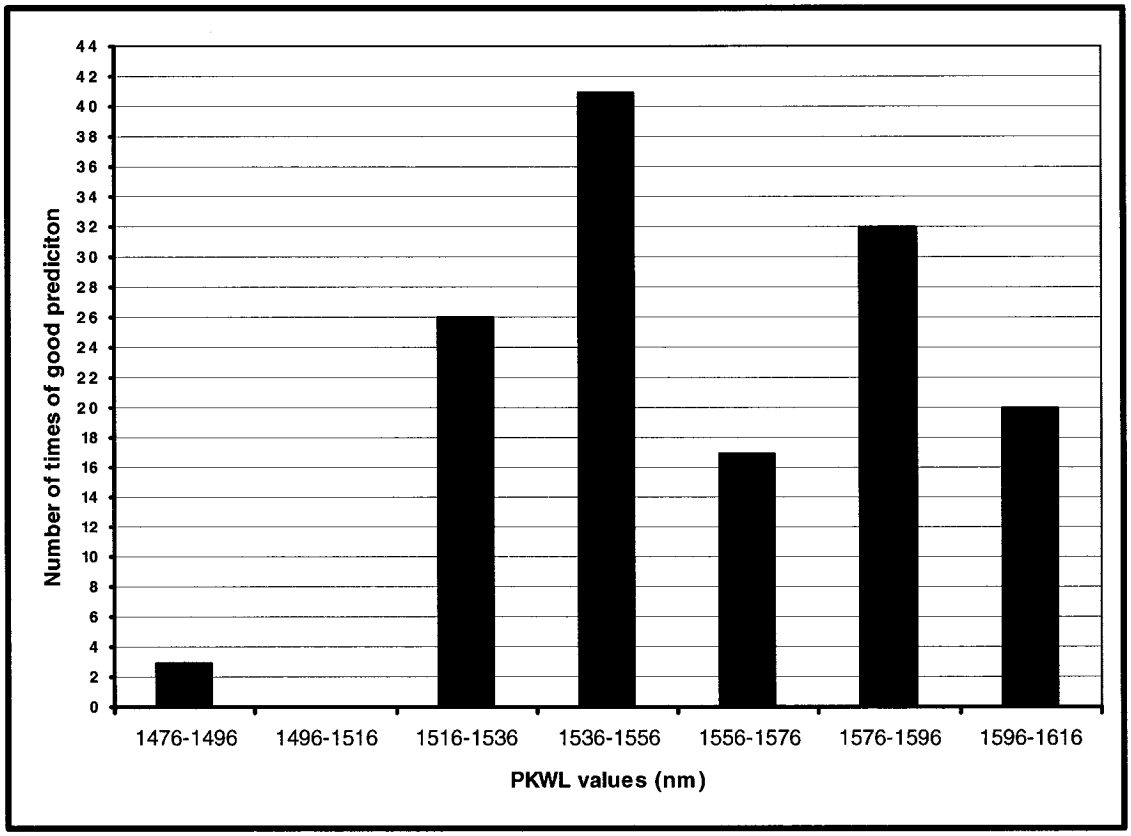

Figure 5.2 Histogram of PKWL bars which represents the number of good and wrong predictions in each wavelength segment.

Second, a plot of the residuals is made to visually observe model inadequacies. Figure 5.3 presents the plot of the residuals as a function of the predicted PKWL values. The standard deviation of the residuals is less than 6% of the range of PKWL (Table 5.1). The parity plot of Figure 5.4 is another way to look at the adequacy of the model, as it shows visually the level of correlation between the predicted and actual values, and the scatter of residuals.

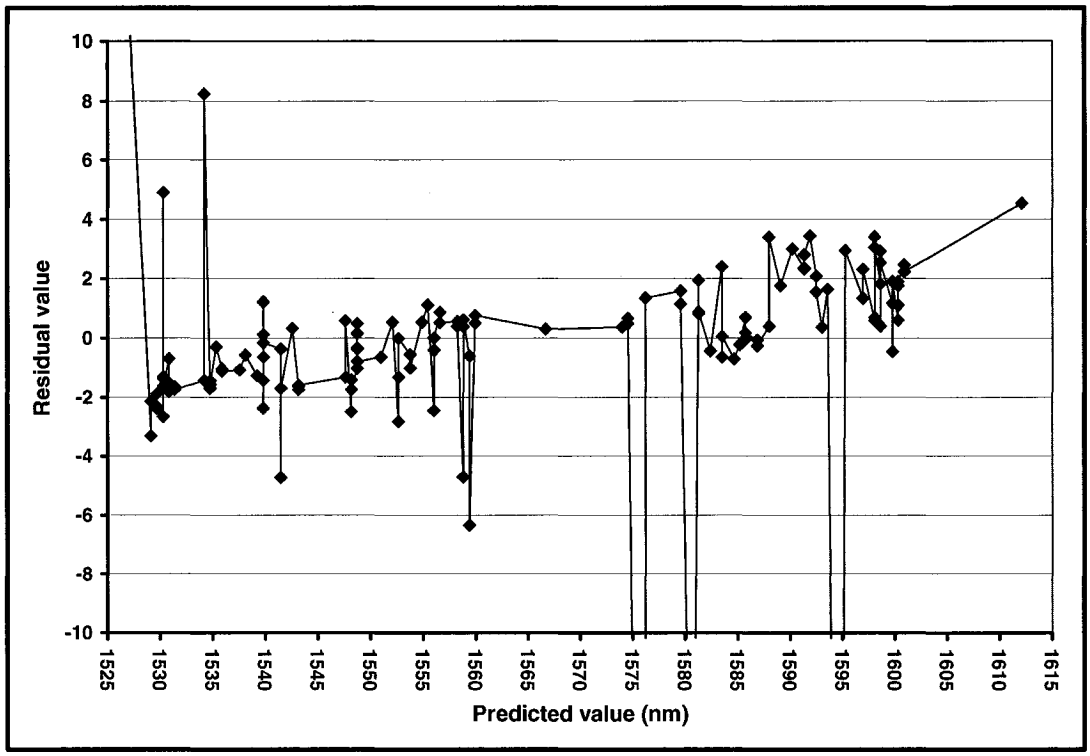

Figure 5.3 PKWL plot of residuals for the one-variable model as a function of the predicted values

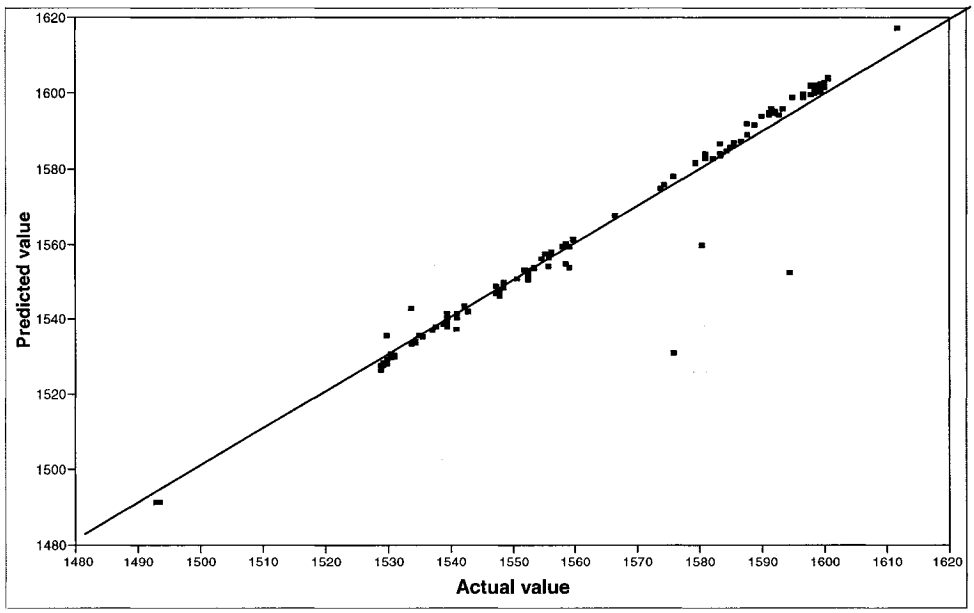

Figure 5.4 Plot of PKWL: Predicted versus Actual values with one variable

5.1.4 *Forward Voltage (VF) Model*

The next output variable with the highest correlation coefficient is the Forward Voltage (Column 9 in the databank). Table 5-2 presents the statistics for models with one to four input variables. The correlation coefficient increases from 0.606 to 0.751 when the number of input variables is increased from one to four. It is interesting to note that the best models for different numbers of input variables do not use the same input variables. For one-input variable, the overgrowth layer single point intensity (Column 43) is used whereas the two-input model was generated using the overgrowth layer average intensity (Column 46) and the overgrowth layer intensity standard deviation (Column 41). All these three input variables are very closely related being a single point, an average and standard deviation of a map, respectively. The actual specification is a Forward Voltage between 0.15 and 3V at current of 10 mA.

Table 5-2 Summary of best models for output VF (Column 9)

Number of inputs	Number of points	Input value	Min	Max	Parameter Values (using scaled inputs and outputs)					σ	ε̄	Correlation coefficient (y, ŷ)	|ε̄|
					β0	β1	β2	β3	β4				
1	147	43	0.81	1.00	-0.4958	-0.5208				0.02	0.0000	0.606	0.02
2	147	46 41	0.81	1.00	-0.3134	-0.5504	0.3772			0.02	0.0000	0.680	0.02
3	145	43 49 41	0.81	1.00	-0.3434	-0.4140	-0.1406	0.2836		0.02	0.0000	0.720	0.02
4	145	46 49 41 44	0.81	1.00	-0.1752	-0.5294	-0.2260	0.3709	-0.2076	0.02	0.0000	0.751	0.02

The most significant contribution to the VF is the intensity measurement, because most of the model inputs are related to this particular measurement. In the third model, one of the variables is the ridge width measurement whereas the other inputs are related to the intensity measurement. Based on statistical considerations, the second model is the model that appears to be the best compromise between parameter parsimony and precision. However, the two-variable model uses two similar inputs that are highly correlated, and model with three input variables should also be used to make use of the

additional information of the ridge width (Column 49). Ridge measurement is the main Fab process step and the most critical one in the manufacturing of BHet laser. Ridge creation is at a very early stage in the Fab process. If the ridge width is not within specification, there is an opportunity for the rework process.

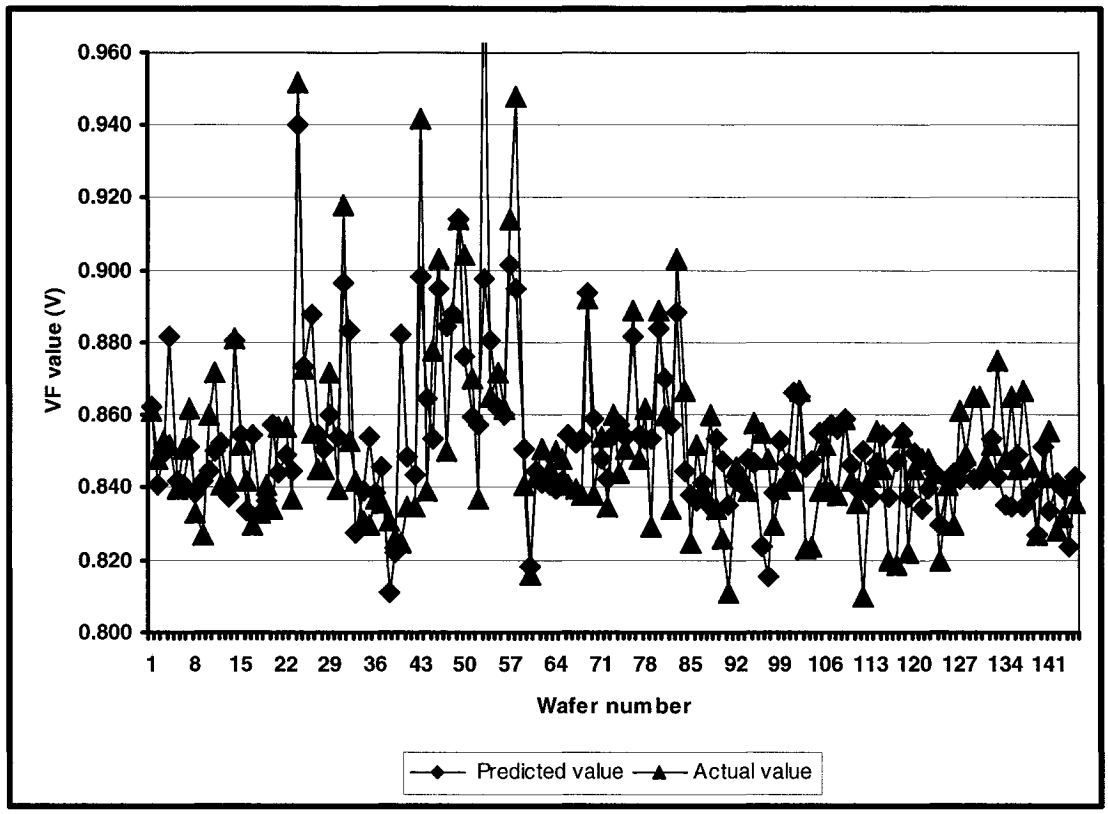

Figure 5.5 Plot of VF with three variables predicted versus actual value.

In the case of VF, there were no failures associated with this output variable. The scatter plot of residuals with three variables is shown on Figure 5.6. Residual plots for all four models showed no significant correlation. Figure 5.7 presents the predicted versus actual VF values where the points are mostly clustered around 45° line. In the case of both PKWL and VF, the predicted values compared very well to the actual values. However, from a practical point of view, these predictions are unfortunately not very useful because most BHet wafers meet the required specifications of these two output variables.

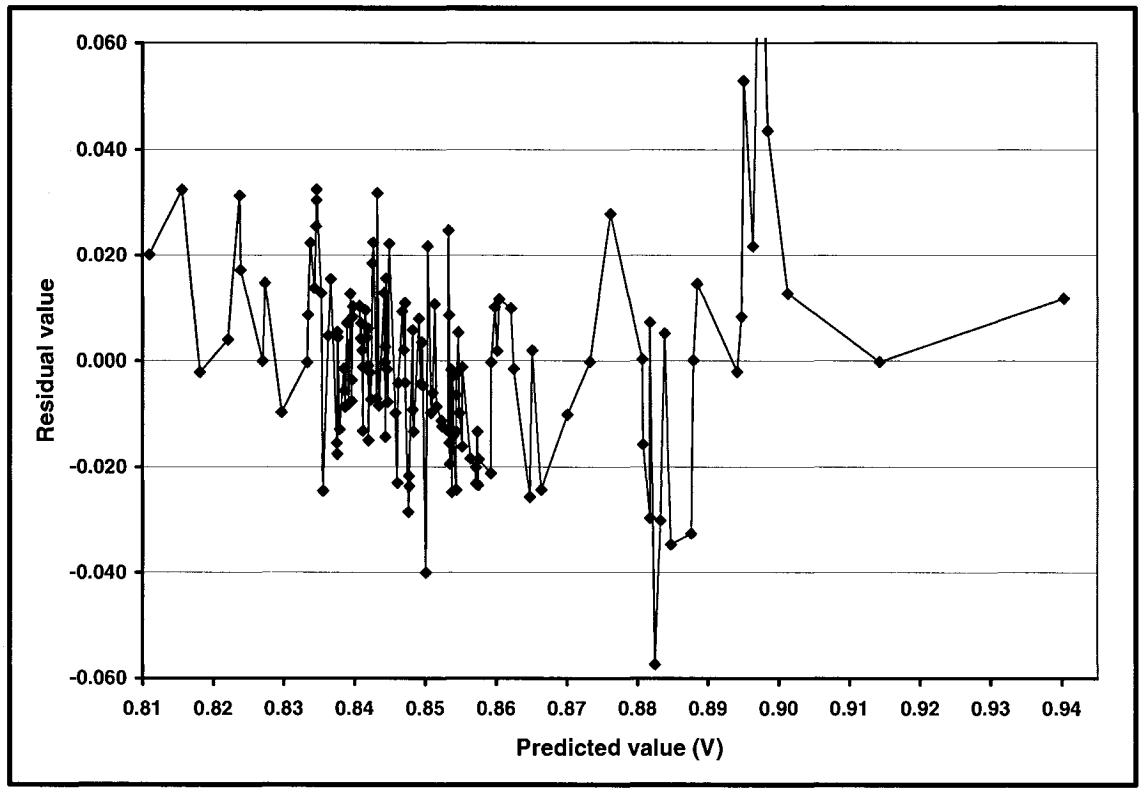

Figure 5.6 Residual Plot of VF with three variables

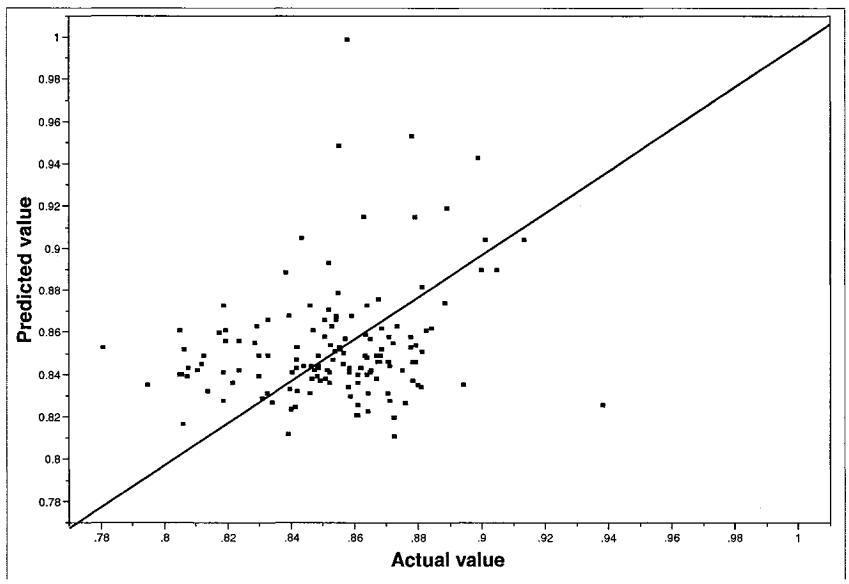

Figure 5.7 Plot of VF: Predicted versus Actual values with three variables

5.1.5 *SMSR Model*

SMSR is one of the output variables for which the largest number of failures for the BHet is recorded. Indeed, 70 wafers from a total of 147 failed for this variable did not meet the specification.

Table 5-3 presents the best prediction models with one to four input variables. For the SMSR model with one input variable selected the grating depth (Column 39) and the resulting correlation coefficient was found to be 0.499. In the two-variable model, the lasing wavelength (Column 33) was added to give a correlation coefficient of 0.560. For the third and fourth models, the correlation coefficients were 0.625 and 0.644 respectively, which does not correspond to a very significant increase in the correlation coefficient. For this reason and mainly because predictions could be made at an earlier stage, the two-variable model is preferred. For each model, the major impact on SMSR is the grating depth. The actual specification for SMSR is 40 dB or higher

Table 5-3 Summary of best models for output SMSR (Column 12)

Number of inputs	Number of points	Input value	Min	Max	Parameter Values (using scaled inputs and outputs)					σ	ε̂	Correlation coefficient (y, ŷ)	|ε̂|
					β0	β1	β2	β3	β4				
1	147	39	29.82	50.67	-0.1776	-0.6862				4.02	-0.0007	0.499	4.00
2	138	39 33	29.82	50.67	-0.2333	-0.6058	0.2019			3.68	-0.0002	0.560	3.66
3	138	39 43 33	29.82	50.67	-0.1407	-0.5533	-0.3862	0.0721		3.43	0.0003	0.625	3.42
4	137	39 43 33 36	29.82	50.67	-0.0820	-0.4502	-0.4089	0.1335	0.1249	3.36	0.0002	0.644	3.35

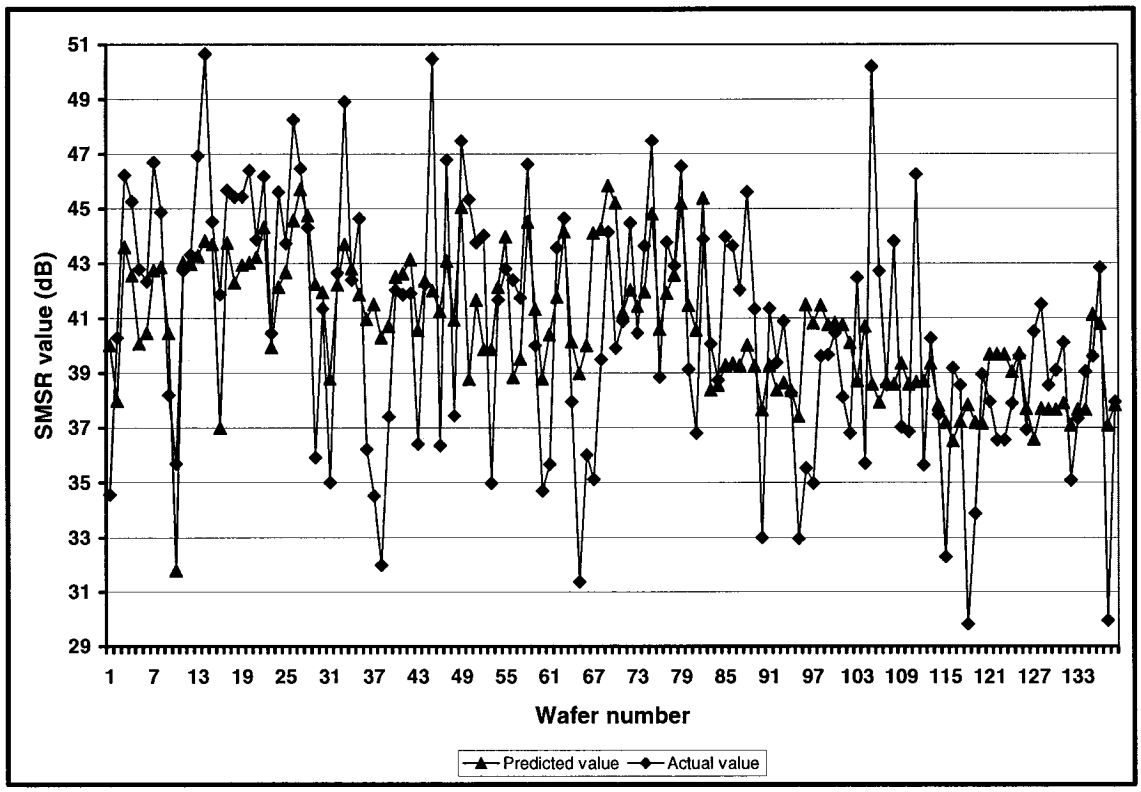

Figure 5.8 Plots of the actual and predicted SMSR values with the two input variables (grating depth and lasing wavelength).

To check the prediction accuracy, data were divided into two groups: good and wrong predictions. Figure 5.8 presents a plot of the actual and predicted SMSR values with the two input variables. Figure 5.9 presents a histogram of the number of good and wrong predictions as a function of the actual values of the SMSR. The highest probability of a wrong prediction occurs in the vicinity of the 40 dB threshold SMSR value. The accuracy of prediction does not change at this threshold point. However, the probability of being wrong increases. This then becomes a critical decision for the engineers, to decide if the wafer should continue further down the fabrication line or not. Possibly the use of more than one model could help in increasing the probability of the right outcome.

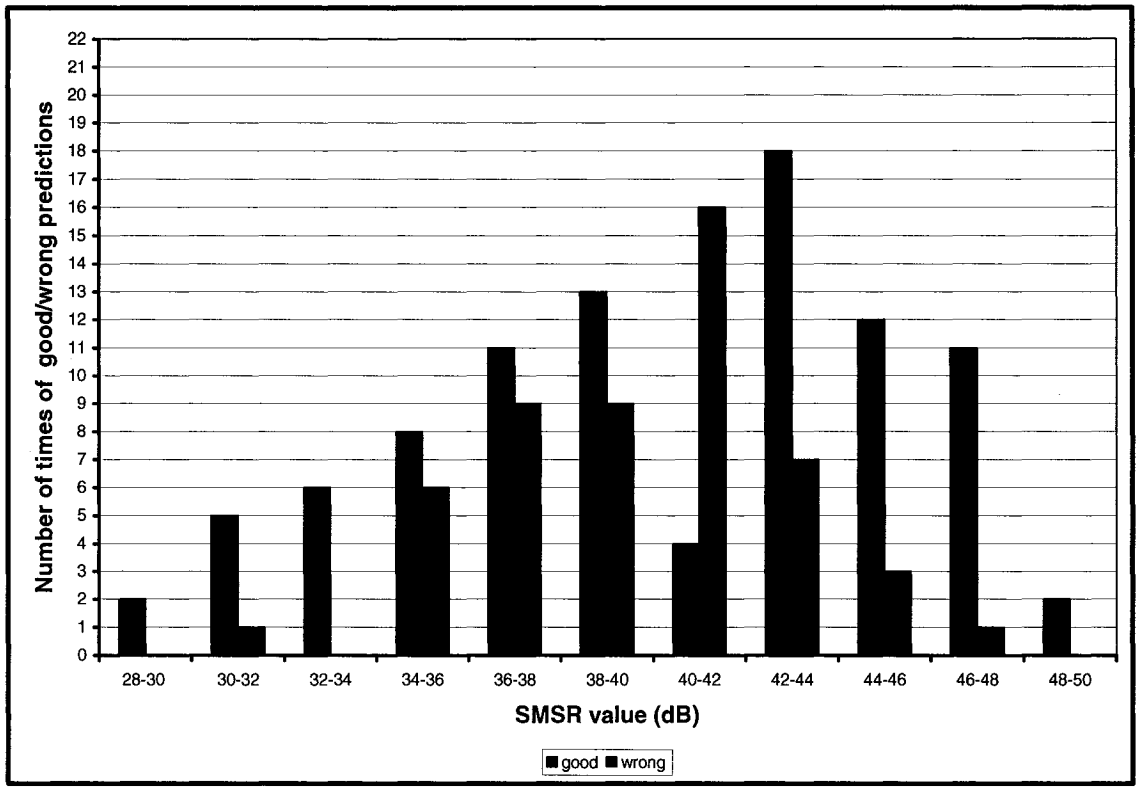

Figure 5.9 Histogram of good and wrong SMSR predictions as a function of actual SMSR values.

Figures 5.10 and 5.11 present the plot of the prediction residuals for SMSR as a function of the predicted value, respectively for the one- and two-variable models. Figure 5.10 clearly shows that residuals are correlated as evidenced by the "saw-tooth" pattern in the first half of the data, which indicates that there was some adjustment being made in the grating depth process. Figure 5.11 shows that the two-variable model provides a much better fit of SMSR with the addition of the lasing wavelength.

Figure 5.12 presents the scatter plot of predicted value versus actual value. From this figure, it can be seen that there exist an acceptable correlation. Data are clustered along the 45° line.

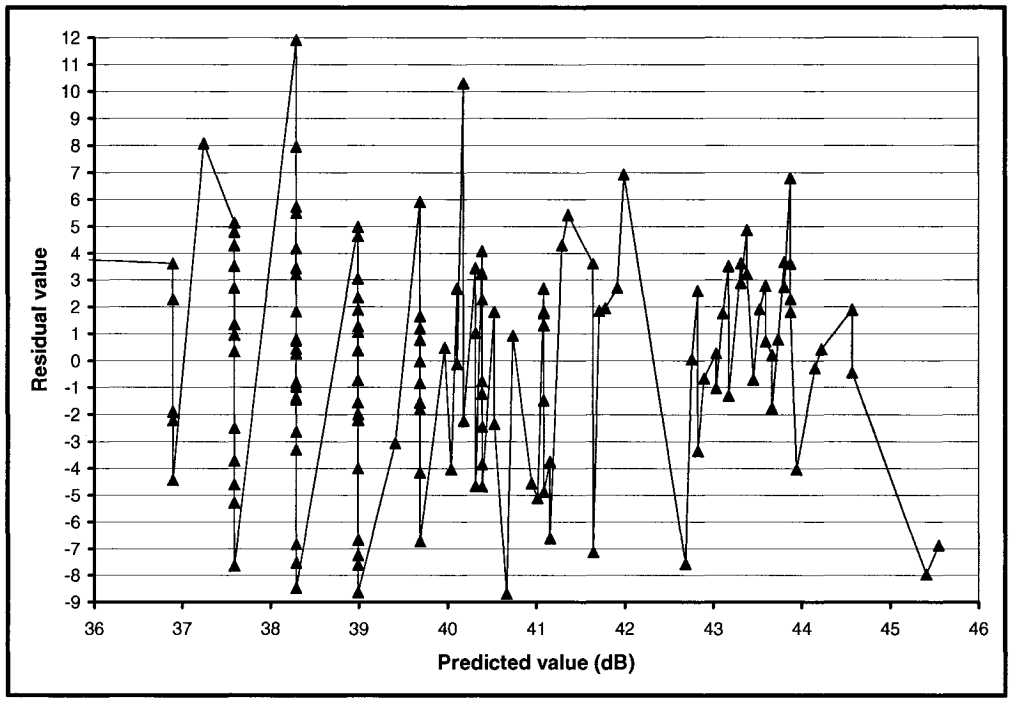

Figure 5.10 SMSR residual plot with one-variable model

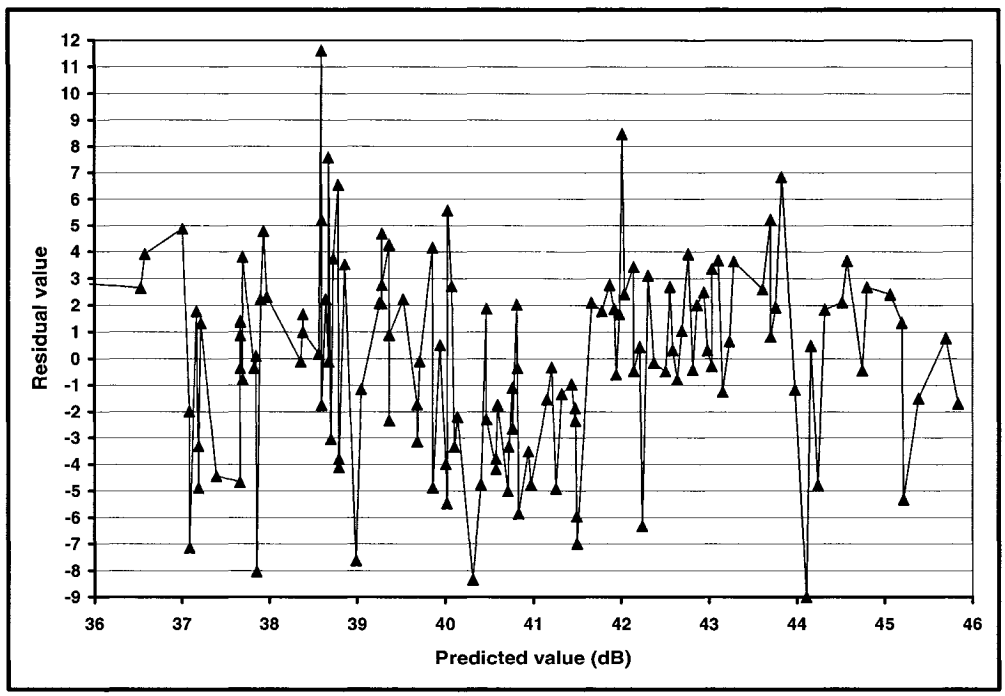

Figure 5.11 SMSR residual plots for the two variable model.

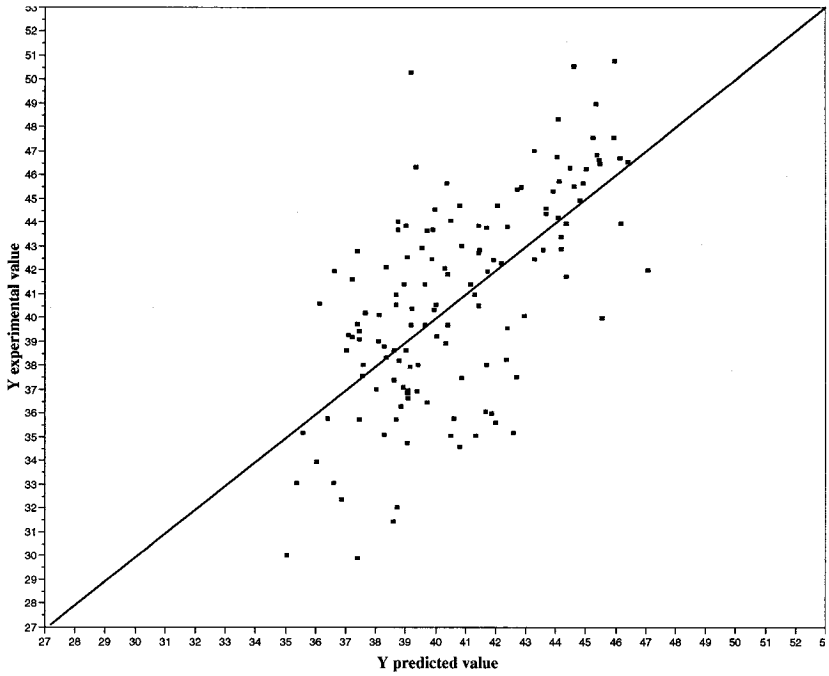

Figure 5.12 Plot of SMSR: Predicted versus Actual values with two input variables.

5.1.6 *SBand Model*

One of the most frequent failures is caused by SBand (Column 13). Table 5-4 presents the best models for one to four input variables. The SBand model with one input variable uses the grating depth (Column 39) and the correlation coefficient was found to be 0.386. The two-variable model uses the average N-metal value (Column 59) in addition to the grating depth, giving a correlation coefficient of 0.434. In the three-variable model by adding the oxide thickness (Column 51) and in the four-variable model by adding the ridge width (Column 49), the correlation coefficients increase to 0.456 and 0.476, respectively. The values of the correlation coefficient, even for the four-variable model, are not very high and the models have to be used with caution. In all models, the most important variable affecting the SBand is the grating. To meet the specification, the SBand must lie between 2.4 to 10 nm.

Table 5-4 Summary of best models for SBand (Column 13)

Number of inputs	Number of points	Input value	Min	Max	Parameter Values (using scaled inputs and outputs)					σ	ε	Correlation coefficient (y, ŷ)	|ε|
					β0	β1	β2	β3	β4				
1	145	39	2.01	4.37	-0.2452	-0.4608				0.41	-0.0001	0.386	0.41
2	145	39 59	2.01	4.37	-0.4542	-0.4950	0.3398			0.40	-0.0004	0.434	0.40
3	144	39 51 59	2.01	4.37	-0.4570	-0.4676	0.1312	0.3833		0.40	0.0000	0.456	0.40
4	143	39 51 49 59	2.01	4.37	-0.4741	-0.4805	0.1244	0.0858	0.3568	0.40	0.0003	0.476	0.40

Basing the selection of the model strictly on the correlation coefficient to have the best prediction, the four-variable model would be the best model. However, there are many, often contradicting, criteria that must be considered for the selection of the model. It is desired to have the smallest number of model parameters, the highest correlation coefficient, and to use input variables associated with early steps in the fabrication process. Based on these considerations, the most appropriate model is the one-variable model because it is the only model that does not use the average N-metal value (Column

59), which is the last step in the process. Using the other three models does not allow taking remedial action and they cannot be used as diagnostic tools.

Figure 5.13 compares the actual and predicted values of the SBand with one input variable. The predictions are not very good and it was not possible to obtain a reliable model.

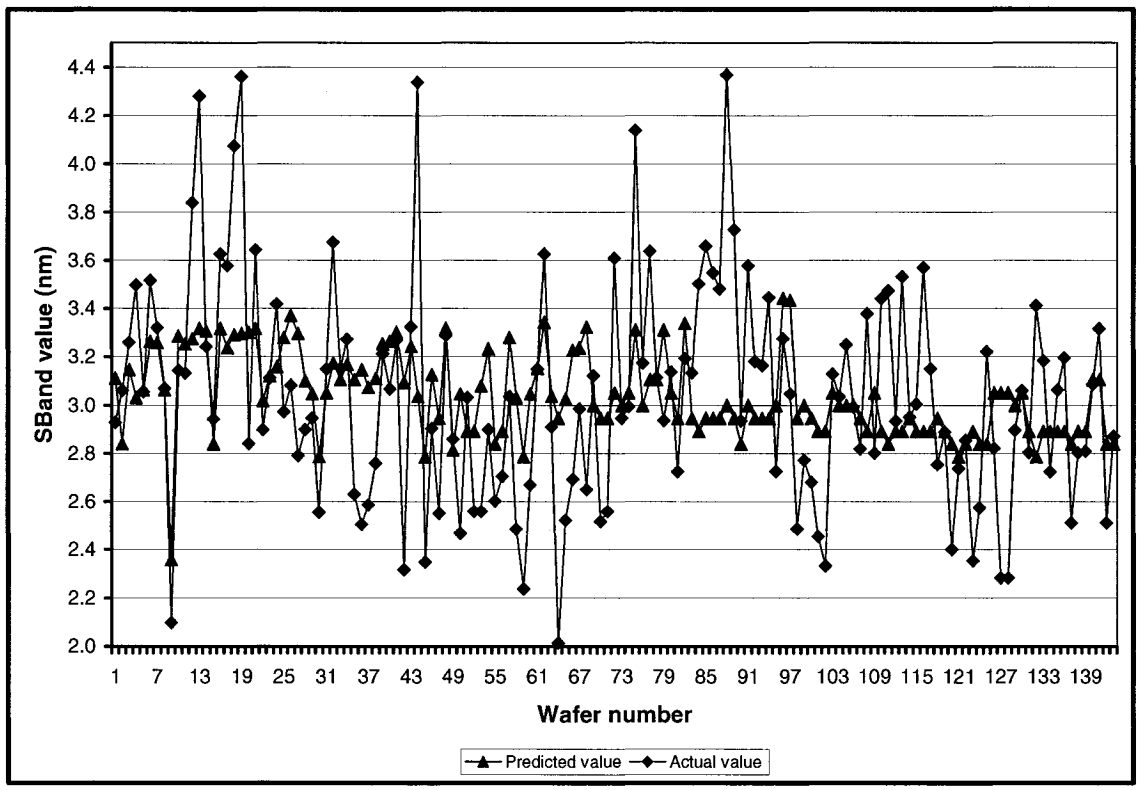

Figure 5.13 Plot of SBand with one input variable: predicted versus actual values.

Figure 5.14 presents a histogram of the number of good and wrong predictions as a function of the actual values of the SBand. The model predicted only one failure that was actually a failure whereas all the other wafers were assumed to meet specification. However, in reality, a total of 10 wafers failed so that the success rate for predicting the right outcome with respect to failures is only 10%. This model is obviously not very useful for predicting failed wafers close to the specification value. The correlation coefficient is too low to provide this level of accuracy.

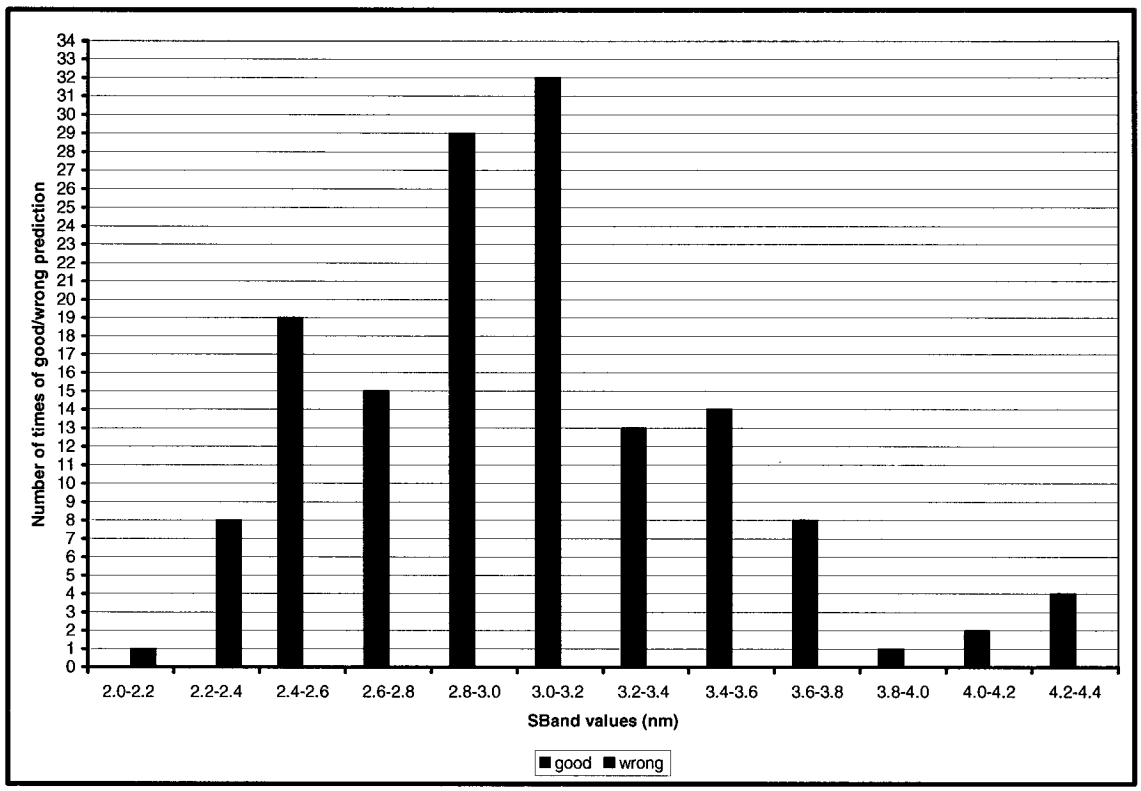

Figure 5.14 Histogram bars of SBand which represents a ratio of the good and wrong predictions in each segment.

The plot of residuals for the one-variable model is presented on Figure 5.15. The residual plot shows no definite trend with the mean centred at zero. Figure 5.16 presents the plot of the predicted versus actual SBand values. It is clear that the model is not very good because there is no information in the databank that could be used to adequately explain the SBand behaviour with linear models.

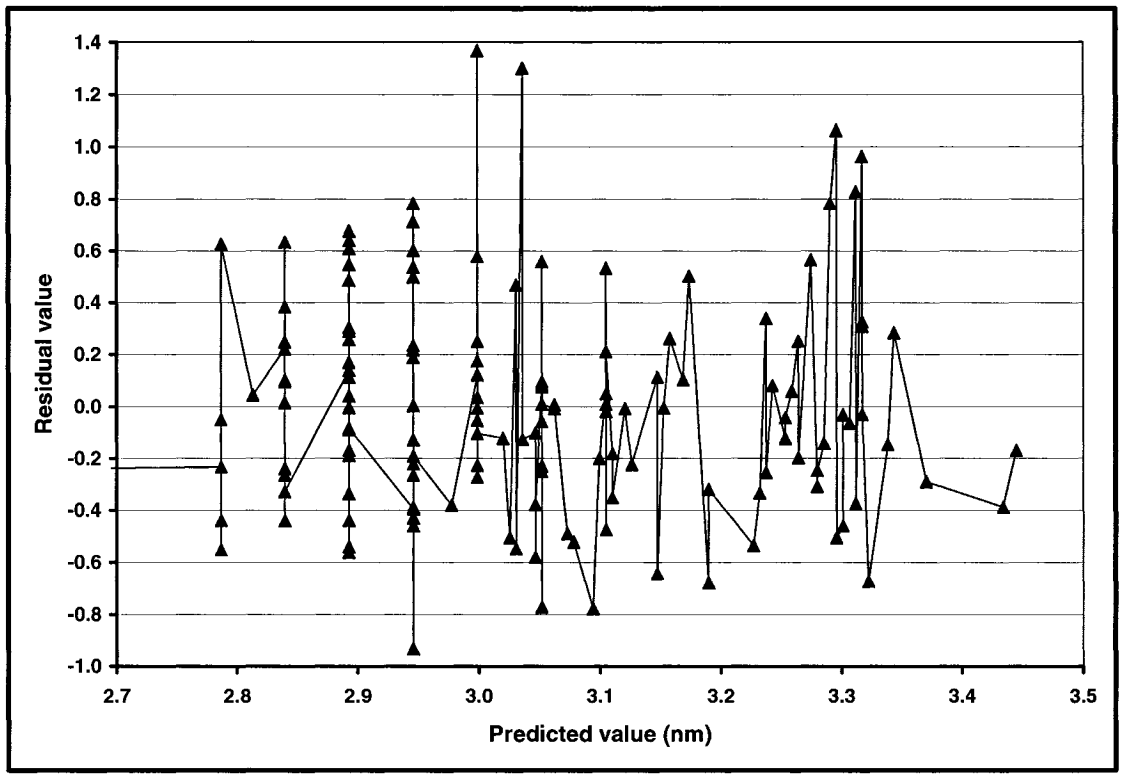

Figure 5.15 SBand residual plots for the one-variable model.

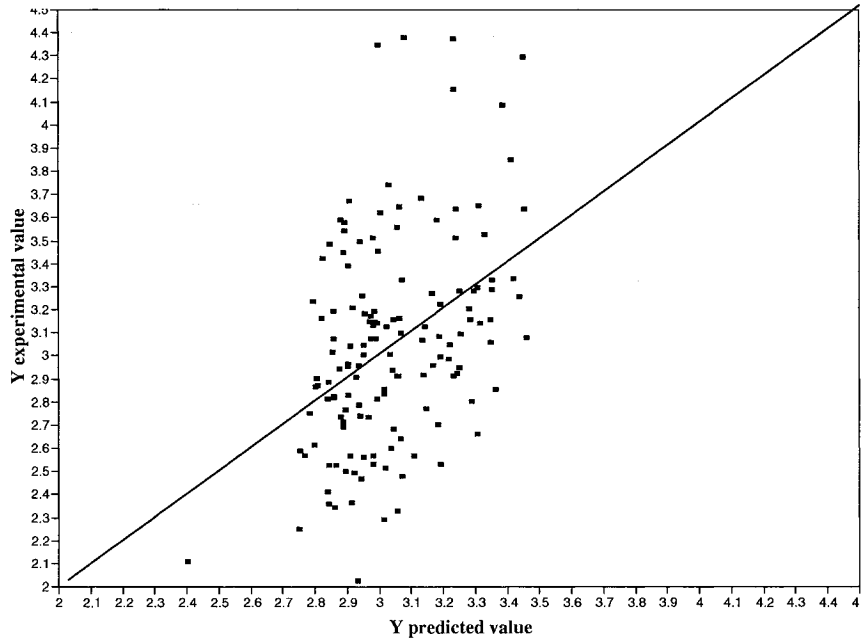

Figure 5.16 Plot of SBand: predicted versus actual values.

5.2 Neural Network (NN)

All the previous models have used a simple linear structure in order to predict some output variables. In some cases, the prediction was very good and, in many other cases, the prediction was too unreliable to be used with confidence in process diagnostic. The reasons for the poor performance of some models may be caused by many sources: (1) the data do not contain the right information to develop an adequate model; (2) the variability in the data is too important such that the pertinent information is indiscernible, and (3) the structure of the model does not have the right degree of complexity to capture the underlying of the process. There is not much that can be done for the first two points. However, for the third point, it is possible to change the structure of the model to examine if better predictions could be obtained. In this section, a general class of nonlinear models, neural networks, will be briefly tested to see if non-linear models could capture more adequately the relationship existing between input and output variables.

Neural networks can be viewed as a general class of non-linear models that possess a certain degree of plasticity that allows these models to mold themselves to the data landscape.

There are different types of connections used between layers, called feedforward and feedback networks. Feedforward NNs allow signals to travel one way only; from input to output. There is no feedback (loops) i.e. the output of any layer does not affect that same layer. Feedback networks can have signals travelling in both directions by introducing loops in the network. Feedback networks are very powerful and can get extremely complicated. Feedforward neural networks have been the most widely applied neural network for modelling and control purposes. In this section a three-layer feedforward neural network is used to model output variables as a function of input variables. A schematic representation of a three-layer feedforward neural network is presented in Figure 5.17. The input vector I is the scaled vector of the independent variables of the

model that is distributed to all functional neurons[17] of the second or hidden layer. The functional neurons of the hidden layer perform two simple tasks: the weighted sum of the inputs and the non-linear transformation of this sum to generate the output of each neuron. The outputs of the hidden layer are then distributed to the next layer where the same two tasks are accomplished to finally generate the scaled outputs or dependent variables of the neural model. Using the nomenclature of Figure 5.17, the neural model can be expressed by the following set of equations:

Hidden layer:

$$H_k = \phi\left(\sum_{j=1}^{J} W_{j,k}\, I_j\right) \qquad 1 \le k \le K-1 \tag{5.2}$$

Output layer:

$$O_\ell = \phi\left(\sum_{k=1}^{K} W_{k,\ell}\, H_k\right) \qquad 1 \le \ell \le L \tag{5.3}$$

Sigmoid function:

$$\phi(x) = \frac{1}{\left(1+e^{-x}\right)} \tag{5.4}$$

Once the number of layers, and number of units in each layer, has been selected, the network's weights and thresholds must be set so as to minimize the prediction error made by the network. This is the role of the *training algorithms*. The historical cases that which have been gathered are used to automatically adjust the weights and thresholds in order to minimize this error. This process is equivalent to fitting the model represented by the network to the training data available. The error of a particular configuration of the network can be determined by running all the training cases through the network, comparing the actual output generated with the desired or target In this section, the weights were determined using the quasi-Newton optimization algorithm and on-line validation with 15% of the data for validation and 85% for training. From an initially random configuration of weights and thresholds (i.e., a random point on the error

[17] The most basic element of the human brain is a specific type of cell, which provides us with the abilities to remember, think, and apply previous experiences to our every action. These cells are known as neurons. The basic unit of neural networks, the artificial neurons, simulates the four basic functions of natural neurons.

surface), the training algorithms incrementally seek for the global minimum. Typically, the gradient (slope) of the error surface is calculated at the current point, and used to make a downhill move. Eventually, the algorithm stops in a low point, which may be a local minimum.

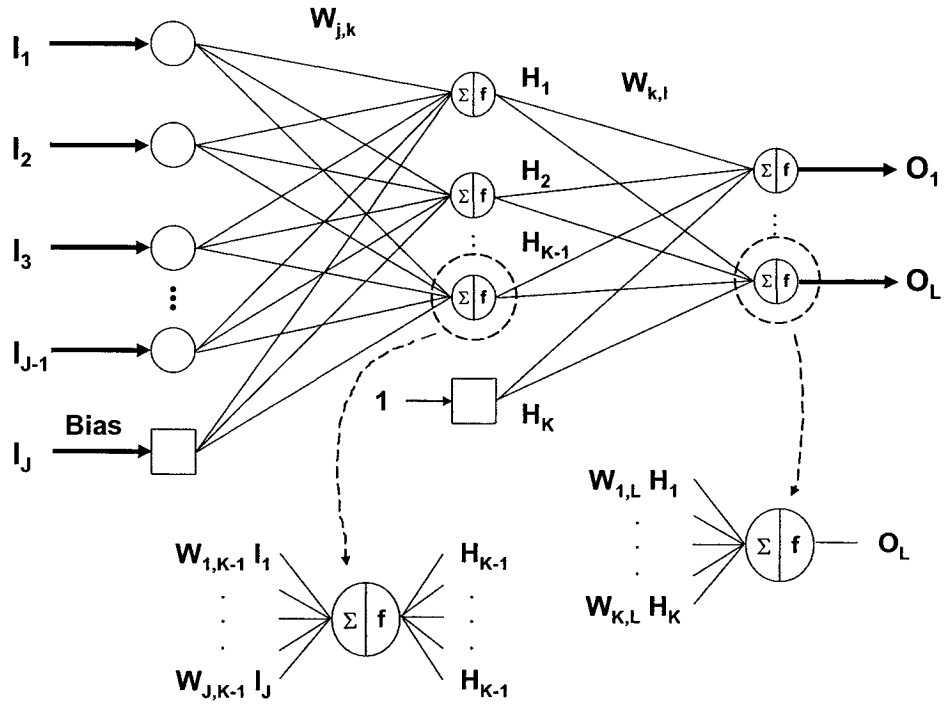

Figure 5.17 Architecture of a neural network.

Neural network models were generated for the SMSR using the same input variables as in the previous section. Table 5-5 gives a summary of the statistics for the models with 1 to 4 input variables obtained with neural networks having different numbers of hidden neurons. In general, the results obtained with neural networks are fairly equivalent to those obtained with linear models since the correlation coefficients are relatively equal. Unlike linear models, neural network models are not unique because there exist more than one set of weights that is the solution of the model. In other words, there exist multiple local minima. In addition, for each solution a random set of data points was chosen for the learning and validation data sets. To test the variation of the solution to this random choice, the neural network model with 4 input variables and 4 hidden neurons was fitted 20 additional times in order to evaluate the mean value and the

standard deviation of the correlation coefficient. The mean value of the 21 correlation coefficients was found to be 0.680 with a standard deviation 0.043. The value for the linear model for the same model was 0.644. Similar results were obtained with the other models. Neural networks did not improve significantly the precision of the models to justify their use in this investigation.

5.3 Implementation Strategy

Models developed in the previous sections of this chapter can be used to predict some output values and their probability of failure during the process sequence. The models can use one or more variables to estimate probability of failure before the manufacture of the wafer is completed. Depending on the accuracy of the models, process engineers could decide not to proceed further with the fabrication of a given wafer or to take remedial action to bring the wafer closer to its specification. The benefit of using a predictive model becomes more attractive when the inputs used by the model are measured early in the wafer process. The efficiency of this strategy strongly depends on the reliability of the models and the quality of the information that was used to generate these models.

To be useful, this early failure-prediction model must have the following constituent:

- Using the inverse model it may be possible to establish the limits of the input variables, and thus create new range of operating conditions in order to meet specifications.
- For the models to be accepted and used by examination staff, they must be simple and easy to understand.
- To yield the greatest benefits, an early-warning system's data must be timely and accurate.

Table 5-5 Summary of statistics of neural networks for SMSR models with 1 to 4 input variables

Number of inputs	Number of points	Input Variable	Number of hidden neurons	σ	έ	Correlation coefficient $(\hat{y}, y)$
1	147	39	2	3.960	-0.255	0.5172
			3	3.873	-0.334	0.5519
			4	4.018	0.092	0.5087
			5	3.884	0.169	0.5464
			6	3.861	-0.051	0.554
2	138	39, 33	2	3.449	-0.160	0.6197
			3	3.523	0.168	0.5992
			4	3.645	-0.036	0.5586
			5	8.490	1.134	0.5155
			6	3.627	-0.237	0.5651
3	138	39, 43, 33	2	3.431	-0.012	0.6252
			3	3.338	0.074	0.6574
			4	3.220	0.464	0.6856
			5	3.370	-0.115	0.642
			6	2.930	-0.013	0.7452
4	137	39, 43, 33, 36	2	3.374	-0.122	0.6407
			3	3.293	-0.063	0.6636
			4	2.914	0.053	0.7486
			5	2.998	-0.005	0.7313
			6	3.842	0.524	0.6205

To achieve this objective, one or more models are used with their inputs from as early as possible in the process sequence in order to provide information to process engineers to allow them to take the necessary action. This strategy is demonstrated using a few of the most frequent failures

5.3.1 *SMSR Failure Mode*

Results presented in Chapter 4 have shown that one of most frequent failures is SMSR (Side Mode Suppression Ratio in Decibels), which is defined as the ratio between the main device lasing wavelength and the next brightest peak. The grating is the filter that promotes one particular wavelength to dominate, and to suppress all the others. SMSR is a measurement of the strength of the grating. This strength is dependent on the grating depth, the natural lasing wavelength of the "First Growth", and the wavelength of the stack after grating overgrowth.

This grating strength depends on the grating quality, which is defined by the depth of the grating, and the uniformity of the grating along the device, the grating pitch, and the Mark to Space ratio. Also as the difference between the grating pitch wavelength and the First Growth wavelength increases, the grating strength decreases.

The last variables that have an effect on grating strength are the MOCVD overgrowth on top of the grating, and the wavelength match of this material to the previous grown layers and the grating.

As the most frequent device failure is by far the SMSR, the benefit of a prediction model for this failure would be enormous. During the correlation exercise of all the input data to the output data, the input variables that most affect SMSR do in fact control its manufacturing sequence. It is fortunate that these input process variables are associated with process steps that occur early in the process. These variables are the wafer first growth wavelength, the grating and the overgrowth. With these variables, a prediction can be done for SMSR before the wafer even enters the main wafer fabrication process centre. In the previous section, it was shown that all these input variables have reasonable correlation coefficients with SMSR. The highest correlation coefficient is with the grating depth with a correlation coefficient of 0.499. This is not a very high correlation coefficient but still provides some information as to the probability of failure. Table 5.2 shows that the grating depth as predicted by the models should be higher than 0.785 (SRS units) for the SMSR to exceed the threshold value of 40 dB.

Table 5.3 presents the number of times the one-input and two-input models predicted a failure correctly. The success rates in predicting the right outcome was higher than 63% in both cases. The greater fraction of these wrong predictions occurs in the vicinity of the 40 dB threshold.

Table 5-6 Impact of grating depth on SMSR

1 VARIABLE (grating depth)		**2 VARIABLES** (grating depth and lasing wavelenght)	
Grating Depth	**SMSR**	**Grating Depth**	**SMSR**
0.500	59.90	0.500	59.00
0.600	52.90	0.600	52.40
0.700	45.90	0.700	45.70
0.785	40.00	**0.785**	40.10
0.800	38.90	0.800	39.10

Table 5-7 Summary of SMSR Model Failure prediction

Number of Input Variables	**Wrong predicted wrong**	**Wrong predicted good**	**Good predicted wrong**	**Good predicted good**
1 VARIABLE (grating depth)	45.00	25.00	28.00	49.00
2 VARIABLE (grating depth and lasing wavelenght)	34.00	28.00	23.00	53.00

5.3.2 *SBand Failure Mode*

Another important failure code is the SBand (Stop Band). The SBand is defined as the wavelength in nm between the main lasing wavelength peak and the second largest peak. The value of this measurement is the combination of all the MOCVD growth layers, the ridge width and dielectric clad, and the grating interaction with them. The one-variable SBand model, with correlation coefficient of 0.386, has a success rate of 94% in predicting the right outcome, i.e. 9 wrong predictions out of 145 wafers. Table 5.4 shows the impact of the depth on the value of SBand. Table 5.5 presents the number of times the one-input model would have predicted correctly a failure. This result should be interpreted with caution since out of the 10 recorded failures, only one was predicted correctly. These failures occurred very close to the SBand threshold value where the probability of being wrong is much higher. On the other hand, a reliable prediction can be made for a wafer that was accepted. It is interesting to note that the same specification for the grating depth, i.e. a threshold of 0.785 (SRS units), was also obtained for the SBand model.

Table 5-8 Impact of grating depth on SBand

1 VARIABLE (grating depth)	
Grating Depth	**SBand**
0.500	4.54
0.600	4.01
0.700	3.48
0.785	**3.03**
0.800	2.95
0.900	2.42

Table 5-9 Summary of SBand Model Failure prediction

Number of Input Variables	Wrong predicted wrong	Wrong predicted good	Good predicted wrong	Good predicted good
1 (grating depth)	1	9	0	136

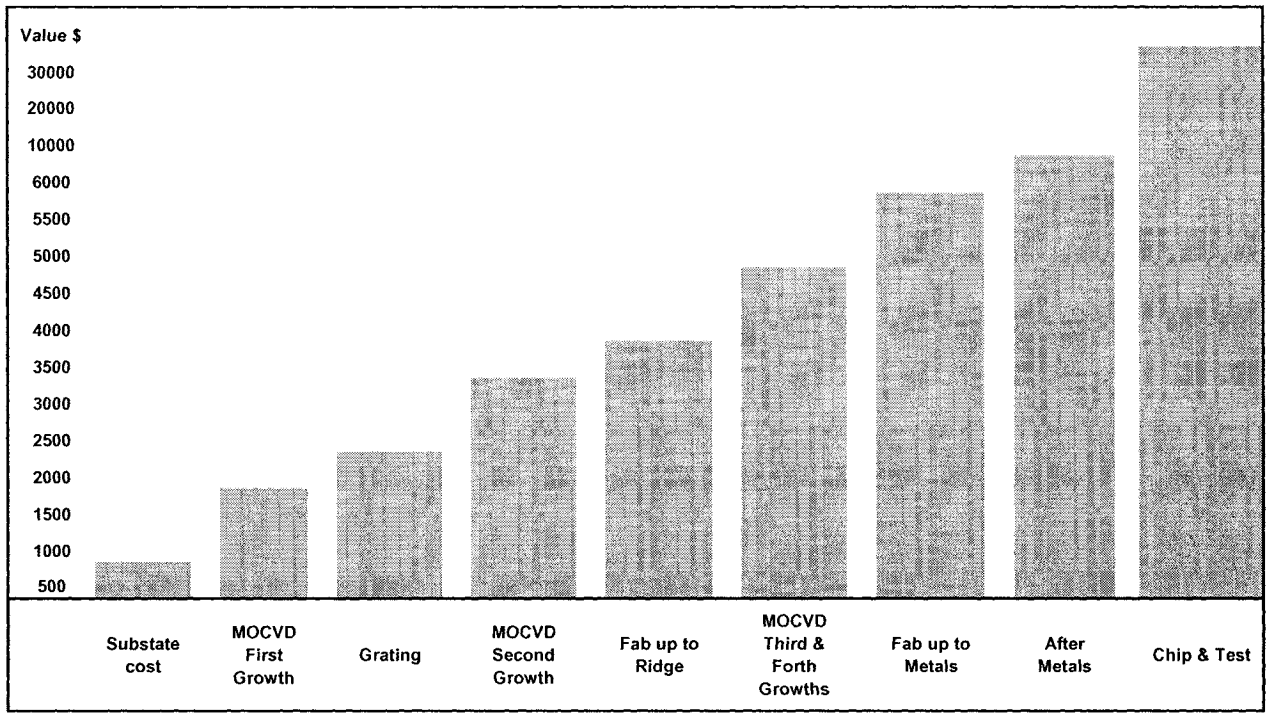

Figure 5.18 Summary of manufacturing costs

Figure 5.18 provides an insight of the cost of fabrication of a wafer. This analysis helps in assessing the advantage of using a prediction model to diagnose possible failures. Using the historical data bank of the BHet wafers, there were a total of 147 wafers from which 77 were accepted and 70 were discarded due to SMSR. From the results of the one-variable SMSR model, 74 wafers would have been allowed to proceed. From those 74 wafers, 49 would have passed the final test and 25 would have failed. Out of the 74 wafers that would have been rejected, 28 would have passed. This strategy could be made more permissive or rigid depending on the cost analysis.

The saving would be the cost of processing the extra 73 wafers, minus the cost of the 28 that did pass the test but would not have been allowed to proceed further. The net gain in cost of the 45 Fab processed wafers, at $6000 per wafer, would be $200 700. Realistically in both cases, SMSR and SBand, the models allow to predict with a fair to moderate probability the actual measured value.

While these predictive models cannot replace entirely the on-site examination, they allow employees to have first-hand evaluation of operating procedures, levels of risk-taking, and long-range strategic planning. An effective warning system can complement the on-site examination process by identifying troubled places that need early examination or possible intervention.

The goal of these models is to identify a process weakness in production at the initial stage of the process and to warn interested parties of its potential failure before they have a major impact on the cost.

We also compared the prediction results of SMSR and SBand with different one-variable models. Different models were implemented in the way illustrated in the previous section and according to equation (5.1) attempts to use models, without including the grating depth, did not result in successful predictions.

Following the Opto Electronics industry's explosive growth, and subsequent freefall, we have entered a period of reduced demand and customer required product cost reduction. Increased wafer size and the move from batch tools to the latest generation of single wafer equipment have significantly reduced the cost of the chip on wafer manufacture, leaving sixty to seventy five percent of the cost of the finished device coming in the individual chip building and testing.

Accurate failure-prediction models, such as those developed in this study, have massive advantages for engineers involved in production. Firstly, relationships between the process inputs and tested outputs have been identified. Secondly, hard specification values can be defined for critical inputs, which will ensure an increased yield in the final test process. Undoubtedly the most important advantage is the cost saving due to the model being able to predict the outcome of the test results before the wafer fabrication is completed. Process engineers, using this early-warning strategy, could decide whether to

proceed with the next step of fabrication without large parts of being processed through the Fab and Test processes.

CHAPTER 6

CONCLUSIONS

The objective of this thesis was to develop prediction models, based on input process variables, to forecast as early as possible key output variables and probabilities of failure. To achieve this objective, a series of steps were followed. The first step, and the most time-consuming, was to assemble a complete databank of the entire wafer fabrication. This step was tedious because process information was scattered in different databanks and changes in the way the information was stored frequently occurred over the years. The second step was to perform data mining using statistical tools to identify process variables that have strong correlations and to develop predictive models that can be used in an early-warning diagnostic strategy.

Two different types of models, linear models and neural networks, were used to relate the seven failure codes and the 37 input variables. The practical relevance of this research lies in the predictions that can be realized using these models as a source of information on the state of the process. These predictions heavily rely on the quality of the process data. Despite the inherent variability of the industrial databank used in this work, it was possible to propose useful models that could assist plant engineers to better control the process.

- It was possible to determine that some output variables had sufficiently high correlation coefficients with some input variables to develop predictive models that could serve as a diagnostic tool.
- Neural Networks provided slightly better predictions than linear models. However, given the variability of the databank, the use of linear models is recommended because of their simplicity and ease to understand from an operator point of view.
- In case of SMSR results indicate that grating depth is the most important process variable to the success yield improvement.

- The predictive models can be used to detect the weakest point in the manufacturing of the BHet, and provide good feedback to the engineering personnel insight as to the reasons of wafer failure.
- For most output variables, and failure probability models with one or two process input variables were sufficient. Most models, however, had a very low regression coefficient and were not very useful as a diagnostic tool. Fortunately, the highest correlation and the more accurate models were obtained for the SMSR, which account for the most frequent failure.
- One major disadvantage of the linear model is that the prediction is less accurate for values closer to lower specification limit, which can be attributed to the fact that an average value for an entire wafer was used.
- A strategy has been presented to use these models for early-warning diagnostic.
- This exercise highlighted a serious problem with the data collection methods used for this product at Nortel. The multiple databases and changes in identifiable tracking numbers through the process and time, made the data collection extremely time consuming and very manual. To use the predictive models on-line, it would be necessary to identify the wafer with a single unique number and to record in a single databank all the data with a strict protocol for the entire process.

REFERENCES

- Bose, M., Basa, D.K., Bose, D.N., "Effect of ammonia plasma pretreatment on the plasma enhanced chemical vapor deposited silicon nitride films", Department of Physics, Utkal U., Bhubaneswar, Advanced Technology Center, Indian Inst. of Technology, Kharagpur, 48 (2001) 336-341.
- Briggs, R. D., Howard, A. J., Baca, A.G., Hafich, M.J., Vawter, G. A., "A study of P-type ohmic contact to InAlAs / InGaAs Heterostructure", Sandia National Lab., Center of Compound Semicond. Technology, Thin Solid Films, 290-291 (1996)5.8-512.
- Cambell, S.A., "The Science and Engineering of Microfabrication, 2nd Ed., Oxford University Press (2001).
- Dautremont, W.C. S., and Feldman, L.C., "Surface Structural Damage Produced in InP (100) by R.F. Plasma or Sputter Deposition", Electronics and Optics, Thin Solid Films, 105 (1983)187-196 (1983).
- Gromova, T.I., Davydova E.I., Uspenslkii, M.B., and Shishkin, V.A., "SEM evidence for near-surface carrier passivation by hydrogen in CH_4/H_2 reactive ion etching p-InP", Analytical Center, Research and Development Institute'Poljus', Semicond. Sci. Technol, 10 (1995) 536-539.
- Hong, S. J., and Sholom, M. W., "Advances in Predictive Model generation for Data Mining", IBM Research Report RC-21570.
- Ivey, D. G., Jian, P., "Microstructural analysis of Au/Pt/Ti contacts to p-type InGaAs", Department of Mining, Metallurgical and Petroleum Eng., Bell Northern Research, Journal of Materials Science , Materials in Electronics 6 (1995)219-227
- Kachigan, K., "Multivariate Statistical Analysis", A Conceptual Introduction, 2nd Ed., Radius Press (1991).
- Kapon, E., "Semiconductor Lasers 1, fundamentals", Optics and Photonics, Academic Press (1999).

- Kaman, V., Student Member, IEEE, Reynolds, T., Petersen, A., and Bowers, J. E., Fellow, IEEE, "A 100-kHz to 50-GHz Traveling-Wave Amplifier IC Module", IEEE Microwave and Guided Wave Letters, Vol. 9, No.10, October 1999.
- McLean, D.D., Burn, N.B., "Data Collection and Interpretation", Course Note, (2002).
- Medou, M. J., "Fundamentals of Microfabrication", CRC Press (1997).
- Mierry, de P., Etchegoing, P., and Stutzmann, M., "Plasma damage and acceptor passivation in D_2-plasma-treated InP Zn: A photoluminescence and ellipsometry study", Max-Planck Institut für Feskörperforshung, Physical Review B., vol. 49, No. 8 (1993).
- Montgomery, D.C., "Introduction to Statistical Quality Control", 4th Ed., Wiley (2001).
- Simon, K. J., and Small, R., "The Effect of DI Water and Intermediate Rinse Solution on Post Metal Etch Residue Removal Using Semi-Aqueous Cleaning Chemistries", Ekc Technology, Inc., Solid State Phenomena Vols. 76-77 (2001)pp. 307-310, Switzerland.
- Thibault, J., Van Breusegem V., and Cheruy, A., "Online Prediction of Fermentation Variables Using Neural Networks", Biotechnol. Bioeng., 36, 1041-1048 (1990).
- Van Zant, P., "Microchip Fabrication", A Practical Guide to Semiconductor Processing 3rd Ed., McGraw-Hill, (1997).
- Zhao, L., Chen,Y., and Shaffner, D. W., "Comparison of Logistic Regression and Linear Regression in Modeling Percentage Data", Applied and Environmental Microbiology , May 2001, p. 2129–2135 Vol. 67, No. 5.
- http://www.denselight.com, (June, 2003)
- http://www.intenseco.com, (June, 2003)

Appendix A

List of Columns in the Data Bank

COLUMN NUMBER	NAME	COLUMN NUMBER	NAME
1	WAFERID	31	Wavelenght Standard Deviation
2	ITH2L	32	Grating Pitch Calcualtion
3	REAR POWER	33	Lasing Wavelenght
4	I_5MW	34	Grating Period
5	EFF_M2	35	Grating Exposure Energy
6	POWERSAT_10MW	36	Grating Exposure Time
7	KINKCURRENTM1	37	Grating Etch Time
8	KINKPOWERM1	38	Grating Blitz Etch Time
9	VF_5MW	39	Grating depth from SRS
10	VF_10MW	40	STDEV of depth from SRS mapper
11	PKWL_ITHX	41	Overgrowth Layers,Intensity StDev
12	SMSR_5MW	42	Overgrowth Single Pt Wavelength
13	SBAND_5MW	43	Overgrowth Layers,Single Pt Intensity
14	Pass %	44	Overgrowth Layers,Single Pt UpperHM
15	SMSR	45	Overgrowth Layers,Single Pt Wavelength
16	RearP...too high	46	Overgrowth Layers,Average Intensity
17	Sband...too low	47	1000A SiO2 Thickness
18	FB_Tracking	48	500A SiN Thickness
19	Bragg	49	Ridge Resist CDs
20	RearP...too low	50	Ridge After Etch CDs
21	Ith...too high	51	3000A SiO Thickness
22	QWQB	52	Ridge heights 1
23	ZOM	53	Ridge heights 2
24	1st growth on Lasers,Avg PL Wavelength	54	Ridge heights 3
25	1st growth on Lasers,InP Peak	55	2500A SiO2 Thickness
26	Intensity Standard Deviation	56	P-metal Average Thickness
27	Single Pt FWHM	57	EP-Metal Thickness
28	Single Pt Intensity	58	Polish Average Thickness
29	Single Pt UpperHM	59	N-metal Average Thickness
30	Single Pt. Wavelenght		

Appendix B

Data Bank

1	2	3	4	5	6	7	8	9	10	11	12	13
WAFERID	ITH2L	REAR POWER	I_5MW	EFF_M2	POWERSAT_10MW	KINKCURRENTM1	KINKPOWERM1	VF_5MW	VF_10MW	PKWL_ITHX	SMSR_5MW	SBAND_5MW
A-2931-2	9.934	2.905	33.646	0.222	1.27	115	22.345	0.861	0.952	1581.6	34.556	2.928
A-3255-8	8.642	2.342	29.508	0.256	0.398	100.554	23.345	0.848	0.929	1537.9	40.29	3.06
A-3311-2	7.773	2.21	30.034	0.246	1.007	110.325	24.917	0.853	0.941	1541.5	46.208	77.948
A-3327-5	9.429	2.122	33.149	0.229	1.025	111.043	22.931	0.852	0.926	1530.4	45.245	3.26
A-3346-2	8.428	2.32	29.944	0.252	0.995	92.405	21.149	0.84	0.918	1547.7	42.783	3.498
A-3346-4	9.538	2.069	29.975	0.259	0.994	112.978	26.159	0.851	0.938	1548.9	42.338	3.055
A-3346-5	8.865	2.733	31.986	0.246	0.846	106.515	23.483	0.862	0.95	1541.5	46.685	3.516
A-3346-6	9.394	2.185	30.677	0.253	0.849	80.849	18.587	0.833	0.905	1546.3	44.869	3.319
A-3347-4	9.157	2.297	29.902	0.253	1.218	89.183	19.736	0.827	0.899	1548.4	38.184	3.07
A-3350-4	11.829	2.284	30.163	0.288	0.894	111.667	26.966	0.86	0.923	1549.8	35.684	2.098
A-3352-2	8.066	2.102	29.148	0.248	1.308	111.292	25.008	0.872	0.96	1541.4	42.753	3.144
A-3353-2	8.691	2.951	29.428	0.264	-0.6	108.13	26.214	0.841	0.921	1532.1	43.308	3.131
A-3353-3	7.553	2.214	28.192	0.259	0.843	90.744	21.433	0.842	0.916	1533.6	46.93	3.839
A-3355-6	8.109	2.373	31.112	0.234	9.789	79.635	17.056	0.881	0.97	1530.5	50.665	4.281
A-3356-4	9.679	2.216	31.119	0.25	1.106	84.057	19.021	0.852	0.935	1532.7	44.524	3.243
A-3357-4	7.836	2.112	29.195	0.249	1.125	83.726	19.286	0.842	0.925	1525.8	41.879	2.942
A-3357-8	7.086	1.878	27.67	0.26	1.043	112.27	26.668	0.83	0.9	1532.5	45.673	3.626
A-3365-1	7.657	2.604	29.67	0.248	1.464	80.107	18.791	0.833	0.909	1538.3	45.412	3.577
A-3366-5	8.709	2.253	32.093	0.232	1.342	83.193	17.724	0.841	0.92	1537.9	45.431	4.074
A-3366-6	6.722	2.173	29.957	0.236	1.325	69.609	15.212	0.834	0.912	1537.4	46.391	4.36
A-3370-1	8.632	2.178	30.715	0.247	1.577	109.511	24.55	0.857	0.947	1541.5	43.869	2.842
A-3373-8	9.394	2.393	32.432	0.235	1.372	113.318	23.923	0.857	0.948	1567	46.163	3.644
A-3376-7	9.96	2.929	31.555	0.25	1.217	79.851	17.999	0.837	0.911	1549.2	40.446	2.898
A-3425-4	12.676	2.106	37.651	0.214	4.602	113.738	19.939	0.952	1.054	1574.3	45.588	3.112
A-3426-4	11.574	2.3	33.275	0.243	0.876	78.77	16.36	0.831	0.903	1577.6	43.723	3.418
A-3427-2	13.743	1.988	36.735	0.233	1.955	113.396	22.567	0.873	0.96	1586.4	48.246	2.973
A-3427-3	10.738	2.257	33.796	0.229	6.108	110.117	20.959	0.908	1.004	1586.4	46.461	3.081
A-3427-5	10.712	2.345	33.618	0.234	1.023	92.566	19.039	0.855	0.945	1584.9	44.304	2.792
A-3427-8	13.33	2.883	34.788	0.244	1.262	88.059	18.097	0.845	0.923	1585.9	35.917	2.899
A-3428-1	12.989	2.401	34.577	0.245	1.143	110.044	22.89	0.845	0.921	1595.2	41.334	2.945
A-3429-8	11.622	3.368	34.811	0.229	2.249	112.189	22.192	0.872	0.971	1600.9	35.001	2.555
A-3430-1	13.241	2.191	36.837	0.228	2.881	94.73	18.398	0.84	0.919	1600.4	42.658	3.148
A-3430-6	13.819	1.647	37.813	0.217	5.31	94.253	16.935	0.918	1.022	1598.7	48.914	3.675
A-3431-8	12.409	2.353	34.945	0.235	0.296	109.062	21.897	0.853	0.939	1598.3	42.4	3.153
A-3434-1	8.593	2.086	29.797	0.252	1.11	114.344	26.022	0.842	0.917	1550.3	44.625	3.273
A-3437-5	9.912	3.021	32.245	0.237	1.987	84.694	17.698	0.831	0.906	1545.7	36.219	2.631
A-3438-3	8.605	2.984	30.813	0.24	0.322	86.421	19.058	0.83	0.904	1546.8	34.506	2.505
A-3438-5	11.611	2.665	32.726	0.251	0.74	88.709	19.443	0.837	0.908	1541.1	31.971	2.585
A-3439-2	9.632	2.523	31.108	0.251	1.213	84.524	18.923	0.836	0.911	1541	37.406	2.759
A-3439-4	7.386	2.595	29.315	0.246	0.971	81.343	18.859	0.831	0.91	1539.1	42.017	3.212
A-3440-4	8.125	2.437	28.471	0.264	0.7	80.883	19.901	0.826	0.897	1539.9	41.864	3.067
A-3440-5	7.139	2.011	28.737	0.246	0.835	112.914	25.558	0.825	0.895	1536.7	41.91	3.27
A-3440-7	10.575	2.75	32.705	0.242	1.619	88.215	18.804	0.835	0.908	1539.7	36.403	2.317
A-3440-8	8.33	2.309	28.986	0.261	-2.344	97.806	23.23	0.835	0.91	1539.6	42.227	3.324
A-3465-3	13.685	1.585	41.594	0.184	7.503	98.166	14.639	0.942	1.059	1599	50.485	4.337
A-3466-8	16.026	2.872	39.352	0.23	2.519	78.231	14.993	0.839	0.914	1601.5	36.353	2.598
A-3467-4	10.92	3.115	33.909	0.228	2.77	111.249	21.672	0.878	0.983	1600.9	32.473	2.349
A-3467-6	13.085	2.13	37.198	0.218	5.306	113.382	20.275	0.903	1.005	1598.8	46.784	2.903
A-3467-8	16.56	-54.309	39.621	0.228	3.137	89.064	16.576	0.85	0.933	1601.4	37.435	2.551
A-3468-1	11.393	1.994	35.874	0.221	4.64	111.261	21.055	0.888	0.98	1586.8	47.476	3.288
A-3468-2	14.404	2.207	38.906	0.212	4.417	111.134	19.199	0.914	1.001	1586.6	45.321	2.858
A-3468-4	14.528	2.354	38.676	0.213	4.422	110.034	19.309	0.904	1.002	1585.7	43.754	2.468
A-3469-1	10.298	2.255	32.077	0.24	2.326	113.516	23.509	0.87	0.961	1593.4	44.02	3.032
A-3469-3	10.049	2.396	31.64	0.239	0.769	111.043	23.603	0.837	0.904	1551.9	34.989	2.558
A-3470-8	13.63	2.561	37.244	0.222	4.337	95.939	17.268	0.998	1.114	1588.4	41.669	2.558
A-3471-2	11.476	2.642	34.144	0.241	2.791	102.726	21.363	0.865	0.957	1585.9	42.808	2.899
A-3471-8	10.776	2.853	33.523	0.233	1.764	110.126	22.149	0.872	0.967	1582.8	42.388	2.602
A-3472-4	10.726	2.337	32.152	0.246	1.235	112.152	23.865	0.862	0.948	1583.5	41.734	2.704
A-3472-5	12.307	2.443	36.061	0.224	8.273	111.493	20.976	0.914	1.012	1583.9	46.622	3.034
A-3472-8	13.276	2.439	36.552	0.222	4.864	114.683	20.491	0.948	1.047	1581.9	39.997	2.485
A-3473-1	10.993	3.68	33.787	0.236	3.404	108.519	21.747	0.841	0.919	1599.3	34.698	2.237
A-3476-5	9.822	2.522	31.329	0.248	1.356	110.497	24.675	0.816	0.875	1551.3	35.662	2.669
A-3476-6	9.788	2.844	31.177	0.254	0.204	77.518	17.887	0.843	0.92	1553.2	43.556	3.148
A-3476-8	8.108	2.717	31.619	0.243	6.059	77.271	17.373	0.851	0.931	1552.8	44.645	3.627
A-3478-4	9.437	3.029	31.259	0.246	0.823	102.907	22.729	0.845	0.919	1548.4	37.946	2.91
A-3479-1	10.326	2.636	31.562	0.251	0.752	106.139	23.791	0.85	0.929	1546.4	31.363	2.013
A-3479-2	10.246	3.533	32.878	0.238	2.029	87.722	18.86	0.848	0.932	1547.9	36.009	2.521
A-3568-4	10.923	3.142	33.674	0.233	1.023	108.971	22.153	0.841	0.933	1593.7	35.119	2.692

1	22	23	24	25	26	27	28	29	30	31	32	33
WAFERID	QWQB	ZOM	1st growth on Lasers,Avg PL Wavelength	1st growth on Lasers,InP Peak	Intensity Standard Deviat	Single Pt FWHM	Single Pt Intensity	Single Pt UpperHM	Single Pt Wavelength	Lasers,Wavelength Standard Deviation	Pitch calculation	Enter Lasing WaveLength
A-2931-2	144	-703.5	1002.9	1540.4	64.8	75.4	949.3	1572	1536.2	1.1	238	1517
A-3255-8	156	-1010	1031.2	1557	118.8	71.3	1050.2	1585.3	1555.4	1.17	0	1557
A-3311-2	149	-925	806.1	1563.6	106.4	69.5	792.9	1591.1	1562.2	1.84	0	1563.6
A-3327-5	154	-1017.9	958.3	1602.6	89.7	77.6	860.7	1635.2	1604.6	1.63	248.1	1579.5
A-3346-2	154	-930	1070.6	1566.6	121.8	75.3	998.6	1600.8	1568.6	1.06	243.2	1548.5
A-3346-4	155	-920	1058.2	1567.9	127.1	71.1	903	1599.7	1569.8	1.14	243.2	1548.5
A-3346-5	155	-900	1059.2	1563.7	120.8	74.7	966.9	1599.1	1565	1.37	242.2	1542.1
A-3346-6	152	-920	1174	1564.8	124.1	75.9	1088.2	1597.7	1564.8	1	243	1546.9
A-3347-4	154	-931.8	1005.4	1566.7	110.7	71.5	876.2	1600.5	1570.8	1.09	243.2	1548.5
A-3350-4	154	-917.3	1162.6	1574.1	117	73.7	1034.5	1607.1	1573	1.05	243.9	1552.5
A-3352-2	157	-965.9	1120.1	1563.7	119.8	76.7	992.9	1600.5	1568.2	1.17	242.2	1542.1
A-3353-2	153	-906.8	1177.6	1552.6	135.7	76.5	1009.4	1590.2	1556.2	1.87	0	1552.6
A-3353-3	152	-911.2	1134.4	1553.7	110.1	71.3	969.7	1587.5	1566	1.02	0	1553.7
A-3355-6	153	-894.1	1207.2	1554	139.5	91.5	1036.7	1596.8	1557.8	2.05	0	1554
A-3356-4	152	-917.1	1288.1	1554.3	141	73.7	1166.9	1587.3	1555	1.21	0	1554.3
A-3357-4	154	-863.7	1222.9	1546.3	135.7	69.8	1114.5	1577.4	1547.6	0.96	239.7	1528
A-3357-8	154	-901.3	1263.2	1552	134.7	73.3	1263.3	1584.1	1553.2	1.05	0	1552
A-3365-1	153	-888.6	927.5	1560.6	111.4	72.5	909.5	1590.2	1559.8	0.98	241.6	1538.2
A-3366-5	154	-881.2	1057.7	1559.2	137.4	77.1	1080.3	1590.6	1558	1.16	241.5	1537.4
A-3366-6	154	-899.2	862	1561	96.5	71.7	822.8	1592	1561.8	0.91	241.6	1538.2
A-3370-1	156	-885	1094.4	1563.8	115.4	75.6	972.2	1599.4	1567.2	1.08	242.2	1542.1
A-3373-8	155	-923	1012.4	1590.1	65.7	77.9	855.9	1628.6	1596.8	2.62	246.4	1568.8
A-3376-7	160	-875	1199.1	1566.8	150.7	75.2	1139.4	1602.4	1570.6	1.11	243.2	1548.5
A-3425-4	151	-895.8	568.6	1598.9	72.9	69.4	476.4	1633.4	1605	2	247.7	1577
A-3426-4	158	-855	639	1602.3	76	78.9	574.1	1638.6	1610.8	2.46	248.1	1579.5
A-3427-2	158	-850	641.1	1609.7	92.5	72.1	546.9	1640.3	1613.2	2.83	249.8	1590.4
A-3427-3	157	-855	628.8	1609.7	94.7	71.6	550.2	1641.6	1616.6	2	249.8	1590.4
A-3427-5	157	-815	638.2	1609	86	68.9	486.8	1640.2	1612.4	2.64	249.7	1589.6
A-3427-8	157	-815	689.1	1606.3	87.4	71.5	591.1	1639.5	1611.8	1.69	249.4	1587.9
A-3428-1	161	-885	571	1618.5	100	65.3	454.8	1643.2	1621.8	3.17	251.2	1598.9
A-3429-8	156	-830	580.8	1620.6	75.5	69.6	519.9	1645.2	1624.2	2.41	252.4	1601.5
A-3430-1	162	-915	682.1	1622.4	101	69.4	562.5	1647.1	1625.4	2.38	252.1	1604.9
A-3430-6	158	-805	685.7	1622.6	87.8	69.1	626	1645.4	1623.6	1.63	252	1604
A-3431-8	159	-870	651.3	1622.4	87.7	62.8	448.4	1647.2	1628.6	1.91	251.8	1603.2
A-3434-1	156	-845	914.1	1570.6	102.9	72.8	819.6	1605.8	1575.6	2.53	243.6	1550.9
A-3437-5	159	-879	908.2	1566.5	101.8	76.5	862.9	1604.6	1572	2.19	243.1	1547.7
A-3438-3	160	-928.6	844.9	1566.5	96.4	72.4	759.8	1599.8	1570.2	1.23	243.1	1547.7
A-3438-5	160	-909.8	922	1561.7	101.7	74.2	788.7	1598.8	1568.4	1.86	241.9	1539.8
A-3439-2	160	-904.3	898.5	1560.1	102.4	71.8	684.4	1595.3	1562.4	2.11	241.6	1538.2
A-3439-4	159	-900.5	870.1	1560.1	117	71.1	704.7	1596	1565	1.85	241.6	1538.2
A-3440-4	160	-904.2	1559.5	-337	111.4	73.2	793.5	1594.9	1563.6	2.31	241.6	1538.2
A-3440-5	160	-920.9	1561.7	-323.1	104.6	74.4	745.5	1597.3	1566.8	2.02	241.9	1539.8
A-3440-7	160	-919.1	1562.7	-329.3	97.6	70.5	777.5	1596.4	1567.8	2.08	241.9	1539.8
A-3440-8	160	-916.9	1560.9	-342.1	99.5	70.9	664.7	1597.3	1568.4	2.14	241.6	1538.2
A-3465-3	158	-915	1621	0	71.9	68.2	602.8	1647.3	1626	1.22	252.1	1604.9
A-3466-8	159	-905	1621.7	0	61.8	65.7	531.3	1647	1627	1.77	252	1604
A-3467-4	159	-905	838.6	1621	85.9	68.8	780.8	1644.4	1623.4	1.56	252.3	0
A-3467-6	160	-905	1621.9	0	87	73	789.5	1645.8	1623.8	1.72	252	1604
A-3467-8	158	-915	1623.7	0	66.2	66.4	578.4	1646.6	1625.8	1.21	252.4	1606.6
A-3468-1	158	-865	1610.3	0	113.7	74.6	832	1640.1	1613.6	1.52	250	1591.3
A-3468-2	157	-860	1611.4	0	98.9	76.4	969.3	1640	1611.4	1.03	250	1591.3
A-3468-4	158	-865	1609.2	0	116.9	80.2	920.8	1642.9	1612.8	1.41	249.8	1590.4
A-3469-1	158	-880	1614	0	102	76.6	928.8	1642.9	1615	1.61	251.1	1593.8
A-3469-3	156	-880	1614.2	0	88.3	71.6	835.7	1644.4	1619.4	0.95	251.4	1593.8
A-3470-8	157	-885	1612.9	0	110.7	74.9	897.8	1644.1	1616.4	1.58	250.2	1593
A-3471-2	158	-918.2	1609.5	-2620	102.8	71	853.2	1639.2	1611.4	1.47	249.8	1590.4
A-3471-8	155	-885.7	1605.4	-2625.7	98.7	78.2	919.3	1640.1	1609.8	1.42	249.4	1583.7
A-3472-4	157	-899.2	1605.2	-2640.3	106.6	78.3	866.1	1640.3	1609.8	1.43	249.4	1583.7
A-3472-5	158	-907.7	1607.1	-2665.9	112.3	76.4	984.1	1638.2	1609	1.59	249.6	1588.7
A-3472-8	156	-887.2	1604.2	-2679.1	89.9	80.1	1016.9	1639.4	1607.8	1.34	249.2	1586.2
A-3473-1	157	-1010.5	1620.8	-147.2	133.6	75.5	947.9	1643.2	1617.6	1.74	252.3	1601.5
A-3476-5	158	-960.3	1573.3	-908.3	110.4	76.1	1024.7	1606.7	1574.2	1.11	243.9	1552.5
A-3476-6	158	-965.6	1574.2	-854.1	99.6	76.1	1023.3	1607.4	1574.8	1.17	244.1	1554.1
A-3476-8	157	-953.1	1572.1	-898.7	102.9	70.3	885.9	1604.7	1575.2	1.22	244.1	1554.1
A-3478-4	158	-936.6	1567.8	-443.1	161	80.4	2516.1	1600.9	1570	1.06	243.2	1548.5
A-3479-1	160	-975	1565.7	-516	181.8	77.5	1677.2	1602.7	1570.6	1.09	243.1	1547.7
A-3479-2	160	-970	1567.8	-469	163.5	78.3	1643.1	1604	1572	1.17	243.2	1548.5
A-3568-4	161	-1074.4	1617.1	-427.1	59	65.7	511.5	1637	1617.4	1.32	250.8	1596.3

1	34	35	36	37	38	39	40	41	42	43	44	45
WAFERID	Enter GRATING PERIOD	Enter EXPOSURE ENERGY	Enter EXPOSURE TIME	Etch time (sec)	Enter blitz etch time	Grating depth from SRS	Stdev of depth from SRS mapper	Overgrowth Layers,Intensity Standard Deviation	Overgrowth Single Pt# FWHM	Overgrowth Layers,Single Pt# Intensity	Overgrowth Layers,Single Pt# UpperHM	Overgrowth Layers,Single Pt# Wavelength
A-2931-2	238	15	187	28	28	0.769	33.3	8627.8	106.3	27949.5	1571.4	1531.3
A-3255-8	241.6	17.5	372	31	26	0.82	67.2	6166	114	32738.1	1585	1541.4
A-3311-2	242.3	17.5	453	36	26	0.738	56.5	6678.2	111.8	29450.4	1589.9	1548.1
A-3327-5	248.1	14.5	187	29	40	0.762	0	5100.7	122	21911.9	1636.8	1590.7
A-3346-2	243.2	18	573	29	29	0.784	29.9	7255.8	110	34259.2	1599.7	1560
A-3346-4	243.4	18	577	29	29	0.778	23.1	6735.5	109	33486.7	1602.5	1562.7
A-3346-5	242.2	18	578	33	26	0.74	27	8012.5	108	31633.9	1598	1558.9
A-3346-6	243	18	557	33	26	0.741	22	3487.3	112	27723.7	1597.2	1558
A-3347-4	243.4	18	577	29	29	0.778	23.7	5864.2	111	31468.3	1599.8	1560
A-3350-4	243.9	16.83	468.3	28	28	0.911	123.3	4003.7	114	26548.6	1608.8	1568.4
A-3352-2	242.2	18	578	33	26	0.736	29	9142.2	109.4	34752.2	1597.6	1557.8
A-3353-2	240.6	17.5	453	36	36	0.742	43.4	5638.9	112.5	28715.8	1586.5	1543
A-3353-3	240.8	17.5	453	36	36	0.738	38.2	6016.7	111	34091.8	1585.7	1543.7
A-3355-6	240.8	17.5	453	36	36	0.73	50.8	8802.3	132.3	23086.8	1588	1533.8
A-3356-4	240.9	17.5	453	36	26	0.732	27.7	7482.8	109.3	33633.1	1588.7	1546.9
A-3357-4	239.7	10	153	30	30	0.82	8.8	5991.7	108.4	36894.1	1577.4	1537.8
A-3357-8	240.6	17.5	453	36	36	0.73	45.8	8053.8	110.5	31849.8	1584.8	1544.9
A-3365-1	241.7	18	575	33	26	0.745	86	5856.2	107.7	35599.9	1592.4	1553.2
A-3366-5	241.5	18	573	33	26	0.735	23	3729	110	29474.3	1588.8	1549.9
A-3366-6	241.7	18	575	33	26	0.734	28	7013.4	113.8	25786.3	1590.2	1546.9
A-3370-1	242.2	18	578	33	26	0.733	26	6517	111.4	31833.8	1595.4	1556.1
A-3373-8	246.4	17.5	481	36	36	0.73	65.3	6811.3	114.5	29978.7	1626.9	1584.8
A-3376-7	243.4	18	573	29	29	0.786	31	7664.2	110	33888.6	1601.7	1561
A-3425-4	247.8	14.5	188	30	25	0.767	36.1	15510	112	15768.6	1633.3	1592.6
A-3426-4	248.1	14.5	187	29	40	0.76	44.4	8484.3	114	32902.5	1639.8	1599.6
A-3427-2	249.9	14.5	187	27	34	0.737	89.2	11270.7	121	28190.1	1646.8	1601.4
A-3427-3	249.9	14.5	187	27	34	0.72	33	12544.3	120	21102.3	1646.7	1602.3
A-3427-5	249.7	14.5	187	28	34	0.734	41.2	10345.9	118	30711.3	1647.2	1605.7
A-3427-8	249.5	14.5	185	28	31	0.771	39.6	8270	115	30399.2	1644.6	1602.6
A-3428-1	251.1	14.5	212	28	31	0.781	35.9	8770.6	116	33176.4	1658.2	1617
A-3429-8	252.4	15.3	170	26	30	0.83	0.3	7532.8	115.3	34682.7	1657.4	1616.4
A-3430-1	252.1	16	186	30	28	0.78	7.6	6339	117.1	32227.4	1659.9	1616.6
A-3430-6	252	14.5	162	28	0	0.757	42.4	9301.4	120	18203.6	1658.5	1614.9
A-3431-8	251.8	15	183	30	31	0.77	4.4	8581.5	117.6	25431.7	1659.9	1616.5
A-3434-1	243.6	18	575	33	29	0.758	22	6135.8	112.2	43831	1605.7	1565.1
A-3437-5	243.1	14.5	195	28	31	0.77	29.5	9352.5	110	41045.5	1603.5	1563.4
A-3438-3	243.1	14.5	195	28	31	0.762	36.1	9702.4	109	33639.9	1601.8	1562.4
A-3438-5	241.9	14.5	195	28	31	0.776	33	8512.6	110	39435.6	1598.6	1559.9
A-3439-2	241.7	18	563	33	29	0.769	70	10098.7	113	39322.9	1594.9	1554.3
A-3439-4	241.7	18	563	33	29	0.742	34	6356.2	109.3	48326.6	1595.2	1554.3
A-3440-4	241.7	18	563	33	29	0.74	24	5914.3	110.6	41881.1	1595.2	1555.7
A-3440-5	241.9	14.5	195	28	31	0.733	26.2	4749.1	122	9670	1627.9	1580.5
A-3440-7	241.9	14.5	195	28	31	0.772	62.5	9071.8	110	35614.9	1598.7	1561.6
A-3440-8	241.7	18	563	33	29	0.744	36	9478.4	114	38763.1	1595.9	1554.9
A-3465-3	252.2	14.5	139	28	30	0.783	29.1	8452.9	126	15160.1	1658.7	1613.4
A-3466-8	0	0	0	28	31	0.794	51.2	8337.5	120	29234.2	1661	1618.7
A-3467-4	252.3	13.8	130	32	31	0.83	0.2	4474.9	118	27904.5	1658	1615.5
A-3467-6	252	14.5	162	28	0	0.766	48.9	8389.3	127	15918.7	1658.6	1612.4
A-3467-8	252.4	16	186	30	28	0.8	4.9	8627	117.8	21640.7	1661.6	1619.2
A-3468-1	249.9	14.5	186	28	34	0.73	49.6	7652.5	125	24277.8	1649.6	1604
A-3468-2	249.9	14.5	186	28	34	0.825	164.9	9233.9	126	13974.3	1648.7	1602.4
A-3468-4	249.8	14.5	186	28	34	0.781	119.4	6770.2	124	25886.2	1646.2	1601.1
A-3469-1	251.2	14.3	158	36	26	0.81	1.4	5391.9	121.5	27709.7	1651.3	1607.1
A-3469-3	251.5	14.3	158	36	26	0.81	0.2	4801.7	122.2	27732.1	1650.9	1606.2
A-3470-8	250.2	14.5	209	30	35	0.775	23.8	7396.2	127	18715.2	1650.2	1604.8
A-3471-2	249.8	14.5	186	28	34	0.746	37.1	6548.8	124	25430.8	1648.4	1601.9
A-3471-8	249.5	15.3	162	37	25	0.82	0.3	5162	120.9	27396.6	1640.8	1596.2
A-3472-4	249.5	15.3	162	37	25	0.81	0.3	5309.4	119.9	27332.9	1641.7	1596.9
A-3472-5	249.6	14.5	187	27	34	0.737	40.7	8106.6	124	18063.2	1645.5	1600.1
A-3472-8	249.2	14.5	45	28	30	0.784	36.9	6730.3	123	18763.7	1641.2	1598.3
A-3473-1	252.3	14.1	130	32	31	0.83	0	4904.7	116.9	30194.1	1657.9	1615.5
A-3476-5	243.9	16.25	397.5	28	28	0.781	33.9	8542.6	116	50398.8	1607.7	1567
A-3476-6	244.2	14.5	185	28	26	0.761	167.4	9934.1	123	39567.1	1605.7	1561.9
A-3476-8	244.2	14.5	185	28	26	0.725	189.4	8033.9	123	36755.6	1604.2	1561.7
A-3478-4	243.2	18	573	29	29	0.783	28.5	6542.7	117	33283.1	1604.4	1563.5
A-3479-1	243.1	14.5	195	28	28	0.8	85	6542.7	116	35239.6	1603.5	1561.6
A-3479-2	243.2	18	573	29	29	0.785	18.6	6684.8	114	33060.9	1605	1563.5
A-3568-4	250.8	14.5	212	28	31	0.747	102	6363.2	122	34165.7	1655.6	1613.9

1	46	47	48	49	50	51	52	53	54	55	56	57	58	59
WAFERID	Overgrowth Layers,Average Intensity	Thickness for each wafer (1000A SiO2)	Thickness of each wafer (500A SiN)	Ridge litho CD	Ridge after etch CDs	Thickness for each wafer (3000A SiO)	Ridge heights 1	Ridge heights 2	Ridge heights 3	Thickness (2500A SiO2)	Averaage P-metal thickness	EP-Metal thickness (13000A)	Averaage value for polish ticknes	Average value for n-metal
A-2931-2	29381.2	1004.6	492.1	2.04	1.99	2996.7	1.63	3.28	2.99	2476.9	2563	11396	154.1	4561.3
A-3255-8	35310.9	991.6	508.7	2.06	1.96	3121.7	1.58	3.2	2.89	2381.7	2500.3	10609	152.8	4518.3
A-3311-2	33433.6	2059.9	500.5	2.06	2	3012.2	1.75	3.16	2.84	2427.1	2556	10641	155.6	4596
A-3327-5	23462.1	970.4	487.4	1.69	2.03	3055.2	1.55	2.95	2.76	2489	2242	10534	153	4710.2
A-3346-2	33507.7	988.5	519.1	2.07	2.09	3123.8	1.64	3.34	3.01	2555.6	2360.3	10240	153.4	4733
A-3346-4	33085.5	980.9	480.5	2.08	1.93	3025.7	1.5	3.03	2.65	2455.7	2598.3	11395	153.4	4525.3
A-3346-5	32108.3	903.5	508.4	2.06	1.94	3037.3	1.86	3.37	3.03	2510.1	2537	11594	152.8	4634.7
A-3346-6	28324.5	1025.7	495	2.06	2	3062.3	1.68	3.08	2.76	2446.6	2626.3	13791	153.6	4571.3
A-3347-4	33162.4	1025.7	495	2.06	2	3062.3	1.68	3.08	2.76	2446.6	2626.3	13791	154.1	4634.2
A-3350-4	29310.6	990.6	462.4	2.04	1.91	2957.1	1.7	3.35	3.12	2437.9	2446.8	10097	150.8	4661.3
A-3352-2	34865.1	903.5	508.4	2.06	1.94	3037.3	1.86	3.37	3.03	2510.1	2510.2	11472	152.5	4639.2
A-3353-2	31521.3	965.2	493.2	1.97	2.2	3064.2	1.6	2.98	2.68	2482	2688	10902	156.2	4629
A-3353-3	32681.1	991.6	508.7	2.06	1.96	3121.7	1.58	3.2	2.89	2381.7	2500.3	10609	154.1	4518.3
A-3355-6	27061.8	993.8	450.1	1.92	1.86	3121.8	1.62	3.23	2.91	2487.9	2418	11323	152.6	4617.3
A-3356-4	34099.1	993.8	450.1	1.92	1.86	3121.8	1.62	3.23	2.91	2487.9	2418	11323	152	4617.3
A-3357-4	34951.2	984.6	488	2.04	1.93	2988.6	1.61	3.37	3.08	2437	2473.3	11571	155.1	4861
A-3357-8	32132.8	974.3	494.8	2.01	2.32	2967.6	1.61	3.81	3.52	2393.6	2449.7	13074	152.2	4616
A-3365-1	33879.9	1027.9	484.4	2.07	1.93	2945.2	1.7	3.51	3.45	2416.4	2424.3	10916	154.6	4644.7
A-3366-5	28506.1	1025.7	495	2.06	2	3062.3	1.68	3.08	2.76	2446.6	2626.3	13791	153.8	4634.2
A-3366-6	28704.4	1027.9	484.4	2.07	1.93	2945.2	1.7	3.51	3.45	2416.4	2424.3	10916	155.2	4644.7
A-3370-1	33385.5	903.5	508.4	2.06	1.94	3037.3	1.86	3.37	3.03	2510.1	2537	11594	150.8	4639.2
A-3373-8	30209	2059.9	500.5	2.06	2	3012.2	1.75	3.16	2.84	2427.1	2556	10641	156.2	4611
A-3376-7	32334	1028.2	488.8	2.07	1.97	2997.2	1.69	3.34	3.06	2433.2	2525.3	12470	154.4	4608
A-3425-4	24909.6	970.4	487.4	1.69	2.03	3055.2	1.55	2.95	2.76	2489	2242	10534	148.2	4814.7
A-3426-4	34236.5	0	510.4	0	0	0	0	0	2.9	2554.6	2417.7	10484	160	4639
A-3427-2	29471.1	985.4	495.8	2.05	2.01	3008	1.7	2.99	2.74	2448.1	2322.3	12527	155.9	4592.7
A-3427-3	26374.9	0	474.6	0	1.74	2976	1.72	3.76	3.4	2500.8	2428.3	12156	154.6	4650.3
A-3427-5	30139.3	970	498.3	1.7	2.04	3050.1	1.52	3.1	2.71	2384.3	2495.7	27093	147.8	4561.3
A-3427-8	29330.4	1010.5	533.1	2.06	1.96	3007.7	1.66	3.28	2.96	2424.7	2517.3	2824	150.2	4479.7
A-3428-1	30094.5	1040.2	507.7	2.07	1.93	3114.3	1.61	3.2	2.81	2471.5	2524.3	5235	151.1	4604.2
A-3429-8	34883.8	972.9	498.5	1.803	2.064	3019.2	1.64	2.95	2.68	2506.7	2402.3	10706	153.8	4663
A-3430-1	31288.7	967.6	512.2	1.89	1.871	3058.6	1.71	3.21	2.87	2376.7	2505.3	11160	156.3	4109.7
A-3430-6	21315.3	970.2	493.3	1.86	0	3020.6	1.65	3.27	2.84	2596.2	2219	9942	151	4681.3
A-3431-8	27778.8	972.9	498.5	1.8	2.02	3019.2	1.64	2.95	2.68	2506.7	2402.3	10706	153.5	4663
A-3434-1	38824.4	964.2	512.6	1.94	2.18	3040.8	1.67	3.09	2.67	2496.6	2511.3	12196	157.2	4614
A-3437-5	40357.1	1010.5	533.1	2.06	1.96	3007.7	1.66	3.28	2.96	2424.7	2517.3	2824	155.4	4469
A-3438-3	37232	1027.9	484.4	2.07	1.93	2945.2	1.7	3.51	3.45	2416.4	2424.3	10916	155.3	4644.7
A-3438-5	41274.9	1010.5	533.1	2.06	1.96	3007.7	1.66	3.28	2.96	2424.7	2517.3	2824	155.1	4528
A-3439-2	42747.3	1010.5	533.1	2.06	1.96	3007.7	1.66	3.28	2.96	2424.7	2517.3	2824	152.7	4528
A-3439-4	40258.5	1027.9	484.4	2.07	1.93	2945.2	1.7	3.51	3.45	2416.4	2424.3	10916	155.1	4644.7
A-3440-4	39382.4	995	513.8	2.06	1.85	3139.4	1.62	3.15	2.89	2395	2534	10710	146.8	4609
A-3440-5	10600.5	1002.6	496.3	2.01	2.1	3048.4	1.65	3.13	2.82	2456.6	2513.2	13139	151.8	4593.7
A-3440-7	38487.1	1010.5	533.1	2.06	1.96	3007.7	1.66	3.28	2.96	2424.7	2517.3	2824	155.4	4479.7
A-3440-8	43045.4	986.4	511.6	2.07	2	3121.7	1.52	3.2	2.89	2381.7	2500.3	10609	154.2	4518.3
A-3465-3	17440.6	970.2	493.3	1.86	0	3020.6	1.65	3.27	2.84	2596.2	2219	9942	150.6	4681.3
A-3466-8	30926.8	984.4	512.5	1.95	1.9	3124.7	1.61	3.2	2.94	2467.6	2427.8	11058	150.1	4637.3
A-3467-4	27960.5	967.9	482.1	1.9	2.03	3057.2	1.55	3.64	3.27	2485	2515	10682	156	4524.8
A-3467-6	20692.3	967.6	512.2	1.89	1.88	3058.6	1.71	3.21	2.87	2376.7	2505.3	11160	157.2	3627
A-3467-8	29591.2	967.6	512.2	1.89	1.88	3058.6	1.71	3.21	2.87	2376.7	2505.3	11160	157.1	4121
A-3468-1	24661.6	970	498.3	1.7	2.04	3050.1	1.52	3.1	2.71	2384.3	2495.7	27093	147.8	4688
A-3468-2	20232.4	963.9	490.1	1.71	2	3010.6	1.62	2.97	2.73	2525.6	2428.3	10188	156.4	4596
A-3468-4	27576.2	970.2	490.3	1.77	0	3052.9	1.7	3.3	3	2366.3	2554.7	10855	155.5	4309.3
A-3469-1	26487.8	965.6	483.2	1.87	2.06	3040	0	3.2	2.91	2450.3	2517.3	12947	158.3	4644
A-3469-3	27256.2	965.6	483.2	1.87	2.06	3040	0	3.2	2.91	2450.3	2517.3	12947	159.2	4644
A-3470-8	21097.6	970	498.3	1.7	2.04	3050.1	1.52	3.1	2.71	2384.3	2495.7	27093	151	4583.5
A-3471-2	25530.7	970	498.3	1.7	2.04	3050.1	1.52	3.1	2.71	2384.3	2495.7	27093	151.2	4647
A-3471-8	27216.7	977.5	502.6	1.83	2.03	3007.3	1.61	3.21	2.94	2451.3	2497.7	15171	155.8	4626
A-3472-4	28355.7	965.6	483.2	1.87	2.06	3040	0	3.2	2.91	2450.3	2517.3	12947	162.6	4634.7
A-3472-5	20035.2	963.9	490.1	1.71	2	3010.6	1.62	2.97	2.73	2525.6	2432.7	10226	156.4	4616.3
A-3472-8	17557.4	969.2	495.5	1.69	2.07	2998.9	1.54	3.47	3.03	2509.4	2417.7	10560	156.2	4626
A-3473-1	29034.1	965.3	496.7	1.9	2.09	2994.3	1.65	3.7	3.37	2470	2522.8	13172	157.5	4723.8
A-3476-5	43701.7	997.1	491.3	2.05	1.96	2994.6	1.71	3.12	2.76	2463.3	2563	10656	155.7	4498.8
A-3476-6	40423.1	995	513.8	2.06	1.85	3139.4	1.62	3.15	2.89	2395	2534	10710	150	4541.7
A-3476-8	37165	995	513.8	2.06	1.85	3139.4	1.62	3.15	2.89	2395	2534	10710	146.8	4609
A-3478-4	33641.6	988.5	519.1	2.07	2.09	3123.8	1.64	3.34	3.01	2555.6	2360.3	10240	152.4	4733
A-3479-1	35494.2	1011.2	470.2	2.03	2.03	3012.8	1.64	3.31	2.95	2501.8	2390	10729	151.2	4647.4
A-3479-2	33008.4	987.1	504.7	2.07	1.95	3091	1.6	3.18	2.89	2563.1	2286	10597	165.2	4639
A-3568-4	34391.8	977.5	502.6	1.83	2.03	3007.3	1.61	3.21	2.94	2451.3	2497.7	15171	156.3	4626

Appendix C

Listing of the FORTRAN Program

```
PROGRAM ILOMOD

DIMENSION COL(150,80),AVG(80),COR(80,80),IROWCOR(80,80)
DIMENSION COROR(80,80),IORDER(80),COL1(150,80),IIN(80)
DIMENSION DATAB1(150,40),INP(10),VMIN(40),VMAX(40)
DIMENSION FBESTMOD(10),INPBES(10,10)
DOUBLE PRECISION PARAM(10),F
CHARACTER*1 EXT1
CHARACTER*2 EXT2
CHARACTER*3 EXT
CHARACTER*31 DRIV
CHARACTER*45 FICH,FICH1
DRIV='C:\Folder-Jules\ETUDIANT\ILONA\'
FICH=DRIV//'IloData2.csv'
PRINT *, FICH
IROW=149
ICOL=59
CALL READDATA(IROW,ICOL,COL,FICH)
NOPTION=5
IF (NOPTION .EQ. 1) THEN
C
C  Calculate correlation for a number of outputs as a function of a series of inputs
NUMBER=3
IF (NUMBER .LT. 10) THEN
WRITE(EXT1,50) NUMBER
50    FORMAT(I1)
EXT='00'//EXT1
ELSE IF (NUMBER .LT. 100) THEN
WRITE(EXT2,51) NUMBER
51    FORMAT(I2)
EXT='0'//EXT2
ELSE
STOP
END IF
FICH=DRIV//'RESUL'//EXT//'.DAT'
FICH1=DRIV//'RESUL'//EXT//'A.DAT'
JMIN=22
JMAX=59
KMIN=NUMBER
KMAX=NUMBER
CALL CALCORR(IROW,JMIN,JMAX,KMIN,KMAX,IROWCOR,COR,COL,
+            FICH,FICH1)
FICH=DRIV//'ORDER'//EXT//'.DAT'
KOR=NUMBER
CALL ORDER(KOR,JMIN,JMAX,IORDER,COR,COROR,FICH)
ELSE IF (NOPTION .EQ. 2) THEN
C
C  Generate a bank of data to fit a single output as a function of a number of specified inputs
IOUT = 14
NUMBER=IOUT
IF (NUMBER .LT. 10) THEN
WRITE(EXT1,50) NUMBER
EXT='00'//EXT1
ELSE IF (NUMBER .LT. 100) THEN
WRITE(EXT2,51) NUMBER
EXT='0'//EXT2
ELSE
STOP
END IF
FICH=DRIV//'DATA'//EXT//'.DAT'
```

```
FICH1=DRIV//'DATA'//EXT//'A.DAT'
NUMINPUT=1
IIN(1)=40
IIN(2)=40
IIN(3)=36
IIN(4)=59
LEC=1
CALL GENERATEBANK(LEC,IROW,IOUT,NUMINPUT,IIN,NP,COL,DATAB1
+              ,VMIN,VMAX,FICH,FICH1)
ELSE IF (NOPTION .EQ. 3) THEN
C
C  Find the whole matrix of correlation C  Find correlation in order importance for that output C  Generate automatically a data bank of all the inputs with given  characteristics
NUMBER=14
IF (NUMBER .LT. 10) THEN
WRITE(EXT1,50) NUMBER
EXT='00'//EXT1
ELSE IF (NUMBER .LT. 100) THEN
WRITE(EXT2,51) NUMBER
EXT='0'//EXT2
ELSE
STOP
END IF
FICH=DRIV//'RESUL'//EXT//'.DAT'
FICH1=DRIV//'RESUL'//EXT//'A.DAT'
JMIN=2
JMAX=59
KMIN=2
KMAX=59
CALL CALCORR(IROW,JMIN,JMAX,KMIN,KMAX,IROWCOR,COR,COL
+        ,FICH,FICH1)
FICH=DRIV//'ORDER'//EXT//'.DAT'
JMIN=22
JMAX=59
KOR=NUMBER
CALL ORDER(KOR,JMIN,JMAX,IORDER,COR,COROR,FICH)
FICH=DRIV//'DATA'//EXT//'.DAT'
FICH1=DRIV//'DATA'//EXT//'A.DAT'
IOUT=KOR
NUMINPUT=1
IIN(1)=IORDER(JMIN)
DO 10 J=JMIN+1,JMAX
IF (ABS(COROR(J,IOUT)) .LT. .15) GOTO 11
IJ = 0
DO 20 K=1,NUMINPUT
IF (ABS(COR(IIN(K),IORDER(J))) .GT. .7) IJ=IJ+1
20      CONTINUE
IF (IJ .EQ. 0) THEN
NUMINPUT=NUMINPUT+1
IIN(NUMINPUT)=IORDER(J)
END IF
PRINT *, J,IJ,NUMINPUT,IORDER(J),COROR(J,IOUT)
10   CONTINUE
11   CONTINUE
LEC=1
CALL GENERATEBANK(LEC,IROW,IOUT,NUMINPUT,IIN,NP,COL,DATAB1
+              ,VMIN,VMAX,FICH,FICH1)
ELSE IF (NOPTION .EQ. 4) THEN
C
C  Calculate a series of possible models
IOUT = 3
NUMBER=IOUT
IF (NUMBER .LT. 10) THEN
WRITE(EXT1,50) NUMBER
EXT='00'//EXT1
ELSE IF (NUMBER .LT. 100) THEN
WRITE(EXT2,51) NUMBER
EXT='0'//EXT2
ELSE
STOP
```

```
END IF
FICH=DRIV//'MODEL'//EXT//'.DAT'
FICH1=DRIV//'MODEL'//EXT//'A.DAT'
OPEN(2,FILE=FICH)
NINPUT=6
INP(1)=59
INP(2)=33
INP(3)=43
INP(4)=55
INP(5)=34
INP(6)=27
INP(7)=40
INP(8)=36
INP(9)=41
INP(10)=35
DO 19 I=1,4
FBESTMOD(I)=1.0E+30
19  CONTINUE
LEC=0
DO 100 I=1,NINPUT
IF (I .EQ. 1) THEN
NPA=I+1
NUMINPUT=I
DO 15 J=1,NINPUT
IIN(1)=INP(J)
CALL
GENERATEBANK(LEC,IROW,IOUT,NUMINPUT,IIN,NP,COL,DATAB1
+             ,VMIN,VMAX,FICH,FICH1)
DO 16 N=1,NPA
PARAM(N)=0.1
16      CONTINUE
CALL OPTIM(NPA,NP,DATAB1,PARAM,F)
WRITE(2,200) NPA,NP,(IIN(JJ),JJ=1,NUMINPUT)
PRINT *, NPA,NP,(IIN(JJ),JJ=1,NUMINPUT)
WRITE(2,201) (PARAM(JJ),JJ=1,NPA),SQRT(F/FLOAT(NP))
PRINT *, (PARAM(JJ),JJ=1,NPA),SQRT(F/FLOAT(NP))
CALL DENORMOUT(NPA,NP,DATAB1,PARAM,VMIN,VMAX,FD,AVER,STD)
WRITE(2,201) VMIN(1),VMAX(1),AVER,STD,SQRT(FD/FLOAT(NP))
PRINT *, VMIN(1),VMAX(1),AVER,STD,SQRT(FD/FLOAT(NP))
IF ((FD/FLOAT(NP)) .LT. FBESTMOD(I)) THEN
FBESTMOD(I)=FD/FLOAT(NP)
DO 90 JJ=1,NUMINPUT
INPBES(JJ,I)=IIN(JJ)
90        CONTINUE
END IF
15     CONTINUE
ELSE IF (I .EQ. 2) THEN
NPA=I+1
NUMINPUT=I
DO 25 J=1,NINPUT-1
DO 26 K=J+1,NINPUT
IIN(1)=INP(J)
IIN(2)=INP(K)
CALL
GENERATEBANK(LEC,IROW,IOUT,NUMINPUT,IIN,NP,COL,DATAB1
+             ,VMIN,VMAX,FICH,FICH1)
DO 27 N=1,NPA
PARAM(N)=0.1
27      CONTINUE
CALL OPTIM(NPA,NP,DATAB1,PARAM,F)
WRITE(2,200) NPA,NP,(IIN(JJ),JJ=1,NUMINPUT)
WRITE(2,201) (PARAM(JJ),JJ=1,NPA),SQRT(F/FLOAT(NP))
CALL DENORMOUT(NPA,NP,DATAB1,PARAM,VMIN,VMAX,FD,AVER,STD)
WRITE(2,201) VMIN(1),VMAX(1),AVER,STD,SQRT(FD/FLOAT(NP))
PRINT *, VMIN(1),VMAX(1),AVER,STD,SQRT(FD/FLOAT(NP))
IF ((FD/FLOAT(NP)) .LT. FBESTMOD(I)) THEN
FBESTMOD(I)=FD/FLOAT(NP)
DO 91 JJ=1,NUMINPUT
INPBES(JJ,I)=IIN(JJ)
91        CONTINUE
```

```
END IF
26      CONTINUE
25     CONTINUE
ELSE IF (I .EQ. 3) THEN
NPA=I+1
NUMINPUT=I
DO 35 J=1,NINPUT-2
DO 36 K=J+1,NINPUT-1
DO 37 L=K+1,NINPUT
IIN(1)=INP(J)
IIN(2)=INP(K)
IIN(3)=INP(L)
CALL GENERATEBANK(LEC,IROW,IOUT,NUMINPUT,IIN,NP,COL
+              ,DATAB1,VMIN,VMAX,FICH,FICH1)
DO 38 N=1,NPA
PARAM(N)=0.1
38        CONTINUE
CALL OPTIM(NPA,NP,DATAB1,PARAM,F)
WRITE(2,200) NPA,NP,(IIN(JJ),JJ=1,NUMINPUT)
WRITE(2,201) (PARAM(JJ),JJ=1,NPA),SQRT(F/FLOAT(NP))
CALL
DENORMOUT(NPA,NP,DATAB1,PARAM,VMIN,VMAX,FD,AVER,STD)
WRITE(2,201) VMIN(1),VMAX(1),AVER,STD,SQRT(FD/FLOAT(NP))
PRINT *, VMIN(1),VMAX(1),AVER,STD,SQRT(FD/FLOAT(NP))
IF ((FD/FLOAT(NP)) .LT. FBESTMOD(I)) THEN
FBESTMOD(I)=FD/FLOAT(NP)
DO 92 JJ=1,NUMINPUT
INPBES(JJ,I)=IIN(JJ)
92        CONTINUE
END IF
37       CONTINUE
36      CONTINUE
35     CONTINUE
ELSE IF (I .EQ. 4) THEN
NPA=I+1
NUMINPUT=I
DO 45 J=1,NINPUT-3
DO 46 K=J+1,NINPUT-2
DO 47 L=K+1,NINPUT-1
DO 48 M=L+1,NINPUT
IIN(1)=INP(J)
IIN(2)=INP(K)
IIN(3)=INP(L)
IIN(4)=INP(M)
CALL GENERATEBANK(LEC,IROW,IOUT,NUMINPUT,IIN,NP,COL
+              ,DATAB1,VMIN,VMAX,FICH,FICH1)
DO 49 N=1,NPA
PARAM(N)=0.1
49        CONTINUE
CALL OPTIM(NPA,NP,DATAB1,PARAM,F)
WRITE(2,200) NPA,NP,(IIN(JJ),JJ=1,NUMINPUT)
WRITE(2,201) (PARAM(JJ),JJ=1,NPA),SQRT(F/FLOAT(NP))
CALL
DENORMOUT(NPA,NP,DATAB1,PARAM,VMIN,VMAX,FD,AVER,STD)
WRITE(2,201) VMIN(1),VMAX(1),AVER,STD,SQRT(FD/FLOAT(NP))
PRINT *, VMIN(1),VMAX(1),AVER,STD,SQRT(FD/FLOAT(NP))
IF ((FD/FLOAT(NP)) .LT. FBESTMOD(I)) THEN
FBESTMOD(I)=FD/FLOAT(NP)
DO 93 JJ=1,NUMINPUT
INPBES(JJ,I)=IIN(JJ)
93        CONTINUE
END IF
48       CONTINUE
47       CONTINUE
46      CONTINUE
45     CONTINUE
ELSE
END IF
100  CONTINUE
PRINT *, IOUT
```

```
DO 105 I=1,4
PRINT *,(INPBES(JJ,I),JJ=1,I),FBESTMOD(I)
105  CONTINUE
200  FORMAT(2I4,12X,15(5X,I2,5X))
201  FORMAT(8X,15E12.4)
CLOSE(2)
ELSE IF (NOPTION .EQ. 5) THEN
C
C  Calculate the output of a given model
IOUT = 3
NUMBER=IOUT
IF (NUMBER .LT. 10) THEN
WRITE(EXT1,50) NUMBER
EXT='00'//EXT1
ELSE IF (NUMBER .LT. 100) THEN
WRITE(EXT2,51) NUMBER
EXT='0'//EXT2
ELSE
STOP
END IF
FICH=DRIV//'MORES'//EXT//'.DAT'
FICH1=DRIV//'MORES'//EXT//'A.DAT'
OPEN(2,FILE=FICH)

NINPUT=4
INP(1)=59
INP(2)=43
INP(3)=55
INP(4)=27
NPA=NINPUT+1
CALL GENERATEBANK(LEC,IROW,IOUT,NINPUT,INP,NP,COL,DATAB1
+     ,VMIN,VMAX,FICH,FICH1)
DO 300 N=1,NPA
PARAM(N)=0.1
300  CONTINUE
CALL OPTIM(NPA,NP,DATAB1,PARAM,F)
PRINT *, NPA,NP,(IIN(JJ),JJ=1,NUMINPUT)
PRINT *, (PARAM(JJ),JJ=1,NPA),SQRT(F/FLOAT(NP))
CALL FINMODEL(NPA,NP,DATAB1,PARAM,VMIN,VMAX,FICH,FICH1)
CLOSE(2)
ELSE
STOP
END IF
END
C
C**********************************
C    SUBROUTINE CALCORR(IROW,JMIN,JMAX,KMIN,KMAX,IROWCOR,COR,COL
+        ,FICH,FICH1)
DIMENSION COL(150,80),COR(80,80),IROWCOR(80,80)
CHARACTER*45 FICH,FICH1
OPEN(2,FILE=FICH)
WRITE(2,110) (K,K=KMIN,KMAX)
110 FORMAT(6X,80(2X,I2,2X))
DO 10 J=JMIN,JMAX
DO 15 K=KMIN,KMAX
CALL CORREL(J,K,IROW,IROWCOR,COL,COR)
C                                          PRINT *, J,K,IROWCOR(J,K),COR(J,K)
15  CONTINUE
WRITE(2,111) J,(COR(J,K),K=KMIN,KMAX)
111  FORMAT(2X,I2,2X,80(1X,F5.2))
10 CONTINUE
CLOSE(2)
OPEN(2,FILE=FICH1)
WRITE(2,112) (K,K=KMIN,KMAX)
112 FORMAT(4X,80(1X,I3))
DO 20 J=JMIN,JMAX
WRITE(2,113) J,(IROWCOR(J,K),K=KMIN,KMAX)
113                                                FORMAT(80(1X,I3))
20 CONTINUE
CLOSE(2)
```

```
RETURN
END
C*******************************
SUBROUTINE CORREL(J,K,IROW,IROWCOR,COL,COR)
DIMENSION COL(150,80),AVG(80),STD(80),COR(80,80),IROWCOR(80,80)
DIMENSION COL1(150,80)
SUMJ=0.
SUMK=0.
II = 0
DO 10 I=1,IROW
IF ((COL(I,J) .EQ. 0.) .OR. (COL(I,K) .EQ. 0.)
+   .OR. ((J .EQ. 14) .AND. (COL(I,J) .LT. .001))
+   .OR. ((K .EQ. 14) .AND. (COL(I,K) .LT. .001))
+   .OR. ((J .EQ. 13) .AND. (COL(I,J) .GT. 2.))
+   .OR. ((K .EQ. 13) .AND. (COL(I,K) .GT. 20.))
+   .OR. ((J .EQ. 3) .AND. (COL(I,J) .LT. .0))
+   .OR. ((K .EQ. 3) .AND. (COL(I,K) .LT. .0))) THEN
C                                                  PRINT *, I,J,K,COL(I,J),COL(I,K)
ELSE
II = II + 1
COL1(II,J)=COL(I,J)
COL1(II,K)=COL(I,K)
SUMJ=SUMJ+COL(I,J)
SUMK=SUMK+COL(I,K)
END IF
10 CONTINUE
AVG(J)=SUMJ/FLOAT(II)
AVG(K)=SUMK/FLOAT(II)
IROWCOR(J,K)=II
IROWCOR(K,J)=II
SUMJ=0.
SUMK=0.
DO 20 I=1,II
SUMJ=SUMJ+(COL1(I,J)-AVG(J))**2
SUMK=SUMK+(COL1(I,K)-AVG(K))**2
20 CONTINUE
STD(J)=SQRT(SUMJ/FLOAT(II-1))
STD(K)=SQRT(SUMK/FLOAT(II-1))
SUMI=0.
DO 30 I=1,II
SUMI=SUMI+(COL1(I,J)-AVG(J))*(COL1(I,K)-AVG(K))
30 CONTINUE
COR(J,K)=SUMI/(STD(J)*STD(K)*FLOAT(II-1))
COR(K,J)=COR(J,K)
RETURN
END
C
C**************************
C
SUBROUTINE GENERATEBANK(LEC,IROW,IOUT,NUMINPUT,IIN,II,COL,
+                DATAB1,VMIN,VMAX,FICH,FICH1)
DIMENSION DATAB(150,40),DATAB1(150,40),VMIN(40),VMAX(40)
DIMENSION COL(150,80),IIN(80)
CHARACTER*45 FICH,FICH1
II=0
DO 10 I=1,IROW
ICHECK=0
IF ((COL(I,IOUT) .EQ. 0.).OR.((IOUT .EQ. 14).AND.
+    (COL(I,IOUT) .LT. .001)).OR.((IOUT .EQ. 13).AND.
+    (COL(I,IOUT) .GT. 20.)).OR.((IOUT .EQ. 3).AND.
+    (COL(I,IOUT) .LT. .0))) THEN
ICHECK=ICHECK+1
ENDIF
DO 20 J=1,NUMINPUT
IF ((COL(I,IIN(J)).EQ.0.).OR.((IOUT.EQ.14).AND.
+     (COL(I,IIN(J)) .LT. .001)).OR.((IOUT .EQ. 13).AND.
+    (COL(I,IIN(J)) .GT. 20.)).OR.((IOUT .EQ. 3).AND.
+    (COL(I,IIN(J)) .LT. .0)))  THEN
ICHECK=ICHECK+1
C     PRINT *, I,J,ICHECK,IIN(J),COL(I,IIN(J))
```

```
ENDIF
20  CONTINUE
IF (ICHECK .EQ. 0) THEN
II=II+1
DATAB(II,1)=COL(I,IOUT)
DO 30 J=1,NUMINPUT
DATAB(II,J+1)=COL(I,IIN(J))
30    CONTINUE
END IF
10 CONTINUE
DO 40 J=1,NUMINPUT + 1
VMIN(J)=1.0E+30
VMAX(J)=-1.0E+30
DO 50 I=1,II
IF (DATAB(I,J) .LT. VMIN(J)) VMIN(J)=DATAB(I,J)
IF (DATAB(I,J) .GT. VMAX(J)) VMAX(J)=DATAB(I,J)
50  CONTINUE
DO 60 I=1,II
DATAB1(I,J)=2*(DATAB(I,J)-VMIN(J))/(VMAX(J)-VMIN(J))-1
C       PRINT *, I,J,DATAB(I,J),DATAB1(I,J)
60  CONTINUE
40 CONTINUE
IF (LEC .EQ. 1) THEN
OPEN(2,FILE=FICH)
DO 70 I=1,II
WRITE(2,100) (DATAB1(I,J),J=1,NUMINPUT+1)
70  CONTINUE
100  FORMAT(20E12.4)
CLOSE(2)
OPEN(2,FILE=FICH1)
WRITE(2,101) II
WRITE(2,102) IOUT,VMIN(1),VMAX(1)
101  FORMAT(I5)
102  FORMAT(I5,2E12.4)
DO 80 J=1,NUMINPUT
WRITE(2,102) IIN(J),VMIN(J+1),VMAX(J+1)
80  CONTINUE
DO 85 I=1,II
WRITE (2,100) (DATAB(I,J),J=1,NUMINPUT+1)
85  CONTINUE
CLOSE(2)
END IF
RETURN
END
C
C*****************************
C
SUBROUTINE ORDER(KOR,JMIN,JMAX,IORDER,COR,COROR,FICH)
DIMENSION COR(80,80),COROR(80,80),IORDER(80)
CHARACTER*45 FICH
DO 10 J=JMIN,JMAX
COROR(J,KOR)=COR(J,KOR)
IORDER(J) = J
10 CONTINUE
DO 20 I=JMIN,JMAX - 1
IMAX = I
DO 30 J=I+1,JMAX
IF (ABS(COROR(J,KOR)) .GT. ABS(COROR(IMAX,KOR))) IMAX=J
30  CONTINUE
CC=COROR(I, KOR)
COROR(I, KOR)=COROR(IMAX, KOR)
COROR(IMAX, KOR)=CC
IC=IORDER(I)
IORDER(I)=IORDER(IMAX)
IORDER(IMAX)=IC
20 CONTINUE
OPEN(3,FILE=FICH)
WRITE(3,100) FLOAT(KOR)
100 FORMAT(7X,F7.3)
DO 40 J=JMIN,JMAX
```

```
WRITE(3,101) FLOAT(IORDER(J)),COROR(J, KOR)
40 CONTINUE
101 FORMAT(2F7.3)
CLOSE(3)
RETURN
END
C
C**********************************
C
SUBROUTINE READDATA(IROW,ICOL,COL,FICH)
DIMENSION COL(150,80)
CHARACTER*45 FICH
CHARACTER*8 DUM

OPEN(1,FILE=FICH)
DO 10 I=1,IROW
READ(1,*) DUM,(COL(I,J),J=2,ICOL)
C       PRINT *, I,(COL(I,J),J=2,ICOL)
10 CONTINUE
CLOSE(1)
RETURN
END
C
C**************************************************************************
C     SUBROUTINE OPTIM(NPA,NP,DATAB1,PA,F)
C OPTIMISATION
DIMENSION DATAB1(150,80),PACON(10)
DOUBLE PRECISION PA(10),G(10),SCA(10),W(8000),F,ACC
COMMON /VA13B/IPRINT,LP,MAXFUN,MODE,NFUN
IPRINT=0
ACC=1.0D-14
LINK=0
MAXITN=200
FCON=1.0E+30
ITER=0
DO 15 I=1,NPA
SCA(I)=0.1
15 CONTINUE
20 CONTINUE
ITER=ITER+1
F=0.
DO 30 I=1,NP
Y=PA(1)
DO 35 J=2,NPA
Y=Y+PA(J)*DATAB1(I,J)
35    CONTINUE
F=F+(Y-DATAB1(I,1))*(Y-DATAB1(I,1))
30  CONTINUE
IF (F .LT. FCON) THEN
FCON=F
DO 19 K=1,NPA
PACON(K)=PA(K)
19    CONTINUE
END IF
F0=F
DO 40 J=1,NPA
DPAR=ABS(PA(J)*.001)
IF (ABS(DPAR) .LT. 1.0E-15) DPAR=.0001
PA(J)=PA(J)+DPAR
F=0.
DO 41 I=1,NP
Y=PA(1)
DO 42 K=2,NPA
Y=Y+PA(K)*DATAB1(I,K)
42      CONTINUE
F=F+(Y-DATAB1(I,1))*(Y-DATAB1(I,1))
41    CONTINUE
IF (F .LT. FCON) THEN
FCON=F
DO 21 K=1,NPA
```

```
PACON(K)=PA(K)
21     CONTINUE
END IF
F1=F
G(J)=(F1-F0)/DPAR
PA(J)=PA(J)-DPAR
40   CONTINUE
CALL VA13A(NPA,PA,F,G,SCA,ACC,W,LINK)
IF((LINK .NE. 2) .AND. (ITER .LE. MAXITN)) GOTO 20
DO 61 J=1,NPA
PA(J)=PACON(J)
61   CONTINUE
F=FCON
RETURN
END
C
C*************************************************************************
C     SUBROUTINE DENORMOUT(NPA,NP,DATAB1,PA,VMIN,VMAX,FD,AVER,STD)
C OPTIMISATION
DIMENSION DATAB1(150,80),Y(150),YP(150),E(150),VMIN(40),VMAX(40)
DOUBLE PRECISION PA(10)
FD=0.
DO 30 I=1,NP
Y(I)=PA(1)
DO 35 J=2,NPA
Y(I)=Y(I)+PA(J)*DATAB1(I,J)
35   CONTINUE
Y(I)=VMIN(1)+0.5*(VMAX(1)-VMIN(1))*(Y(I)+1.)
YP(I)=VMIN(1)+0.5*(VMAX(1)-VMIN(1))*(DATAB1(I,1)+1.)
E(I)=Y(I)-YP(I)
FD=FD+E(I)**2
30 CONTINUE
SUM=0.
DO 10 I=1,NP
SUM=SUM+E(I)
10 CONTINUE
AVER=SUM/FLOAT(NP)
SUM=0.
DO 20 I=1,NP
SUM=SUM+(E(I)-AVER)**2
20 CONTINUE
STD=SQRT(SUM/FLOAT(NP-1))
RETURN
END
C
C*************************************************************************
C     SUBROUTINE FINMODEL(NPA,NP,DATAB1,PA,VMIN,VMAX,FICH,FICH1)
C OPTIMISATION
DIMENSION DATAB1(150,80),Y(150),YP(150),E(150),VMIN(40),VMAX(40)
DOUBLE PRECISION PA(10)
CHARACTER*45 FICH,FICH1
SUMJ=0.
SUMK=0.
DO 30 I=1,NP
Y(I)=PA(1)
DO 35 J=2,NPA
Y(I)=Y(I)+PA(J)*DATAB1(I,J)
35   CONTINUE
YP(I)=VMIN(1)+0.5*(VMAX(1)-VMIN(1))*(Y(I)+1.)
Y(I)=VMIN(1)+0.5*(VMAX(1)-VMIN(1))*(DATAB1(I,1)+1.)
E(I)=Y(I)-YP(I)
SUMJ=SUMJ+Y(I)
SUMK=SUMK+YP(I)
WRITE(2,201) I,Y(I),YP(I),E(I)
PRINT *, I,Y(I),YP(I),E(I)
30 CONTINUE
201 FORMAT(I5,10E15.5)
AVGJ=SUMJ/FLOAT(NP)
AVGK=SUMK/FLOAT(NP)
SUMJ=0.
```

```
SUMK=0.
DO 20 I=1,NP
SUMJ=SUMJ+(Y(I)-AVGJ)**2
SUMK=SUMK+(YP(I)-AVGK)**2
20 CONTINUE
STDJ=SQRT(SUMJ/FLOAT(NP-1))
STDK=SQRT(SUMK/FLOAT(NP-1))
SUMI=0.
DO 10 I=1,NP
SUMI=SUMI+(Y(I)-AVGJ)*(YP(I)-AVGK)
10 CONTINUE
CORY=SUMI/(STDJ*STDK*FLOAT(NP-1))
PRINT *, CORY
RETURN
END
```

Appendix D

Specification Limits for Output Variables

Dataname	Description	Min	Max	Units
Open Cct	Open Circuit flag	0.00E+00	0.00E+00	NONE
OpAbort	Operator test abort early	0.00E+00	0.00E+00	NONE
Vf@10mA	Forward voltage at current	0.15	3	V
Ith2L	Threshold two line fit ref 10mW	5	19	mA
RearP	Rear facet power	0.7	7	mW
Eff_m2	Efficiency between 1 and 9mW any temp	0.15	99.9	%
Lin_m4@10mW	Linearity between 1 and 9mW any temp	-7	7	%
RS_2L	Two line fit Resistance	0	8	ohm
PowerSat@10mW	PowerSatM1	-18	18	%
Vf@5mW	Forward voltage	0.5	1.8	V
Kink2DPowerFront	2nd derivative Kink up to 115mA any temp	12	99.9	mW
SMSR@5mW	SMSR@Pf	40	999	dB
Pkwl@Ith+X	Pkwl at Ith+Xma at 10.00mW	1516	1625	nm
Bragg@5mW	Bragg mode at 5mW	R	R	NONE
SBand@5mW	Stop Band at 5 mW	2.4	10	nm
FB_Tracking	ratio of FB ratios at Ith+10 and 100mA	0.5	2	NONE
Kink2DCurrentRear	kink location in current on back facet	113	999	mA

Appendix E

All fail codes presented in percentage

WAFEID	Pass %	FB_Track.	SMSR	Bragg	RearP...too high	KinkPower	Sband... too low	Effic.. too low	RearP ...too low	PowerSaturation too high	PowerSatu. too low	KinkCurrent too low	Ith...too high	ManKink Power too low	Ith...too low
A-2931-2	47.62	4.76	30.95	4.76	7.14	4.76									
A-3255-8	65.93		18.68	4.4	7.69	1.1	1.1	1.1							
A-3311-2	43.9	9.76	4.07	13.82	4.88		15.45		4.88	2.44	0.81				
A-3311-3	64.86	5.41		2.7	2.7		18.92		5.41						
A-3327-5	57.97	9.42	4.35	0.72	2.9		20.29	1.45	2.9						
A-3346-2	66.67	2.5	10.83	0.83	7.5		2.5		8.33			0.83			
A-3346-4	66.3	6.52	13.04	2.17	1.09		5.43		1.09				2.17		
A-3346-5	60.61	12.12			12.12		3.03		6.06					6.06	
A-3346-6	69.42		7.44	1.65	4.96			0.83	10.74				0.83	3.31	0.83
A-3347-4	62.5		23.44	1.56	6.25									3.31	
A-3350-4	20	0.83	32.5	2.5	2.5		35						3.33	3.33	
A-3352-2	71.43	3.57	3.57	7.14	3.57		7.14	3.57							
A-3353-2	57.97	5.8	10.14	1.45	14.49	1.45	2.9		4.35	1.45					
A-3353-3	70.93		2.33	10.47	6.98		3.49		3.49	1.16	1.16				
A-3355-6	70.18			5.26	12.28				8.77				3.51		
A-3356-4	67.23		3.36	0.84	12.61				10.08				2.52	2.52	
A-3357-4	65		13.33	13.33	5				2.5						
A-3357-8	76.69	6.13	1.23	3.68	3.68		6.13	1.23	0.61						
A-3365-1	67.96		3.88	17.48					9.71					0.97	
A-3366-5	58.39		4.38	2.92	10.22			3.65	18.98					0.73	
A-3366-6	75.83				7.5				11.67				0.83	0.83	3.33
A-3370-1	58.39	6.57	7.3	2.19	3.65		13.87	4.38	0.73					2.92	
A-3373-8	74.77	11.21	1.87	1.87	4.67		1.87	1.87	1.87						
A-3376-7	54.67		18.67	2.67	16			0.67	5.33				0.67	1.33	
A-3425-4	61.54	10.77	9.23		1.54		10.77	4.62	1.54						
A-3426-4	74.11		11.61	3.57	7.14				1.79				0.89	0.89	
A-3427-2	39.58	16.67		2.08			31.25						8.33		
A-3427-3	58.74	11.65	2.91	2.91	3.88		14.56	0.97	0.49	1.94			1.94		
A-3427-5	50.29	2.89	5.78	15.03	5.2		12.14	2.31	2.89		0.58		1.16	1.16	
A-3427-8	52.63		25.44	4.39	7.89			0.88	0.88				6.14	1.75	
A-3428-1	59.12	4.38	14.6	5.84	2.19	3.65	7.3					0.73	2.19		
A-3429-8	55.07	2.2	28.63	0.44	5.29	0.44	1.76	1.32		0.88	0.44		3.08	0.44	
A-3430-1	65.75	3.87	8.29	1.66	6.08	0.55	3.31	1.1	4.97	1.1			1.66	1.66	
A-3430-6	69.09		1.82	2.73	5.45				16.36				4.55		
A-3431-8	68.36	5.65	11.3	4.52	1.69	1.13	3.95				0.56		1.13	1.13	
A-3434-1	64.8	8.8	9.6	4	1.6		8		2.4	0.8					
A-3435-3	52.27	6.82	13.64	2.27	4.55	9.09	6.82				2.27				
A-3437-5	51.92		30.13	2.56	13.46								0.64	1.28	
A-3438-3	48.5		28		15				5					3.5	
A-3438-5	45.98		27.59	1.15	13.22				1.72				8.62	1.15	
A-3439-2	49.68		23.87		10.32			0.65	10.32				0.65	4.52	
A-3439-4	66.67		10.37		11.11			0.74	8.89					1.48	
A-3439-5	69.57		11.96	1.09	10.87			1.09	5.43						
A-3440-4	62.5		17.19	1.56	9.38				9.38						
A-3440-5	58.57	6.43	12.86	3.57	2.14	0.71	12.14	2.14	0.71				0.71		
A-3440-7	51.96		27.93		10.06				5.03				1.12	3.35	
A-3440-8	75.93		8.33	0.93	8.33	0.93	4.63			0.93					
A-3465-3	79.35			3.26	1.09			8.7	4.35				3.26		
A-3466-8	44.44		5.56		11.11			2.78	11.11				19.44	5.56	
A-3467-4	42.79	0.87	31	4.8	5.24		6.11	0.87					0.44		
A-3467-6	50.96	17.83	3.18	7.64	2.55		11.46	1.27					5.1		
A-3467-8	48.18		13.14	0.73	6.57				12.41				18.25	0.73	
A-3468-1	62.83	6.19	0.88	9.29	1.33		11.06	2.21	0.88	2.21			2.21	0.88	
A-3468-2	52.68	9.82	5.36	0.89	1.79	0.89	15.18	2.68	0.89	0.89			8.93		
A-3468-3				12.5									87.5		
A-3468-4	47.59	3.45	7.59	4.14	1.38	0.69	19.31	4.83					11.03		
A-3469-1	69.35	11.29	11.29			1.61	3.23	1.61		1.61					
A-3469-3	51.28	3.42	30.77	4.27	1.71	3.42	4.27		0.85						
A-3470-8	60	3.48	9.57	3.48	6.96		0.87	0.87					6.09	1.74	
A-3471-2	51.11	7.78	8.15	6.3	6.67	2.59	11.85	0.74	0.37	1.48	0.37	0.37	1.48	0.37	
A-3471-8	55.63	5.3	9.27	4.64	4.64		10.6	2.65		1.32	1.32		1.32	3.31	
A-3472-4	58.79	4.85	15.76	3.03	3.03	1.21	11.52	0.61			0.61			0.61	
A-3472-5	68.49	6.16	3.42	4.79	3.42		5.48	3.42	0.68	0.68			3.42		
A-3472-8	65.08		17.46	1.59	1.59		9.52	1.59					3.17		
A-3473-1	23.31	1.5	22.56	13.53	12.03	5.26	21.05	0.75							
A-3476-5	48.5	4.79	29.94	4.79	4.19	1.8	4.19	0.6		0.6					0.6
A-3477-3	46.59	3.41	32.95	2.27	4.55	3.41	5.68	1.14							
A-3477-5	41.18	11.76	26.47	5.88	2.94	2.94	8.82								
A-3478-4	51.95	1.95	20.13	5.19	14.94	0.65	2.6				0.65		0.65		
A-3479-1	25.17	2.65	36.42	11.26	4.64		11.92	1.32					0.66	5.96	

WAFEID	Pass %	FB_Track.	SMSR	Bragg	RearP...too high	KinkPower	Sband... too low	Effic.. too low	RearP ...too low	PowerSaturation too high	PowerSatu. too low	KinkCurrent too low	Ith...too high	ManKink Power too low	Ith...too low
A-3570-6	59.55	3.18	18.18	1.36	6.36	2.27	3.64	3.18		0.45	0.45		0.91		
A-3570-7	55.46	5.8	7.56	7.56	3.36	0.84	14.29	4.2							
A-3575-7	81.05		1.05	2.11	7.37				7.37					1.05	
A-3576-5	64.13	2.72	19.02	1.09	3.8	1.09	2.17	4.35	0.54					1.09	
A-3578-1	69.12	5.88	6.62	2.21	3.68	1.47	0.74	4.41	4.41	0.74		0.74			
A-3579-1	57.14	14.29	17.14				11.43								
A-3579-3	57.14	10.48	4.76	6.67	1.9		14.29	1.9	1.9	0.95					
A-3580-8	52.45	8.82	14.71	0.98	6.37	5.39	8.82	1.96		0.49					
A-3583-1	45.59	7.35	23.53	12.5	2.21		1.47	1.47			0.74	0.74		4.41	
A-3583-4	55.48	10.27	3.42	4.11	2.05	2.74	15.07	3.42	0.68	0.68	0.68	0.68			
A-3695-7	66.13	0.81	20.97	0.81	6.45		0.81		4.03						
A-3696-2	61.22		26.53	2.04	6.12				3.06					1.02	
A-3696-7	87.5	2.78	2.78		1.39	1.39	1.39	2.78							
A-3696-8	71.83		7.75		9.86			0.7	6.34				1.41	1.41	
A-3698-3	69.17	6.02	11.28	1.5	1.5	0.75	3.01	5.26				1.5			
A-3698-5	64		4	0.8	12			0.8	17.6					0.8	
A-3698-8	69.57		7.83	1.74	11.3			1.74	3.48					4.35	
A-3699-6	49.69	6.21	36.02	0.62	1.86	2.48	1.24	1.86							
A-3700-3	72.29	1.2	14.46	6.02	2.41			2.41			1.2				
A-3700-4	62.79	4.65	16.28	0.78	2.33		1.55	2.33	5.43	0.78				3.1	
A-3700-5	62.99	5.51	11.81	1.57	3.15	0.79	10.24	2.36		0.79					
A-3700-7	60.38	1.89	21.7	2.83	6.6		0.94	0.94	1.89					2.83	
A-3740-4					9.09	9.09									18.18
A-3740-5			12.5		6.25			6.25							
A-3740-6			20		6.67			3.33							
A-3741-7	19.23		6.41	1.28					70.51					2.56	
A-3747-1	42.42	3.03	12.12	9.09	3.03									3.3	
A-3823-1	43.86	2.19	35.96	7.02	3.95	4.39	1.32	0.44		0.44					
A-3823-2	52.9	2.58	29.68	2.58	4.52	1.29	2.58	1.94			0.65			1.29	
A-3823-4	44.91	2.99	36.53	2.99	5.99	0.6	2.4	2.99		0.6					
A-3823-5	35.55	3.79	38.39	5.21	9.48	3.32	3.79		0.47						
A-3823-8	55.63		27.46	1.41	2.82	4.23	6.34	1.41					0.7		
A-3826-2	59.53	6.98	19.53	3.26	3.26	3.26	3.26	0.47		0.47					
A-3826-3	66.67	5.83	19.17	1.67	0.83	1.67	1.67	0.83				0.83	0.83		
A-3826-4	67.91	5.88	16.04	2.14	2.67		1.07	2.67						1.07	
A-3826-5	63.55	3.45	23.15	0.49	2.46	2.96	0.99	1.97			0.99				
A-3861-1	54.42	7.48	21.77	4.08	4.08	3.4	2.04	0.68			0.68	0.68	0.68		
A-3862-1	72.07	5.41	8.11		2.7		7.21	4.5							
A-3862-8	52.68	3.57	28.57		4.46		0.89	0.89						8.04	0.89
A-3864-1									4.55						
A-3864-2	61.36	3.79	9.09	10.61	4.55	3.03	4.55	2.27							
A-3864-4	58	5	25	3	2	1	4	2							
A-3864-5	76.92	4.81	7.69	2.88	1.92		1.92	2.88	0.96						
A-3864-8	52.91	3.88	30.1	1.46	3.88	1.46	3.4	1.94			0.49				
A-3865-5	53.69	6.71	26.85	0.67	6.04	2.68	2.01	0.67	0.67						
A-3866-1	71.43	7.14	7.14	7.14	3.57							3.57			
A-3866-4	46.05	7.24	23.03		1.97	8.55	3.29	7.24	4.55			1.32			
A-3866-7	4.55														
A-3866-8	55.13	1.28	18.59	2.56	4.49	1.28	16.03	0.64							
A-3867-1	58.57	3.57	24.29	2.14	0.71	2.14	7.14	0.71			0.71				
A-3867-2	32.84	3.92	35.78	3.92	4.41	5.39	8.33	0.98		0.98	0.49			2.94	
A-3867-3	53.63	5.03	21.23	0.91	2.23	2.23	9.5	0.56	1.12				0.56		
A-3867-4	57.34	4.9	19.58	2.8	5.59	2.1	3.5	0.7	3.5						
A-3867-7	38.36	3.42	46.58	3.42	4.11	0.68		0.68	0.68		0.68			1.37	
A-3868-6	46.47	0.59	38.24	2.35	1.76		5.8	2.35		0.59				1.76	
A-3869-2	53.33	3.33	26	4.67	2.67	2	6	0.67		1.33					
A-3869-4	50	6.17	29.01	1.23	3.7	2.47	4.94	0.62		1.23	0.62				
A-3869-7	61.07	5.34	16.79	0.76	2.29	0.76	6.11	3.82	1.53	0.76	0.76				
A-3870-1	46.76	0.72	19.42	2.16	4.32	5.76	14.39		5.04	0.72					
A-3870-2	46.15	6.92	27.69	1.54	3.85	2.31	6.15	1.54		0.77	0.77				0.77
A-3870-3	56.94	4.17	23.61	2.08	2.08	2.08	7.64	1.39							
A-3870-4	56.3	5.19	17.04	3.7	2.96	2.22	8.89	2.22		0.74	0.74				
A-3871-2	55.56	2.78	24.31	0.69	5.56	2.78	6.25	1.39		0.69					
A-3871-3	60		15	25											
A-3871-5	71.43	3.57	10.71		7.14	3.57		3.57							
A-3871-6	43.48	13.04	23.91	1.09	2.17	2.17	8.7	4.35			1.09				
A-3871-7	58.82	8.4	14.29	2.52	3.36	5.04	4.2	2.52	0.84						
A-3871-8	51.9	1.27	13.92	10.13	3.8	5.06	8.86	1.27	1.27			1.27			
A-3872-1	54.84	3.23	32.26		6.45		3.23								
A-3872-3	46.24	11.83	25.81		5.38	2.15	5.38	2.15				1.08			

Appendix F

Averaged Output Variables

WAFER ID	ITH2L 1	REAR POWER 2	I_5MW 3	EFF_M2 4	POWSAT_10MW 5	KINKCURRENT 6	KINKPOWER 7	VF_5MW 8	VF_10MW 9	PKWL_5MW 10	PKWL_ITHX 11	SMSR_5MW 12	SBAND_5MW 13
	mean	mean	mean	mean	mean	mean	mean	mean	mean	mean	mean	mean	mean
A-2931-2	9.93	2.90	33.65	0.22	1.27	115.00	22.35	0.86	0.95	1581.5795	1581.5547	34.56	2.93
A-3255-8	8.64	2.34	29.51	0.26	0.40	100.55	23.34	0.85	0.93	1537.9323	1537.8823	40.29	3.06
A-3311-2	7.77	2.21	30.03	0.25	1.01	110.33	24.92	0.85	0.94	1541.5812	1541.5121	46.21	77.95
A-3327-5	9.43	2.12	33.15	0.23	1.03	111.04	22.93	0.85	0.93	1530.4858	1530.4184	45.25	3.26
A-3346-2	8.43	2.32	29.94	0.25	1.00	92.41	21.15	0.84	0.92	1547.7271	1547.7095	42.78	3.50
A-3346-4	9.54	2.07	29.98	0.26	0.99	112.98	26.16	0.85	0.94	1548.9175	1548.8980	42.34	3.05
A-3346-5	8.86	2.73	31.99	0.25	0.85	106.52	23.48	0.86	0.95	1541.5345	1541.4910	46.69	3.52
A-3346-6	9.39	2.18	30.68	0.25	0.85	80.85	18.59	0.83	0.91	1546.2766	1546.2906	44.87	3.32
A-3347-4	9.16	2.30	29.90	0.25	1.22	89.18	19.74	0.83	0.90	1548.3586	1548.3928	38.18	3.07
A-3350-4	11.83	2.28	30.16	0.29	0.89	111.67	26.97	0.86	0.92	1549.8528	1549.8487	35.68	2.10
A-3352-2	8.07	2.10	29.15	0.25	1.31	111.29	25.01	0.87	0.96	1541.4113	1541.3840	42.75	3.14
A-3353-2	8.69	2.95	29.43	0.26	-0.60	108.13	26.21	0.84	0.92	1532.1597	1532.1378	43.31	3.13
A-3353-3	7.55	2.21	28.19	0.26	0.84	90.74	21.43	0.84	0.92	1533.6031	1533.5854	46.93	3.84
A-3355-6	8.11	2.37	31.11	0.23	9.79	79.63	17.06	0.88	0.97	1530.4976	1530.4708	50.66	4.28
A-3356-4	9.68	2.22	31.12	0.25	1.11	84.06	19.02	0.85	0.94	1532.7272	1532.7047	44.52	3.24
A-3357-4	7.84	2.11	29.20	0.25	1.12	83.73	19.29	0.84	0.92	1525.8239	1525.7994	41.88	2.94
A-3357-8	7.09	1.88	27.67	0.26	1.04	112.27	26.67	0.83	0.90	1532.4788	1532.4611	45.67	3.63
A-3365-1	7.66	2.60	29.67	0.25	1.46	80.11	18.79	0.83	0.91	1538.3742	1538.3466	45.41	3.58
A-3366-5	8.71	2.25	32.09	0.23	1.34	83.19	17.72	0.84	0.92	1537.9765	1537.9431	45.43	4.07
A-3366-6	6.72	2.17	29.96	0.24	1.32	69.61	15.21	0.83	0.91	1537.4084	1537.3912	46.39	4.36
A-3370-1	8.63	2.18	30.71	0.25	1.58	109.51	24.55	0.86	0.95	1541.5595	1541.5313	43.87	2.84
A-3373-8	9.39	2.39	32.43	0.23	1.37	113.32	23.92	0.86	0.95	1567.0151	1566.9771	46.16	3.64
A-3376-7	9.96	2.93	31.56	0.25	1.22	79.85	18.00	0.84	0.91	1549.2102	1549.2180	40.45	2.90
A-3425-4	12.68	2.11	37.65	0.21	4.60	113.74	19.94	0.95	1.05	1574.3785	1574.3209	45.59	3.11
A-3426-4	11.57	2.30	33.27	0.24	0.88	78.77	16.36	0.83	0.90	1577.5713	1577.5503	43.72	3.42
A-3427-2	13.74	1.99	36.74	0.23	1.95	113.40	22.57	0.87	0.96	1586.4714	1586.4348	48.25	2.97
A-3427-3	10.74	2.26	33.80	0.23	6.11	110.12	20.96	0.91	1.00	1586.4658	1586.4255	46.46	3.08
A-3427-5	10.71	2.35	33.62	0.23	1.02	92.57	19.04	0.86	0.95	1585.0237	1584.9481	44.30	2.79
A-3427-8	13.33	2.88	34.79	0.24	1.26	88.06	18.10	0.85	0.92	1585.8938	1585.8903	35.92	2.90
A-3428-1	12.99	2.40	34.58	0.24	1.14	110.04	22.89	0.85	0.92	1595.2480	1595.2218	41.33	2.94
A-3429-8	11.62	3.37	34.81	0.23	2.25	112.19	22.19	0.87	0.97	1600.9406	1600.9107	35.00	2.55
A-3430-1	13.24	2.19	36.84	0.23	2.88	94.73	18.40	0.84	0.92	1600.4741	1600.4403	42.66	3.15
A-3430-6	13.82	1.65	37.81	0.22	5.31	94.25	16.93	0.92	1.02	1598.6951	1598.6538	48.91	3.68
A-3431-8	12.41	2.35	34.94	0.23	0.30	109.06	21.90	0.85	0.94	1598.3111	1598.2750	42.40	3.15
A-3434-1	8.59	2.09	29.80	0.25	1.11	114.34	26.02	0.84	0.92	1550.3595	1550.3362	44.62	3.27
A-3435-3	10.35	2.98	33.95	0.22	0.49	108.77	21.53	0.87	0.97	1561.7130	1561.6864	36.83	2.82
A-3437-5	9.91	3.02	32.25	0.24	1.99	84.69	17.70	0.83	0.91	1545.6947	1545.6828	36.22	2.63
A-3438-3	8.60	2.98	30.81	0.24	0.32	86.42	19.06	0.83	0.90	1546.8016	1546.7586	34.51	2.51
A-3438-5	11.61	2.67	32.73	0.25	0.74	88.71	19.44	0.84	0.91	1541.1484	1541.0858	31.97	2.58
A-3439-2	9.63	2.52	31.11	0.25	1.21	84.52	18.92	0.84	0.91	1541.0071	1540.9899	37.41	2.76
A-3439-4	7.39	2.59	29.31	0.25	0.97	81.34	18.86	0.83	0.91	1539.1445	1539.1296	42.02	3.21
A-3439-5	8.69	2.30	30.91	0.24	1.81	91.22	19.94	0.83	0.90	1539.1984	1539.1736	41.97	3.68
A-3440-4	8.13	2.44	28.47	0.26	0.70	80.88	19.90	0.83	0.90	1539.8857	1539.8925	41.86	3.07
A-3440-5	7.14	2.01	28.74	0.25	0.84	112.91	25.56	0.83	0.89	1536.7423	1536.7202	41.91	3.27
A-3440-7	10.58	2.75	32.71	0.24	1.62	88.22	18.80	0.84	0.91	1539.7732	1539.7478	36.40	2.32
A-3440-8	8.33	2.31	28.99	0.26	-2.34	97.81	23.23	0.84	0.91	1539.6047	1539.6183	42.23	3.32
A-3465-3	13.69	1.59	41.59	0.18	7.50	98.17	14.64	0.94	1.06	1599.0906	1599.0279	50.48	4.34
A-3466-8	16.03	2.87	39.35	0.23	2.52	78.23	14.99	0.84	0.91	1601.3723	1601.4744	36.35	2.60
A-3467-4	10.92	3.12	33.91	0.23	2.77	111.25	21.67	0.88	0.98	1600.9592	1600.9140	32.47	2.35
A-3467-6	13.08	2.13	37.20	0.22	5.31	113.38	20.27	0.90	1.00	1598.7974	1598.7524	46.78	2.90
A-3467-8	16.56	-54.31	39.62	0.23	3.14	89.06	16.58	0.85	0.93	1601.4444	1601.4078	37.44	2.55
A-3468-1	11.39	1.99	35.87	0.22	4.64	111.26	21.05	0.89	0.98	1586.8320	1586.7907	47.48	3.29
A-3468-2	14.40	2.21	38.91	0.21	4.42	111.13	19.20	0.91	1.00	1586.6378	1586.5894	45.32	2.86
A-3468-3	30.90	1.55	51.02	0.23	14.48	109.17	16.31	0.95	1.03	1585.7316	1585.7139	35.46	5.31
A-3468-4	14.53	2.35	38.68	0.21	4.42	110.03	19.31	0.90	1.00	1585.7005	1585.6855	43.75	2.47
A-3469-1	10.30	2.25	32.08	0.24	2.33	113.52	23.51	0.87	0.96	1593.4091	1593.3837	44.02	3.03
A-3469-3	10.05	2.40	31.64	0.24	0.77	111.04	23.60	0.84	0.90	1551.8981	1551.8844	34.99	2.56
A-3470-8	13.63	2.56	37.24	0.22	4.34	95.94	17.27	1.00	1.11	1588.4325	1588.3837	41.67	2.56
A-3471-2	11.48	2.64	34.14	0.24	2.79	102.73	21.36	0.87	0.96	1585.9398	1585.9040	42.81	2.90
A-3471-6	10.78	2.85	33.52	0.23	1.76	110.13	22.15	0.87	0.97	1582.8800	1582.8462	42.39	2.80
A-3472-4	10.73	2.34	32.15	0.25	1.23	112.15	23.87	0.86	0.95	1583.5639	1583.5399	41.73	2.70
A-3472-5	12.31	2.44	36.06	0.22	8.27	111.49	20.98	0.91	1.01	1583.9457	1583.9045	46.62	3.03
A-3472-8	13.28	2.44	36.55	0.22	4.86	114.68	20.49	0.95	1.05	1581.9832	1581.9395	40.00	2.49
A-3473-1	10.99	3.68	33.79	0.24	3.40	108.52	21.75	0.84	0.92	1599.3178	1599.2806	34.70	2.24
A-3476-8	9.82	2.52	31.33	0.25	1.36	110.50	24.67	0.82	0.88	1551.3558	1551.3317	35.66	2.67
A-3476-6	9.79	2.84	31.18	0.25	0.20	77.52	17.89	0.84	0.92	1553.2414	1553.2265	43.56	3.15
A-3476-8	8.11	2.72	31.62	0.24	6.06	77.27	17.37	0.85	0.93	1552.7804	1552.7776	44.65	3.63
A-3477-3	9.90	2.99	32.62	0.23	1.21	112.47	23.10	0.86	0.95	1560.7703	1560.7385	35.50	2.60

WAFER ID	ITH2L 1	REAR POWER 2	I_5MW 3	EFF_M2 4	POWSAT_10MW 5	KINKCURRENT 6	KINKPOWER 7	VF_5MW 8	VF_10MW 9	PKWL_5MW 10	PKWL_ITHX 11	SMSR_5MW 12	SBAND_5MW 13
	mean	mean	mean	mean	mean	mean	mean	mean	mean	mean	mean	mean	mean
A-3570-4	11.21	3.21	33.97	0.23	1.25	108.69	21.81	0.83	0.92	1601.1995	1601.1699	30.36	2.56
A-3570-5	9.04	2.37	32.08	0.23	-0.05	110.66	22.69	0.86	0.96	1599.2886	1599.2468	44.46	3.61
A-3570-6	11.02	2.67	34.57	0.23	1.49	110.24	21.59	0.84	0.93	1601.1723	1601.1173	40.47	2.95
A-3570-7	8.88	2.38	30.67	0.24	-0.38	112.62	24.05	0.85	0.95	1598.2657	1598.2037	43.64	3.00
A-3575-7	10.23	2.20	33.13	0.24	1.40	85.29	17.74	0.89	0.98	1583.2246	1583.1909	47.48	4.14
A-3576-5	8.18	2.35	31.38	0.23	1.74	109.95	22.66	0.85	0.94	1575.0370	1575.0076	38.86	3.17
A-3578-1	7.61	2.09	30.70	0.23	1.19	108.81	23.10	0.86	0.96	1575.2207	1575.1831	43.77	3.64
A-3579-1	11.18	2.39	34.30	0.23	1.09	110.17	22.35	0.83	0.92	1594.1773	1594.1397	42.91	3.11
A-3579-3	11.16	2.10	36.00	0.22	2.52	113.39	21.22	0.89	0.98	1595.4222	1595.3336	46.54	2.94
A-3580-8	9.60	2.87	33.58	0.23	1.18	107.73	21.50	0.86	0.96	1583.2466	1583.1824	39.14	3.14
A-3583-1	9.84	2.62	32.72	0.23	1.23	98.68	19.95	0.83	0.93	1593.2509	1593.2139	36.79	2.72
A-3583-4	11.05	2.10	34.50	0.23	1.01	110.86	21.68	0.90	1.00	1591.4151	1591.3712	43.88	3.19
A-3695-7	8.70	2.29	30.08	0.25	1.05	91.01	20.58	0.87	0.96	1529.7279	1529.7053	40.06	3.13
A-3696-2	8.68	2.12	29.51	0.25	0.94	91.06	20.58	0.82	0.90	1555.4849	1555.4398	38.74	3.50
A-3696-7	7.43	1.89	30.67	0.23	1.39	115.00	24.11	0.85	0.94	1557.4980	1557.4565	43.97	3.66
A-3696-8	9.14	2.51	31.98	0.24	1.44	81.60	17.34	0.84	0.92	1554.1508	1554.1204	43.63	3.55
A-3698-3	7.87	2.12	30.96	0.23	1.08	111.10	23.30	0.86	0.95	1557.2100	1557.1086	42.03	3.48
A-3698-5	8.47	2.40	32.49	0.23	1.57	77.19	16.19	0.83	0.92	1559.2448	1559.2025	45.60	4.37
A-3698-8	9.68	2.56	33.42	0.23	1.71	79.26	16.09	0.83	0.90	1556.6054	1556.5735	41.33	3.73
A-3699-6	7.80	2.35	29.59	0.24	1.04	110.12	24.00	0.81	0.88	1548.2520	1548.2047	33.00	2.94
A-3700-3	7.01	2.16	28.79	0.24	1.38	109.57	24.26	0.85	0.92	1536.5198	1536.4538	41.34	3.58
A-3700-4	8.82	2.02	30.38	0.24	1.11	91.43	20.19	0.84	0.93	1530.1364	1530.1112	39.37	3.18
A-3700-5	9.49	2.16	31.93	0.24	1.29	108.78	23.56	0.84	0.91	1537.5173	1537.5106	40.88	3.16
A-3700-7	9.53	2.33	33.91	0.22	1.32	84.33	16.44	0.86	0.95	1528.9394	1528.8634	38.26	3.44
A-3740-4	6.48	3.59	27.50	0.25	1.37	100.36	24.11	0.85	0.94	1476.6432	1476.6230	32.97	2.73
A-3740-5	6.36	2.55	27.32	0.27	0.74	108.75	27.48	0.85	0.93	1490.7166	1490.5834	38.67	3.28
A-3740-6	6.35	2.42	24.88	0.30	0.97	108.53	30.49	0.83	0.90	1490.8355	1490.7152	37.45	3.05
A-3741-7	7.04	0.81	15.67	0.64	1.04	76.74	48.67	0.77	0.80	1517.7353	1517.7825	39.73	3.51
A-3747-1	11.07	2.14	32.03	0.25	1.37	112.24	24.06	0.84	0.93	1616.6301	1616.6121	41.11	3.09
A-3823-1	9.14	2.77	30.30	0.25	1.62	108.61	23.43	0.84	0.93	1601.6727	1601.6491	31.74	2.49
A-3823-2	10.03	2.81	32.24	0.23	1.41	111.08	22.78	0.84	0.94	1603.3592	1603.3234	35.54	2.77
A-3823-4	10.91	3.08	35.87	0.21	0.98	109.03	19.62	0.87	0.97	1603.1483	1603.0931	34.99	2.68
A-3823-5	9.68	3.16	31.49	0.24	1.03	108.76	23.32	0.82	0.90	1602.0786	1602.0594	30.78	2.46
A-3823-8	9.09	2.88	29.54	0.25	1.25	113.02	25.24	0.82	0.90	1602.2154	1602.2096	31.45	2.33
A-3826-2	9.57	2.39	30.92	0.25	0.90	109.48	24.28	0.84	0.93	1582.1025	1582.0687	39.61	3.13
A-3826-3	9.41	2.21	31.29	0.24	1.69	113.02	23.87	0.85	0.94	1581.1803	1581.1504	39.66	3.03
A-3826-4	9.10	2.24	31.01	0.24	1.45	109.27	23.67	0.84	0.93	1582.1858	1582.1417	40.46	3.25
A-3828-5	10.08	2.17	31.82	0.24	0.87	110.61	23.39	0.84	0.92	1580.7433	1580.7163	38.12	2.99
A-3861-1	10.09	2.81	32.62	0.24	0.97	109.45	22.95	0.86	0.95	1559.2154	1559.1833	36.79	2.82
A-3862-1	8.57	2.08	31.04	0.24	-2.30	111.20	23.84	0.84	0.92	1560.5426	1560.4523	42.48	3.38
A-3862-8	10.77	2.73	34.66	0.23	0.95	106.58	21.29	0.84	0.92	1560.7562	1560.7176	35.72	2.80
A-3864-1	8.95	0.64	23.30	0.36	0.48	104.05	33.51	0.81	0.86	1553.5630	1553.5770	50.20	3.44
A-3864-2	8.93	2.17	30.07	0.25	0.84	111.52	25.46	0.84	0.92	1556.1133	1556.0384	42.72	3.47
A-3864-4	10.90	2.20	32.95	0.24	0.79	111.83	23.83	0.86	0.94	1558.8868	1558.8282	38.56	2.93
A-3864-5	9.13	1.86	31.21	0.25	1.05	112.34	25.09	0.85	0.93	1555.6475	1555.6153	43.80	3.53
A-3864-8	9.12	2.40	30.27	0.25	0.23	109.68	24.74	0.82	0.89	1559.4697	1559.4457	37.02	2.95
A-3865-5	8.69	2.54	31.42	0.23	0.69	113.07	24.13	0.82	0.89	1556.0557	1556.0189	36.85	3.00
A-3866-1	8.91	1.92	28.78	0.27	1.01	111.64	26.61	0.85	0.94	1558.6903	1558.6736	46.25	3.57
A-3866-4	8.81	2.61	31.79	0.23	1.27	106.23	22.67	0.82	0.90	1558.8633	1558.7879	35.66	3.15
A-3866-8	8.17	2.23	29.10	0.25	1.63	109.05	24.97	0.85	0.92	1553.0493	1553.0478	40.25	2.75
A-3867-1	8.89	2.32	30.50	0.24	1.13	111.93	24.50	0.85	0.92	1532.7683	1532.7411	37.48	2.89
A-3867-2	9.98	2.85	32.87	0.23	1.64	108.17	22.01	0.85	0.94	1533.2386	1533.1616	32.31	2.40
A-3867-3	9.31	2.21	29.79	0.26	0.87	110.16	25.33	0.84	0.92	1533.2958	1533.2838	39.18	2.74
A-3867-4	9.77	2.39	32.02	0.24	0.18	110.90	24.11	0.82	0.88	1534.9712	1534.9833	38.55	2.86
A-3867-7	10.68	2.77	32.78	0.24	1.41	111.73	23.53	0.84	0.92	1533.0551	1533.0236	29.82	2.35
A-3868-6	9.94	2.21	32.13	0.23	0.69	105.37	21.95	0.83	0.91	1533.2044	1533.1505	33.88	2.58
A-3869-2	9.19	2.14	29.60	0.26	1.20	112.19	25.64	0.85	0.93	1534.4920	1534.4728	38.20	2.79
A-3869-4	9.73	2.31	31.61	0.24	1.22	106.38	23.01	0.85	0.93	1534.6287	1534.5980	36.45	2.78
A-3869-7	8.12	2.04	31.30	0.23	-0.39	110.72	23.32	0.86	0.95	1542.4966	1542.4038	38.94	3.22
A-3870-1	8.71	2.19	29.04	0.26	0.05	102.30	23.29	0.85	0.94	1535.0909	1535.1456	37.95	2.82
A-3870-2	9.19	2.78	32.52	0.23	3.01	115.00	22.50	0.87	0.96	1527.6296	1527.5796	36.55	2.28
A-3870-2	8.74	2.59	30.54	0.24	0.73	106.46	23.32	0.86	0.95	1528.0932	1528.1162	36.88	2.84
A-3870-3	9.04	2.21	31.18	0.24	1.06	112.38	23.95	0.85	0.92	1529.3131	1529.2626	37.88	2.89
A-3870-4	9.87	2.23	31.77	0.24	1.22	109.76	24.23	0.85	0.93	1528.9821	1528.9805	39.61	3.06
A-3871-2	10.60	2.63	33.05	0.24	1.56	110.44	23.36	0.88	0.96	1528.9667	1528.9338	36.92	2.80
A-3871-3	8.50	1.90	29.53	0.25	1.61	110.90	25.36	0.85	0.92	1534.8267	1534.8040	40.51	3.41
A-3871-5	9.71	2.47	32.40	0.24	1.37	111.68	23.74	0.87	0.94	1528.6590	1528.6181	41.51	3.18
A-3871-6	11.57	2.13	33.87	0.24	1.91	110.11	22.96	0.85	0.92	1527.3970	1527.3642	38.55	2.73

Appendix G

Correlation Matrices

The first row and the first column of the correlation matrix contain the column number associated to each variable as defined in Appendix A.

	2	3	4	5	6	7	8	9	10	11	12	13	14	15	16	17	18	19	20
2	1.00	0.09	0.88	-0.47	0.45	0.04	-0.42	0.50	0.49	0.60	-0.02	-0.36	-0.31	0.02	-0.08	0.29	0.17	-0.03	0.01
3	0.09	1.00	0.17	-0.23	-0.02	-0.10	-0.22	-0.11	-0.06	0.10	-0.61	-0.51	-0.55	0.50	0.57	-0.17	-0.19	0.03	0.03
4	0.88	0.17	1.00	-0.81	0.55	0.01	-0.60	0.60	0.63	0.60	0.06	-0.18	-0.19	-0.07	-0.08	0.16	0.29	-0.02	0.04
5	-0.47	-0.23	-0.81	1.00	-0.45	-0.04	0.61	-0.50	-0.58	-0.42	0.00	0.01	0.02	0.04	0.16	0.09	-0.23	0.01	0.00
6	0.45	-0.02	0.55	-0.45	1.00	-0.08	-0.42	0.65	0.63	0.29	0.30	0.08	0.04	-0.21	-0.02	0.19	0.22	0.08	0.09
7	0.04	-0.10	0.01	-0.04	-0.08	1.00	0.74	0.15	0.16	0.17	-0.16	-0.33	-0.20	0.18	-0.66	0.23	0.27	-0.01	-0.68
8	-0.42	-0.22	-0.60	0.61	-0.42	0.74	1.00	-0.29	-0.32	-0.25	-0.14	-0.17	-0.11	0.17	-0.44	0.09	-0.04	0.00	-0.53
9	0.50	-0.11	0.60	-0.50	0.65	0.15	-0.29	1.00	0.98	0.30	0.35	0.01	0.12	-0.33	-0.22	0.22	0.22	0.03	-0.11
10	0.49	-0.06	0.63	-0.58	0.63	0.16	-0.32	0.98	1.00	0.37	0.33	0.02	0.12	-0.32	-0.22	0.15	0.23	0.04	-0.09
11	0.60	0.10	0.60	-0.42	0.29	0.17	-0.25	0.30	0.37	1.00	0.08	-0.12	-0.11	-0.09	-0.13	0.01	0.10	0.12	-0.05
12	-0.02	-0.61	0.06	0.00	0.30	-0.16	-0.14	0.35	0.33	0.08	1.00	0.74	0.67	-0.94	-0.06	0.27	0.54	0.09	0.24
13	-0.12	0.00	-0.08	0.04	-0.03	0.05	0.08	-0.03	-0.01	0.05	0.15	1.00	-0.06	-0.15	0.02	0.06	0.17	0.30	0.03
14	-0.31	-0.55	-0.19	0.02	0.04	-0.20	-0.11	0.12	0.12	-0.11	0.67	0.78	1.00	-0.65	-0.08	-0.40	0.10	-0.19	0.15
15	0.02	0.50	-0.07	0.04	-0.21	0.18	0.17	-0.33	-0.32	-0.09	-0.94	-0.68	-0.65	1.00	0.02	-0.22	-0.44	-0.13	-0.27
16	-0.08	0.57	-0.08	0.16	-0.02	-0.66	-0.44	-0.22	-0.22	-0.13	-0.06	0.05	-0.08	0.02	1.00	-0.18	-0.14	0.00	0.49
17	0.29	-0.17	0.16	0.09	0.19	0.23	0.09	0.22	0.15	0.01	0.27	-0.26	-0.40	-0.22	-0.18	1.00	0.26	0.10	-0.22
18	0.17	-0.19	0.29	-0.23	0.22	0.27	-0.04	0.22	0.23	0.10	0.54	0.27	0.10	-0.44	-0.14	0.26	1.00	-0.03	-0.11
19	-0.03	0.03	-0.02	0.01	0.08	-0.01	0.00	0.03	0.04	0.12	0.09	-0.06	-0.19	-0.13	0.00	0.10	-0.03	1.00	-0.08
20	0.01	0.03	0.04	0.00	0.09	-0.68	-0.53	-0.11	-0.09	-0.05	0.24	0.40	0.15	-0.27	0.49	-0.22	-0.11	-0.08	1.00
21	0.75	-0.13	0.63	-0.27	0.25	-0.12	-0.35	0.22	0.19	0.30	0.04	-0.13	-0.19	-0.27	-0.02	0.50	0.39	-0.25	0.28
22	0.17	0.22	0.20	-0.19	0.08	-0.15	-0.27	0.00	0.05	0.40	-0.12	-0.11	0.01	0.04	0.17	-0.12	-0.04	-0.06	-0.01
23	-0.01	0.02	0.05	-0.14	0.07	-0.11	-0.14	0.11	0.08	-0.38	-0.03	0.03	0.03	-0.03	-0.06	0.08	-0.02	-0.09	0.06
24	-0.05	0.06	-0.03	-0.03	-0.04	0.26	0.20	-0.03	-0.01	0.04	-0.20	-0.14	-0.12	0.15	-0.11	-0.19	-0.13	-0.01	-0.16
25	0.02	-0.05	-0.06	0.14	-0.05	-0.17	-0.07	0.01	-0.01	-0.07	0.16	0.07	0.10	-0.10	0.17	0.13	0.17	0.08	0.11
26	-0.18	0.05	-0.25	0.29	0.00	-0.12	0.12	-0.01	-0.07	-0.41	0.10	-0.02	-0.02	-0.09	0.32	0.21	-0.04	0.10	0.05
27	-0.12	-0.01	-0.12	0.03	0.11	0.02	0.04	0.02	-0.01	-0.12	-0.02	-0.02	-0.05	0.14	0.05	0.07	-0.07	-0.14	-0.07
28	-0.33	0.13	-0.35	0.28	-0.05	-0.11	0.15	-0.05	-0.10	-0.56	-0.09	-0.02	-0.03	0.02	0.28	0.00	-0.15	0.01	0.06
29	0.52	0.00	0.51	-0.36	0.28	0.10	-0.26	0.26	0.30	0.81	0.14	-0.08	-0.04	-0.10	-0.12	0.11	0.07	0.04	-0.11
30	0.55	0.01	0.54	-0.38	0.28	0.11	-0.26	0.27	0.32	0.84	0.14	-0.09	-0.03	-0.12	-0.13	0.09	0.09	0.07	-0.11
31	-0.13	-0.11	-0.08	-0.04	-0.05	-0.04	-0.02	-0.10	-0.09	-0.17	-0.08	0.08	0.06	0.07	-0.13	-0.12	-0.10	-0.10	-0.04
32	0.59	0.08	0.57	-0.39	0.36	0.15	-0.25	0.30	0.36	0.96	0.16	-0.09	-0.05	-0.16	-0.12	0.04	0.13	0.13	-0.06
33	0.59	-0.03	0.59	-0.37	0.35	0.14	-0.23	0.36	0.41	0.94	0.29	-0.01	0.03	-0.30	-0.15	0.11	0.23	0.11	-0.04
34	0.58	0.06	0.57	-0.40	0.30	0.19	-0.23	0.30	0.36	0.95	0.12	-0.11	-0.05	-0.10	-0.17	0.08	0.14	0.08	-0.12
35	-0.19	0.05	-0.21	0.21	-0.08	-0.19	0.01	-0.14	-0.17	-0.19	0.21	0.18	0.14	-0.19	0.30	0.07	0.16	0.02	0.36
36	-0.26	-0.01	-0.28	0.27	-0.11	-0.36	-0.09	-0.15	-0.18	-0.28	0.27	0.22	0.18	-0.24	0.36	0.06	0.10	0.03	0.38
37	-0.30	-0.05	-0.26	0.12	-0.20	0.13	0.22	-0.11	-0.08	-0.15	0.10	0.10	0.11	-0.09	-0.08	-0.16	0.15	-0.07	0.02
38	0.26	0.02	0.28	-0.18	0.30	-0.14	-0.27	0.26	0.24	0.24	0.28	0.10	0.08	-0.31	0.12	0.23	0.24	0.08	-0.18
39	0.13	0.11	0.01	0.04	-0.19	0.26	0.20	-0.15	-0.16	0.02	-0.50	-0.39	-0.35	0.52	-0.24	-0.05	-0.41	-0.12	-0.22
40	0.19	-0.03	0.18	-0.01	0.25	-0.26	-0.26	0.26	0.21	0.01	0.27	0.07	-0.02	-0.29	0.20	0.54	0.20	0.09	0.14
41	0.29	-0.09	0.31	-0.19	0.27	-0.11	-0.25	0.34	0.32	0.11	0.22	0.05	0.10	-0.18	0.07	0.16	0.37	-0.05	-0.04
42	0.50	-0.01	0.54	-0.38	0.54	-0.07	-0.40	0.49	0.50	0.66	0.40	0.05	0.06	-0.37	0.02	0.28	0.30	0.10	0.02
43	-0.48	0.23	-0.53	0.38	-0.51	-0.07	0.28	-0.61	-0.58	-0.40	-0.41	-0.13	-0.06	0.34	0.18	-0.37	-0.29	-0.01	0.04
44	0.62	0.07	0.61	-0.43	0.30	0.16	-0.27	0.30	0.36	0.95	0.10	-0.14	-0.09	-0.11	-0.16	0.07	0.13	0.10	-0.11
45	0.62	0.09	0.61	-0.42	0.27	0.17	-0.25	0.28	0.34	0.95	0.07	-0.16	-0.10	-0.08	-0.17	0.05	0.10	0.10	-0.12
46	-0.45	0.20	-0.50	0.39	-0.49	-0.06	0.27	-0.56	-0.54	-0.44	-0.41	-0.14	-0.09	0.34	0.18	-0.34	-0.22	-0.07	0.03
47	-0.10	-0.03	-0.06	0.02	-0.04	0.00	0.04	-0.03	-0.02	-0.06	0.14	0.13	0.02	-0.15	0.02	0.05	0.19	0.10	0.00
48	0.13	0.19	0.13	-0.08	-0.08	-0.20	-0.21	-0.16	-0.17	0.02	-0.08	-0.08	-0.01	-0.03	0.25	-0.12	0.24	-0.02	0.06
49	-0.43	-0.03	-0.47	0.39	-0.39	-0.28	0.12	-0.48	-0.53	-0.63	-0.11	0.14	0.01	0.13	0.27	0.01	-0.02	-0.14	0.21
50	-0.04	0.01	-0.03	-0.07	-0.17	0.27	0.18	-0.05	-0.05	0.18	-0.06	-0.04	0.03	0.03	-0.11	-0.08	-0.18	0.24	-0.24
51	0.10	0.05	0.06	0.05	0.10	-0.32	-0.23	0.00	-0.01	0.01	0.17	0.17	0.12	-0.22	0.38	-0.13	-0.02	0.02	0.27
52	-0.08	-0.09	-0.07	0.02	-0.13	0.11	0.13	-0.15	-0.16	-0.18	-0.01	-0.05	0.02	0.09	-0.07	0.09	0.14	-0.06	0.05
53	-0.09	0.17	-0.09	0.04	0.14	-0.17	-0.12	-0.04	-0.06	0.00	-0.16	-0.12	-0.13	0.12	0.16	0.03	-0.17	0.18	0.16
54	-0.14	0.25	-0.11	0.03	0.10	-0.25	-0.18	-0.10	-0.10	0.00	-0.15	-0.09	-0.12	0.11	0.24	0.07	-0.14	0.13	0.20
55	0.01	0.08	0.08	-0.14	0.05	0.13	0.03	0.08	0.10	0.03	-0.02	0.14	0.00	0.07	0.03	-0.11	-0.01	-0.22	-0.02
56	-0.22	0.00	-0.31	0.26	-0.26	0.13	0.28	-0.25	-0.23	-0.12	-0.15	-0.09	-0.01	0.06	-0.09	-0.32	-0.20	0.11	-0.14
57	0.04	-0.08	0.08	-0.09	0.12	0.11	0.02	0.24	0.25	0.17	0.20	0.02	0.02	-0.24	-0.15	0.11	0.00	0.24	-0.12
58	-0.01	-0.02	-0.02	0.01	-0.12	0.01	0.02	-0.18	-0.15	0.09	-0.04	0.05	0.04	0.10	0.08	-0.22	0.06	-0.03	-0.04
59	-0.35	0.05	-0.29	0.13	-0.17	0.04	0.17	-0.07	-0.08	-0.25	-0.04	0.14	0.15	0.04	0.01	-0.05	-0.20	-0.14	-0.11

	21	22	23	24	25	26	27	28	29	30	31	32	33	34	35	36	37	38	39	40
2	0.75	0.17	-0.01	-0.05	0.02	-0.18	-0.12	-0.33	0.52	0.55	-0.13	0.59	0.59	0.58	-0.19	-0.26	-0.30	0.26	0.13	0.19
3	-0.13	0.22	0.02	0.06	-0.05	0.05	-0.01	0.13	0.00	0.01	-0.11	0.08	-0.03	0.06	0.05	-0.01	-0.05	0.02	0.11	-0.03
4	0.63	0.20	0.05	-0.03	-0.06	-0.25	-0.12	-0.35	0.51	0.54	-0.08	0.57	0.59	0.57	-0.21	-0.28	-0.26	0.28	0.01	0.18
5	-0.27	-0.19	-0.14	-0.03	0.14	0.29	0.03	0.28	-0.36	-0.38	-0.04	-0.39	-0.37	-0.40	0.21	0.27	0.12	-0.18	0.04	-0.01
6	0.25	0.08	0.07	-0.04	-0.05	0.00	0.11	-0.05	0.28	0.28	-0.05	0.36	0.35	0.30	-0.08	-0.11	-0.20	0.30	-0.19	0.25
7	-0.12	-0.15	-0.11	0.26	-0.17	-0.12	0.02	-0.11	0.10	0.11	-0.04	0.15	0.14	0.19	-0.19	-0.36	0.13	-0.14	0.26	-0.26
8	-0.35	-0.27	-0.14	0.20	-0.07	0.12	0.04	0.15	-0.26	-0.26	-0.02	-0.25	-0.23	-0.23	0.01	-0.09	0.22	-0.27	0.20	-0.26
9	0.22	0.00	0.11	-0.03	0.01	-0.01	0.02	-0.05	0.26	0.27	-0.10	0.30	0.36	0.30	-0.14	-0.15	-0.11	0.26	-0.15	0.26
10	0.19	0.05	0.08	-0.01	-0.01	-0.07	-0.01	-0.10	0.30	0.32	-0.09	0.36	0.41	0.36	-0.17	-0.18	-0.08	0.24	-0.16	0.21
11	0.30	0.40	-0.38	0.04	-0.07	-0.41	-0.12	-0.56	0.81	0.84	-0.17	0.96	0.94	0.95	-0.19	-0.28	-0.15	0.24	0.02	0.01
12	0.04	-0.12	-0.03	-0.20	0.16	0.10	-0.02	-0.09	0.14	0.14	-0.08	0.16	0.29	0.12	0.21	0.27	0.10	0.28	-0.50	0.27
13	-0.13	-0.02	-0.09	-0.04	0.03	-0.03	-0.14	-0.05	0.02	0.04	-0.02	0.09	0.09	0.05	0.09	0.05	0.21	-0.10	-0.21	-0.01
14	-0.19	0.01	0.03	-0.12	0.10	-0.02	-0.05	-0.03	-0.04	-0.03	0.06	-0.05	0.03	-0.05	0.14	0.18	0.11	0.08	-0.35	-0.02
15	-0.27	0.04	-0.03	0.15	-0.10	-0.09	0.14	0.02	-0.10	-0.12	0.07	-0.16	-0.30	-0.10	-0.19	-0.24	-0.09	-0.31	0.52	-0.29
16	-0.02	0.17	-0.06	-0.11	0.17	0.32	0.05	0.28	-0.12	-0.13	-0.13	-0.12	-0.15	-0.17	0.30	0.36	-0.08	0.12	-0.24	0.20
17	0.50	-0.12	0.08	-0.19	0.13	0.21	0.07	0.00	0.11	0.09	-0.12	0.04	0.11	0.08	0.07	0.06	-0.16	0.23	-0.05	0.54
18	0.39	-0.04	-0.02	-0.13	0.17	-0.04	-0.07	-0.15	0.07	0.09	-0.10	0.13	0.23	0.14	0.16	0.10	0.15	0.24	-0.41	0.20
19	-0.25	-0.06	-0.09	-0.01	0.08	0.10	-0.14	0.01	0.04	0.07	-0.10	0.13	0.11	0.08	0.02	0.03	-0.07	0.08	-0.12	0.09
20	0.28	-0.01	0.06	-0.16	0.11	0.05	-0.07	0.06	-0.11	-0.11	-0.04	-0.06	-0.04	-0.12	0.36	0.38	0.02	-0.18	-0.22	0.14
21	1.00	0.00	0.22	0.10	0.24	-0.16	-0.09	-0.19	0.25	0.26	-0.08	0.30	0.40	0.26	-0.09	-0.17	-0.20	0.19	0.09	0.22
22	0.00	1.00	-0.33	0.06	-0.08	-0.18	-0.10	-0.11	0.40	0.42	0.15	0.40	0.39	0.42	-0.14	-0.12	-0.21	0.25	-0.11	0.07
23	0.22	-0.33	1.00	-0.28	0.04	0.07	0.25	0.26	-0.33	-0.37	0.17	-0.43	-0.40	-0.42	-0.07	0.02	-0.05	-0.02	0.12	-0.06
24	0.10	0.06	-0.28	1.00	-0.73	0.02	0.09	0.10	-0.01	0.00	-0.18	0.02	0.01	0.05	-0.25	-0.39	0.08	-0.29	0.27	-0.10
25	0.24	-0.08	0.04	-0.73	1.00	0.17	-0.04	-0.03	-0.04	-0.04	-0.16	-0.03	-0.03	-0.07	0.40	0.47	0.06	0.26	-0.31	0.19
26	-0.16	-0.18	0.07	0.02	0.17	1.00	0.13	0.49	-0.29	-0.31	-0.55	-0.37	-0.26	-0.38	0.43	0.38	0.00	-0.08	-0.17	0.18
27	-0.09	-0.10	0.25	0.09	-0.04	0.13	1.00	0.24	0.11	0.00	0.03	-0.11	-0.27	-0.10	0.08	0.12	0.07	0.09	0.18	-0.04
28	-0.19	-0.11	0.26	0.10	-0.03	0.49	0.24	1.00	-0.59	-0.62	0.14	-0.53	-0.47	-0.53	0.18	0.29	0.04	-0.07	0.00	0.07
29	0.25	0.40	-0.33	-0.01	-0.04	-0.29	0.11	-0.59	1.00	0.99	-0.12	0.80	0.76	0.80	-0.15	-0.19	-0.17	0.30	0.01	0.03
30	0.26	0.42	-0.37	0.00	-0.04	-0.31	0.00	-0.62	0.99	1.00	-0.13	0.83	0.80	0.83	-0.17	-0.21	-0.16	0.30	-0.01	0.03
31	-0.08	0.15	0.17	-0.18	-0.16	-0.55	0.03	0.14	-0.12	-0.13	1.00	-0.19	-0.19	-0.17	-0.33	-0.11	-0.03	0.08	0.13	-0.12
32	0.30	0.40	-0.43	0.02	-0.03	-0.37	-0.11	-0.53	0.80	0.83	-0.19	1.00	1.00	0.99	-0.14	-0.23	-0.06	0.34	-0.02	0.03
33	0.40	0.39	-0.40	0.01	-0.03	-0.26	-0.27	-0.47	0.76	0.80	-0.19	1.00	1.00	0.98	-0.11	-0.24	-0.12	0.30	-0.19	0.14
34	0.26	0.42	-0.42	0.05	-0.07	-0.38	-0.10	-0.53	0.80	0.83	-0.17	0.99	0.98	1.00	-0.19	-0.28	-0.12	0.26	0.00	0.00
35	-0.09	-0.14	-0.07	-0.25	0.40	0.43	0.08	0.18	-0.15	-0.17	-0.33	-0.14	-0.11	-0.19	1.00	0.83	0.20	-0.05	-0.34	0.13
36	-0.17	-0.12	0.02	-0.39	0.47	0.38	0.12	0.29	-0.19	-0.21	-0.11	-0.23	-0.24	-0.28	0.83	1.00	0.18	0.08	-0.37	0.16
37	-0.20	-0.21	-0.05	0.08	0.06	0.00	0.07	0.04	-0.17	-0.16	-0.03	-0.06	-0.12	-0.12	0.20	0.18	1.00	-0.32	-0.01	-0.26
38	0.19	0.25	-0.02	-0.29	0.26	-0.08	0.09	-0.07	0.30	0.30	0.08	0.34	0.30	0.26	-0.05	0.08	-0.32	1.00	-0.33	0.31
39	0.09	-0.11	0.12	0.27	-0.31	-0.17	0.18	0.00	0.01	-0.01	0.13	-0.02	-0.19	0.00	-0.34	-0.37	-0.01	-0.33	1.00	-0.39
40	0.22	0.07	-0.06	-0.10	0.19	0.18	-0.04	0.07	0.03	0.03	-0.12	0.03	0.14	0.00	0.13	0.16	-0.26	0.31	-0.39	1.00
41	0.24	0.06	-0.06	-0.29	0.15	-0.10	-0.31	-0.18	0.05	0.09	0.02	0.07	0.21	0.08	-0.04	-0.02	-0.18	0.22	-0.37	0.27
42	0.29	0.35	-0.31	-0.03	0.05	-0.12	0.01	-0.24	0.63	0.65	-0.18	0.76	0.76	0.71	0.03	0.03	-0.07	0.47	-0.31	0.40
43	-0.30	0.06	-0.10	0.05	-0.03	0.09	-0.18	0.16	-0.42	-0.40	0.10	-0.45	-0.44	-0.42	0.10	0.12	0.16	-0.35	0.13	-0.21
44	0.28	0.43	-0.42	0.05	-0.07	-0.42	-0.12	-0.56	0.81	0.84	-0.17	0.99	0.97	0.98	-0.20	-0.26	-0.12	0.30	0.01	0.01
45	0.26	0.43	-0.42	0.05	-0.08	-0.43	-0.14	-0.58	0.81	0.84	-0.16	0.99	0.97	0.97	-0.21	-0.28	-0.13	0.28	0.04	-0.02
46	-0.20	0.02	-0.11	0.06	-0.04	0.06	-0.24	0.16	-0.49	-0.47	0.11	-0.47	-0.46	-0.45	0.08	0.07	0.16	-0.35	0.14	-0.18
47	-0.18	-0.16	0.02	-0.22	0.16	-0.02	0.01	0.00	-0.03	-0.04	-0.02	-0.04	-0.01	-0.06	0.19	0.22	0.17	0.10	-0.19	0.13
48	0.16	0.18	0.10	-0.16	0.08	0.00	-0.09	-0.01	0.02	0.03	0.03	-0.02	0.04	0.02	0.15	0.13	-0.10	0.11	-0.15	0.08
49	-0.12	-0.26	0.29	-0.14	0.08	0.26	0.08	0.30	-0.51	-0.54	0.11	-0.69	-0.70	-0.69	0.21	0.34	-0.01	-0.17	0.05	0.02
50	-0.23	0.07	-0.20	0.05	0.02	0.07	0.00	0.02	0.13	0.13	-0.02	0.22	0.12	0.19	0.13	0.02	-0.06	0.07	0.04	-0.13
51	0.16	0.08	-0.08	0.07	0.00	0.23	-0.01	0.12	0.05	0.05	-0.16	0.09	0.07	0.01	0.27	0.21	-0.08	0.08	-0.15	0.16
52	0.21	-0.13	-0.02	-0.08	0.22	0.15	0.08	-0.02	-0.09	-0.10	-0.07	-0.22	-0.14	-0.16	0.26	0.19	0.01	-0.26	-0.07	0.04
53	-0.12	0.09	0.09	-0.21	0.11	-0.06	0.06	0.14	0.01	0.00	0.19	0.00	-0.16	-0.02	-0.02	0.14	-0.01	0.16	-0.04	0.08
54	-0.12	0.14	0.10	-0.24	0.12	-0.12	0.08	0.13	0.02	0.00	0.21	0.01	-0.13	-0.02	0.00	0.18	-0.01	0.19	-0.06	0.10
55	-0.22	0.03	0.01	0.12	-0.21	-0.01	0.14	0.07	0.02	0.01	-0.10	0.01	-0.02	0.05	-0.04	-0.12	-0.08	-0.02	0.25	-0.32
56	-0.07	-0.15	-0.01	0.18	0.06	0.09	0.04	-0.02	-0.20	-0.20	-0.10	-0.15	-0.18	-0.15	0.08	0.04	0.33	-0.36	0.04	-0.06
57	-0.05	-0.04	0.01	0.14	-0.14	0.02	0.00	0.01	0.15	0.15	0.00	0.18	0.19	0.18	-0.03	-0.03	0.00	0.15	-0.17	-0.03
58	-0.04	0.09	-0.11	0.17	-0.25	-0.06	0.08	0.05	0.04	0.04	0.07	0.09	0.09	0.12	-0.14	-0.14	0.02	-0.02	0.24	-0.27
59	-0.32	-0.15	0.13	-0.03	-0.02	0.00	0.08	0.20	-0.19	-0.22	0.17	-0.23	-0.29	-0.23	-0.18	0.01	0.11	-0.04	0.12	-0.20

	41	42	43	44	45	46	47	48	49	50	51	52	53	54	55	56	57	58	59
2	0.29	0.50	-0.48	0.62	0.62	-0.45	-0.10	0.13	-0.43	-0.04	0.10	-0.08	-0.09	-0.14	0.01	-0.22	0.04	-0.01	-0.35
3	-0.09	-0.01	0.23	0.07	0.09	0.20	-0.03	0.19	-0.03	0.01	0.05	-0.09	0.17	0.25	0.08	0.00	-0.08	-0.02	0.05
4	0.31	0.54	-0.53	0.61	0.61	-0.50	-0.06	0.13	-0.47	-0.03	0.06	-0.07	-0.09	-0.11	0.08	-0.31	0.08	-0.02	-0.29
5	-0.19	-0.38	0.38	-0.43	-0.42	0.39	0.02	-0.08	0.39	-0.07	0.05	0.02	0.04	0.03	-0.14	0.26	-0.09	0.01	0.13
6	0.27	0.54	-0.51	0.30	0.27	-0.49	-0.04	-0.08	-0.39	-0.17	0.10	-0.13	0.14	0.10	0.05	-0.26	0.12	-0.12	-0.17
7	-0.11	-0.07	-0.07	0.16	0.17	-0.06	0.00	-0.20	-0.28	0.27	-0.32	0.11	-0.17	-0.25	0.13	0.13	0.11	0.01	0.04
8	-0.25	-0.40	0.28	-0.27	-0.25	0.27	0.04	-0.21	0.12	0.18	-0.23	0.13	-0.12	-0.18	0.03	0.28	0.02	0.02	0.17
9	0.34	0.49	-0.61	0.30	0.28	-0.56	-0.03	-0.16	-0.48	-0.05	0.00	-0.15	-0.04	-0.10	0.08	-0.25	0.24	-0.18	-0.07
10	0.32	0.50	-0.58	0.36	0.34	-0.54	-0.02	-0.17	-0.53	-0.05	-0.01	-0.16	-0.06	-0.10	0.10	-0.23	0.25	-0.15	-0.08
11	0.11	0.66	-0.40	0.95	0.95	-0.44	-0.06	0.02	-0.63	0.18	0.01	-0.18	0.00	0.00	0.03	-0.12	0.17	0.09	-0.25
12	0.22	0.40	-0.41	0.10	0.07	-0.41	0.14	-0.08	-0.11	-0.06	0.17	-0.01	-0.16	-0.15	-0.02	-0.15	0.20	-0.04	-0.04
13	-0.08	0.06	-0.03	0.02	0.02	-0.01	0.39	0.05	-0.03	0.03	-0.05	0.03	0.00	0.01	-0.05	0.04	0.07	0.00	0.06
14	0.10	0.06	-0.06	-0.09	-0.10	-0.09	0.02	-0.01	0.01	0.03	0.12	0.02	-0.13	-0.12	0.00	-0.01	0.02	0.04	0.15
15	-0.18	-0.37	0.34	-0.11	-0.08	0.34	-0.15	-0.03	0.13	0.03	-0.22	0.09	0.12	0.11	0.07	0.06	-0.24	0.10	0.04
16	0.07	0.02	0.18	-0.16	-0.17	0.18	0.02	0.25	0.27	-0.11	0.38	-0.07	0.16	0.24	0.03	-0.09	-0.15	0.08	0.01
17	0.16	0.28	-0.37	0.07	0.05	-0.34	0.05	-0.12	0.01	-0.08	-0.13	0.09	0.03	0.07	-0.11	-0.32	0.11	-0.22	-0.05
18	0.37	0.30	-0.29	0.13	0.10	-0.22	0.19	0.24	-0.02	-0.18	-0.02	0.14	-0.17	-0.14	-0.01	-0.20	0.00	0.06	-0.20
19	-0.05	0.10	-0.01	0.10	0.10	-0.07	0.10	-0.02	-0.14	0.24	0.02	-0.06	0.18	0.13	-0.22	0.11	0.24	-0.03	-0.14
20	-0.04	0.02	0.04	-0.11	-0.12	0.03	0.00	0.06	0.21	-0.24	0.27	0.05	0.16	0.20	-0.02	-0.14	-0.12	-0.04	-0.11
21	0.24	0.29	-0.30	0.28	0.26	-0.20	-0.18	0.16	-0.12	-0.23	0.16	0.21	-0.12	-0.12	-0.22	-0.07	-0.05	-0.04	-0.32
22	0.06	0.35	0.06	0.43	0.43	0.02	-0.16	0.18	-0.26	0.07	0.08	-0.13	0.09	0.14	0.03	-0.15	-0.04	0.09	-0.15
23	-0.06	-0.31	-0.10	-0.42	-0.42	-0.11	0.02	0.10	0.29	-0.20	-0.08	-0.02	0.09	0.10	0.01	-0.01	0.01	-0.11	0.13
24	-0.29	-0.03	0.05	0.05	0.05	0.06	-0.22	-0.16	-0.14	0.05	0.07	-0.08	-0.21	-0.24	0.12	0.18	0.14	0.17	-0.03
25	0.15	0.05	-0.03	-0.07	-0.08	-0.04	0.16	0.08	0.08	0.02	0.00	0.22	0.11	0.12	-0.21	0.06	-0.14	-0.25	-0.02
26	-0.10	-0.12	0.09	-0.42	-0.43	0.06	-0.02	0.00	0.26	0.07	0.23	0.15	-0.06	-0.12	-0.01	0.09	0.02	-0.06	0.00
27	-0.31	0.01	-0.18	-0.12	-0.14	-0.24	0.01	-0.09	0.08	0.00	-0.01	0.08	0.06	0.08	0.14	0.04	0.00	0.08	0.08
28	-0.18	-0.24	0.16	-0.56	-0.58	0.16	0.00	-0.01	0.30	0.02	0.12	-0.02	0.14	0.13	0.07	-0.02	0.01	0.05	0.20
29	0.05	0.63	-0.42	0.81	0.81	-0.49	-0.03	0.02	-0.51	0.13	0.05	-0.09	0.01	0.02	0.02	-0.20	0.15	0.04	-0.19
30	0.09	0.65	-0.40	0.84	0.84	-0.47	-0.04	0.03	-0.54	0.13	0.05	-0.10	0.00	0.00	0.01	-0.20	0.15	0.04	-0.22
31	0.02	-0.18	0.10	-0.17	-0.16	0.11	-0.02	0.03	0.11	-0.02	-0.16	-0.07	0.19	0.21	-0.10	-0.10	0.00	0.07	0.17
32	0.07	0.76	-0.45	0.99	0.99	-0.47	-0.04	-0.02	-0.69	0.22	0.09	-0.22	0.00	0.01	0.01	-0.15	0.18	0.09	-0.23
33	0.21	0.76	-0.44	0.97	0.97	-0.46	-0.01	0.04	-0.70	0.12	0.07	-0.14	-0.16	-0.13	-0.02	-0.18	0.19	0.09	-0.29
34	0.08	0.71	-0.42	0.98	0.97	-0.45	-0.06	0.02	-0.69	0.19	0.01	-0.16	-0.02	-0.02	0.05	-0.15	0.18	0.12	-0.23
35	-0.04	0.03	0.10	-0.20	-0.21	0.08	0.19	0.15	0.21	0.13	0.27	0.26	-0.02	0.00	-0.04	0.08	-0.03	-0.14	-0.18
36	-0.02	0.03	0.12	-0.26	-0.28	0.07	0.22	0.13	0.34	0.02	0.21	0.19	0.14	0.18	-0.12	0.04	-0.03	-0.14	0.01
37	-0.18	-0.07	0.16	-0.12	-0.13	0.16	0.17	-0.10	-0.01	-0.06	-0.08	0.01	-0.01	-0.01	-0.08	0.33	0.00	0.02	0.11
38	0.22	0.47	-0.35	0.30	0.28	-0.35	0.10	0.11	-0.17	0.07	0.08	-0.26	0.16	0.19	-0.02	-0.36	0.15	-0.02	-0.04
39	-0.37	-0.31	0.13	0.01	0.04	0.14	-0.19	-0.15	0.05	0.04	-0.15	-0.07	-0.04	-0.06	0.25	0.04	-0.17	0.24	0.12
40	0.27	0.40	-0.21	0.01	-0.02	-0.18	0.13	0.08	0.02	-0.13	0.16	0.04	0.08	0.10	-0.32	-0.06	-0.03	-0.27	-0.20
41	1.00	0.23	-0.05	0.10	0.09	0.09	-0.02	0.11	-0.07	-0.20	0.00	0.00	-0.04	-0.04	-0.07	-0.30	-0.11	-0.17	-0.09
42	0.23	1.00	-0.57	0.73	0.69	-0.58	0.01	0.03	-0.57	0.05	0.20	-0.22	0.01	0.02	-0.13	-0.22	0.25	-0.09	-0.27
43	-0.05	-0.57	1.00	-0.45	-0.42	0.94	-0.03	0.11	0.38	0.01	-0.04	0.10	0.00	0.00	-0.03	0.29	-0.22	0.03	0.15
44	0.10	0.73	-0.45	1.00	1.00	-0.48	-0.06	0.01	-0.67	0.18	0.03	-0.19	-0.02	-0.01	0.03	-0.17	0.18	0.09	-0.23
45	0.09	0.69	-0.42	1.00	1.00	-0.46	-0.07	0.02	-0.66	0.19	0.02	-0.18	-0.01	-0.01	0.05	-0.16	0.17	0.10	-0.22
46	0.09	-0.58	0.94	-0.48	-0.46	1.00	-0.01	0.11	0.38	-0.10	-0.04	0.09	-0.04	-0.03	0.00	0.26	-0.28	0.02	0.12
47	-0.02	0.01	-0.03	-0.06	-0.07	-0.01	1.00	0.05	0.16	-0.02	-0.05	0.15	0.01	0.02	-0.12	0.07	-0.06	0.04	0.00
48	0.11	0.03	0.11	0.01	0.02	0.11	0.05	1.00	0.15	0.08	0.19	0.09	-0.01	0.01	-0.10	0.00	-0.20	-0.13	-0.20
49	-0.07	-0.57	0.38	-0.67	-0.66	0.38	0.16	0.15	1.00	-0.27	-0.01	0.32	0.19	0.21	-0.01	0.01	-0.38	-0.02	0.12
50	-0.20	0.05	0.01	0.18	0.19	-0.10	-0.02	0.08	-0.27	1.00	0.02	0.01	0.02	-0.08	0.00	0.08	0.21	0.12	0.08
51	0.00	0.20	-0.04	0.03	0.02	-0.04	-0.05	0.19	-0.01	0.02	1.00	-0.25	-0.16	-0.25	0.00	-0.01	0.04	-0.04	-0.20
52	0.00	-0.22	0.10	-0.19	-0.18	0.09	0.15	0.09	0.32	0.01	-0.25	1.00	0.00	0.00	0.00	0.07	-0.24	0.02	-0.14
53	-0.04	0.01	0.00	-0.02	-0.01	-0.04	0.01	-0.01	0.19	0.02	-0.16	0.00	1.00	0.92	-0.31	-0.11	-0.04	-0.05	-0.02
54	-0.04	0.02	0.00	-0.01	-0.01	-0.03	0.02	0.01	0.21	-0.08	-0.25	0.00	0.92	1.00	-0.23	-0.25	-0.09	-0.04	0.04
55	-0.07	-0.13	-0.03	0.03	0.05	0.00	-0.12	-0.10	-0.01	0.00	0.00	0.00	-0.31	-0.23	1.00	-0.32	-0.20	0.18	0.36
56	-0.30	-0.22	0.29	-0.17	-0.16	0.26	0.07	0.00	0.01	0.08	-0.01	0.07	-0.11	-0.25	-0.32	1.00	0.02	-0.01	-0.18
57	-0.11	0.25	-0.22	0.18	0.17	-0.28	-0.06	-0.20	-0.38	0.21	0.04	-0.24	-0.04	-0.09	-0.20	0.02	1.00	-0.17	0.10
58	-0.17	-0.09	0.03	0.09	0.10	0.02	0.04	-0.13	-0.02	0.12	-0.04	0.02	-0.05	-0.04	0.18	-0.01	-0.17	1.00	-0.06
59	-0.09	-0.27	0.15	-0.23	-0.22	0.12	0.00	-0.20	0.12	0.08	-0.20	-0.14	-0.02	0.04	0.36	-0.18	0.10	-0.06	1.00

Appendix H

Number of points used in correlation

The first row and the first column of the correlation matrix contain the number of points associated to each variable as defined in Appendix A.

	2	3	4	5	6	7	8	9	10	11	12	13	14	15	16	17	18	19	20	21	22	23	24	25	26	27	28	29	30	31	32	33	34	35	36	37	38	39	40	41	42	43	44	45	46	47	48	49	50	51	52	53	54	55	56	57	58	59
2	147	146	147	147	147	147	147	147	147	147	147	145	143	140	138	106	106	124	71	48	146	146	146	125	146	146	146	146	146	146	140	138	145	144	145	146	144	147	135	147	147	147	147	147	147	145	147	145	143	146	142	146	147	147	147	147	147	147
3	146	146	146	146	146	146	146	146	146	146	146	144	142	139	137	106	106	123	70	47	145	145	145	125	145	145	145	145	145	145	139	137	144	143	144	145	143	146	134	146	146	146	146	146	146	144	146	144	142	145	141	145	146	146	146	146	146	146
4	147	146	147	147	147	147	147	147	147	147	147	145	143	140	138	106	106	124	71	48	146	146	146	125	146	146	146	146	146	146	140	138	145	144	145	146	144	147	135	147	147	147	147	147	147	145	147	145	143	146	142	146	147	147	147	147	147	147
5	147	146	147	147	147	147	147	147	147	147	147	145	143	140	138	106	106	124	71	48	146	146	146	125	146	146	146	146	146	146	140	138	145	144	145	146	144	147	135	147	147	147	147	147	147	145	147	145	143	146	142	146	147	147	147	147	147	147
6	147	146	147	147	147	147	147	147	147	147	147	145	143	140	138	106	106	124	71	48	146	146	146	125	146	146	146	146	146	146	140	138	145	144	145	146	144	147	135	147	147	147	147	147	147	145	147	145	143	146	142	146	147	147	147	147	147	147
7	147	146	147	147	147	147	147	147	147	147	147	145	143	140	138	106	106	124	71	48	146	146	146	125	146	146	146	146	146	146	140	138	145	144	145	146	144	147	135	147	147	147	147	147	147	145	147	145	143	146	142	146	147	147	147	147	147	147
8	147	146	147	147	147	147	147	147	147	147	147	145	143	140	138	106	106	124	71	48	146	146	146	125	146	146	146	146	146	146	140	138	145	144	145	146	144	147	135	147	147	147	147	147	147	145	147	145	143	146	142	146	147	147	147	147	147	147
9	147	146	147	147	147	147	147	147	147	147	147	145	143	140	138	106	106	124	71	48	146	146	146	125	146	146	146	146	146	146	140	138	145	144	145	146	144	147	135	147	147	147	147	147	147	145	147	145	143	146	142	146	147	147	147	147	147	147
10	147	146	147	147	147	147	147	147	147	147	147	145	143	140	138	106	106	124	71	48	146	146	146	125	146	146	146	146	146	146	140	138	145	144	145	146	144	147	135	147	147	147	147	147	147	145	147	145	143	146	142	146	147	147	147	147	147	147
11	147	146	147	147	147	147	147	147	147	147	147	145	143	140	138	106	106	124	71	48	146	146	146	125	146	146	146	146	146	146	140	138	145	144	145	146	144	147	135	147	147	147	147	147	147	145	147	145	143	146	142	146	147	147	147	147	147	147
12	147	146	147	147	147	147	147	147	147	147	147	145	143	140	138	106	106	124	71	48	146	146	146	125	146	146	146	146	146	146	140	138	145	144	145	146	144	147	135	147	147	147	147	147	147	145	147	145	143	146	142	146	147	147	147	147	147	147
13	145	144	145	145	145	145	145	145	145	145	145	145	141	138	136	104	104	122	70	48	144	144	144	123	144	144	144	144	144	144	139	136	143	142	143	144	142	145	133	145	145	145	145	145	145	143	145	143	141	144	140	144	145	145	145	145	145	145
14	143	142	143	143	143	143	143	143	143	143	143	141	144	138	135	106	106	124	70	48	143	143	143	122	143	143	143	143	143	143	137	137	142	141	142	143	141	144	132	144	144	144	144	144	144	142	144	142	140	143	139	143	144	144	144	144	144	144
15	140	139	140	140	140	140	140	140	140	140	140	138	138	140	133	104	104	121	66	44	139	139	139	119	139	139	139	139	139	139	134	131	138	137	138	139	137	140	128	140	140	140	140	140	140	138	140	138	137	139	135	139	140	140	140	140	140	140
16	138	137	138	138	138	138	138	138	138	138	138	136	135	133	138	100	101	118	68	47	137	137	137	118	137	137	137	137	137	137	131	129	136	135	136	137	135	138	127	138	138	138	138	138	138	136	138	136	134	137	134	137	138	138	138	138	138	138
17	106	106	106	106	106	106	106	106	106	106	106	104	106	104	100	106	100	95	42	30	106	106	106	90	106	106	106	106	106	106	101	100	106	105	106	106	105	106	95	106	106	106	106	106	106	105	106	105	105	106	102	106	106	106	106	106	106	106
18	106	106	106	106	106	106	106	106	106	106	106	104	106	104	101	100	106	94	42	28	105	105	105	88	105	105	105	105	105	105	103	100	105	104	105	105	104	106	95	106	106	106	106	106	106	106	105	106	105	105	106	102	106	106	106	106	106	106
19	124	123	124	124	124	124	124	124	124	124	124	122	124	121	118	95	94	124	59	43	123	123	123	105	123	123	123	123	123	123	117	117	123	122	123	123	121	124	113	124	124	124	124	124	124	122	124	122	120	123	120	123	124	124	124	124	124	124
20	71	70	71	71	71	71	71	71	71	71	71	70	70	66	68	42	42	59	71	26	71	71	71	58	71	71	71	71	71	71	65	70	70	70	70	71	70	71	68	71	71	71	71	71	71	69	71	69	68	70	69	70	71	71	71	71	71	71
21	48	47	48	48	48	48	48	48	48	48	48	48	48	44	47	30	28	43	26	48	48	48	48	40	48	48	48	48	48	48	46	44	47	47	47	48	46	48	48	48	48	48	48	48	48	46	48	46	44	47	47	47	48	48	48	48	48	48
22	146	145	146	146	146	146	146	146	146	146	146	144	143	139	137	106	105	123	71	48	148	148	148	127	148	148	148	148	148	148	141	140	147	146	147	148	146	148	137	148	148	148	148	148	148	146	148	146	144	147	143	147	148	148	148	148	148	148
23	146	145	146	146	146	146	146	146	146	146	146	144	143	139	137	106	105	123	71	48	148	148	148	127	148	148	148	148	148	148	141	140	147	146	147	148	146	148	137	148	148	148	148	148	148	146	148	146	144	147	143	147	148	148	148	148	148	148
24	146	145	146	146	146	146	146	146	146	146	146	144	143	139	137	106	105	123	71	48	148	148	148	127	148	148	148	148	148	148	141	140	147	146	147	148	146	148	137	148	148	148	148	148	148	146	148	146	144	147	143	147	148	148	148	148	148	148
25	125	125	125	125	125	125	125	125	125	125	125	123	122	119	118	90	88	105	58	40	127	127	127	127	127	127	127	127	127	127	120	119	127	127	127	127	126	127	116	127	127	127	127	127	127	125	127	125	125	126	124	126	127	127	127	127	127	127
26	146	145	146	146	146	146	146	146	146	146	146	144	143	139	137	106	105	123	71	48	148	148	148	127	148	148	148	148	148	148	141	140	147	146	147	148	146	148	137	148	148	148	148	148	148	146	148	146	144	147	143	147	148	148	148	148	148	148
27	146	145	146	146	146	146	146	146	146	146	146	144	143	139	137	106	105	123	71	48	148	148	148	127	148	148	148	148	148	148	141	140	147	146	147	148	146	148	137	148	148	148	148	148	148	146	148	146	144	147	143	147	148	148	148	148	148	148
28	146	145	146	146	146	146	146	146	146	146	146	144	143	139	137	106	105	123	71	48	148	148	148	127	148	148	148	148	148	148	141	140	147	146	147	148	146	148	137	148	148	148	148	148	148	146	148	146	144	147	143	147	148	148	148	148	148	148
29	146	145	146	146	146	146	146	146	146	146	146	144	143	139	137	106	105	123	71	48	148	148	148	127	148	148	148	148	148	148	141	140	147	146	147	148	146	148	137	148	148	148	148	148	148	146	148	146	144	147	143	147	148	148	148	148	148	148
30	146	145	146	146	146	146	146	146	146	146	146	144	143	139	137	106	105	123	71	48	148	148	148	127	148	148	148	148	148	148	141	140	147	146	147	148	146	148	137	148	148	148	148	148	148	146	148	146	144	147	143	147	148	148	148	148	148	148
31	146	145	146	146	146	146	146	146	146	146	146	144	143	139	137	106	105	123	71	48	148	148	148	127	148	148	148	148	148	148	141	140	147	146	147	148	146	148	137	148	148	148	148	148	148	146	148	146	144	147	143	147	148	148	148	148	148	148
32	140	139	140	140	140	140	140	140	140	140	140	139	137	134	131	101	103	117	65	46	141	141	141	120	141	141	141	141	141	141	142	133	140	139	140	141	139	142	130	142	142	142	142	142	142	140	142	140	138	141	137	141	142	142	142	142	142	142
33	138	137	138	138	138	138	138	138	138	138	138	136	137	131	129	100	100	117	70	44	140	140	140	119	140	140	140	140	140	140	133	140	139	138	139	140	138	140	129	140	140	140	140	140	140	138	140	138	136	139	135	139	140	140	140	140	140	140
34	145	144	145	145	145	145	145	145	145	145	145	143	142	138	136	106	105	123	70	47	147	147	147	127	147	147	147	147	147	147	140	139	147	146	147	147	145	147	136	147	147	147	147	147	147	145	147	145	143	146	142	146	147	147	147	147	147	147
35	144	143	144	144	144	144	144	144	144	144	144	142	141	137	135	105	104	122	70	47	146	146	146	127	146	146	146	146	146	146	139	138	146	146	146	146	144	146	135	146	146	146	146	146	146	144	146	144	142	145	141	145	146	146	146	146	146	146
36	145	144	145	145	145	145	145	145	145	145	145	143	142	138	136	106	105	123	70	47	147	147	147	127	147	147	147	147	147	147	140	139	147	146	147	147	145	147	136	147	147	147	147	147	147	145	147	145	143	146	142	146	147	147	147	147	147	147
37	146	145	146	146	146	146	146	146	146	146	146	144	143	139	137	106	105	123	71	48	148	148	148	127	148	148	148	148	148	148	141	140	147	146	147	148	146	148	137	148	148	148	148	148	148	146	148	146	144	147	143	147	148	148	148	148	148	148
38	144	143	144	144	144	144	144	144	144	144	144	142	141	137	135	105	104	121	70	46	146	146	146	126	146	146	146	146	146	146	139	138	145	144	145	146	146	146	135	146	146	146	146	146	146	144	146	144	143	145	141	145	146	146	146	146	146	146
39	147	146	147	147	147	147	147	147	147	147	147	145	144	140	138	106	106	124	71	48	148	148	148	127	148	148	148	148	148	148	142	140	147	146	147	148	146	149	137	149	149	149	149	149	149	147	149	147	145	148	144	148	149	149	149	149	149	149
40	135	134	135	135	135	135	135	135	135	135	135	133	132	128	127	95	95	113	68	48	137	137	137	116	137	137	137	137	137	137	130	129	136	135	136	137	135	137	137	137	137	137	137	137	137	135	137	135	133	136	132	136	137	137	137	137	137	137
41	147	146	147	147	147	147	147	147	147	147	147	145	144	140	138	106	106	124	71	48	148	148	148	127	148	148	148	148	148	148	142	140	147	146	147	148	146	149	137	149	149	149	149	149	149	147	149	147	145	148	144	148	149	149	149	149	149	149
42	147	146	147	147	147	147	147	147	147	147	147	145	144	140	138	106	106	124	71	48	148	148	148	127	148	148	148	148	148	148	142	140	147	146	147	148	146	149	137	149	149	149	149	149	149	147	149	147	145	148	144	148	149	149	149	149	149	149
43	147	146	147	147	147	147	147	147	147	147	147	145	144	140	138	106	106	124	71	48	148	148	148	127	148	148	148	148	148	148	142	140	147	146	147	148	146	149	137	149	149	149	149	149	149	147	149	147	145	148	144	148	149	149	149	149	149	149
44	147	146	147	147	147	147	147	147	147	147	147	145	144	140	138	106	106	124	71	48	148	148	148	127	148	148	148	148	148	148	142	140	147	146	147	148	146	149	137	149	149	149	149	149	149	147	149	147	145	148	144	148	149	149	149	149	149	149
45	147	146	147	147	147	147	147	147	147	147	147	145	144	140	138	106	106	124	71	48	148	148	148	127	148	148	148	148	148	148	142	140	147	146	147	148	146	149	137	149	149	149	149	149	149	147	149	147	145	148	144	148	149	149	149	149	149	149
46	147	146	147	147	147	147	147	147	147	147	147	145	144	140	138	106	106	124	71	48	148	148	148	127	148	148	148	148	148	148	142	140	147	146	147	148	146	149	137	149	149	149	149	149	149	147	149	147	145	148	144	148	149	149	149	149	149	149
47	145	144	145	145	145	145	145	145	145	145	145	143	142	138	136	105	105	122	69	46	146	146	146	125	146	146	146	146	146	146	140	138	145	144	145	146	144	147	135	147	147	147	147	147	147	144	147	143	141	144	140	144	145	145	145	145	145	145
48	147	146	147	147	147	147	147	147	147	147	147	145	144	140	138	106	106	124	71	48	148	148	148	127	148	148	148	148	148	148	142	140	147	146	147	148	146	149	137	149	149	149	149	149	149	147	149	147	145	148	144	148	149	149	149	149	149	149
49	145	144	145	145	145	145	145	145	145	145	145	143	142	138	136	105	105	122	69	46	146	146	146	125	146	146	146	146	146	146	140	138	145	144	145	146	144	147	135	147	147	147	147	147	147	144	147	143	141	144	140	144	145	145	145	145	145	145
50	143	142	143	143	143	143	143	143	143	143	143	141	140	137	134	105	105	120	68	44	144	144	144	125	144	144	144	144	144	144	138	136	143	142	143	144	143	145	133	145	145	145	145	145	145	144	145	144	142	145	141	145	145	145	145	145	145	145
51	146	145	146	146	146	146	146	146	146	146	146	144	143	139	137	106	106	123	70	47	147	147	147	126	147	147	147	147	147	147	141	139	146	145	146	147	145	148	136	148	148	148	148	148	148	147	148	147	145	148	144	148	148	148	148	148	148	148
52	142	141	142	142	142	142	142	142	142	142	142	140	139	135	134	102	102	120	69	47	143	143	143	124	143	143	143	143	143	143	137	135	142	141	142	143	141	144	132	144	144	144	144	144	144	143	144	143	141	144	140	144	144	144	144	144	144	144
53	146	145	146	146	146	146	146	146	146	146	146	144	143	139	137	106	106	123	70	47	147	147	147	126	147	147	147	147	147	147	141	139	146	145	146	147	145	148	136	148	148	148	148	148	148	147	148	147	145	148	144	148	148	148	148	148	148	148
54	147	146	147	147	147	147	147	147	147	147	147	145	144	140	138	106	106	124	71	48	148	148	148	127	148	148	148	148	148	148	142	140	147	146	147	148	146	149	137	149	149	149	149	149	149	147	149	147	145	148	144	148	149	149	149	149	149	149
55	147	146	147	147	147	147	147	147	147	147	147	145	144	140	138	106	106	124	71	48	148	148	148	127	148	148	148	148	148	148	142	140	147	146	147	148	146	149	137	149	149	149	149	149	149	147	149	147	145	148	144	148	149	149	149	149	149	149
56	147	146	147	147	147	147	147	147	147	147	147	145	144	140	138	106	106	124	71	48	148	148	148	127	148	148	148	148	148	148	142	140	147	146	147	148	146	149	137	149	149	149	149	149	149	147	149	147	145	148	144	148	149	149	149	149	149	149
57	147	146	147	147	147	147	147	147	147	147	147	145	144	140	138	106	106	124	71	48	148	148	148	127	148	148	148	148	148	148	142	140	147	146	147	148	146	149	137	149	149	149	149	149	149	147	149	147	145	148	144	148	149	149	149	149	149	149
58	147	146	147	147	147	147	147	147	147	147	147	145	144	140	138	106	106	124	71	48	148	148	148	127	148	148	148	148	148	148	142	140	147	146	147	148	146	149	137	149	149	149	149	149	149	147	149	147	145	148	144	148	149	149	149	149	149	149
59	147	146	147	147	147	147	147	147	147	147	147	145	144	140	138	106	106	124	71	48	148	148	148	127	148	148	148	148	148	148	142	140	147	146	147	148	146	149	137	149	149	149	149	149	149	147	149	147	145	148	144	148	149	149	149	149	149	149